Dominion Nuclear North Anna, LLC
5000 Dominion Boulevard, Glen Allen, VA 23060

Dominion®

August 5, 2004

U. S. Nuclear Regulatory Commission
Attention: Document Control Desk
Washington, D.C. 20555

Serial No. 04-347
ESP/JDH
Docket No. 52-008

DOMINION NUCLEAR NORTH ANNA, LLC
NORTH ANNA EARLY SITE PERMIT APPLICATION
RESPONSE TO REQUEST FOR ADDITIONAL INFORMATION NO. 5

In its June 1, 2004 letter titled "Request for Additional Information Letter No. 5," the NRC requested additional information regarding certain aspects of Dominion Nuclear North Anna, LLC's (Dominion's) Early Site Permit application. This letter contains our responses to the following requests for additional information:

2.5.1-5, 2.5.1-6, 2.5.2-5, 2.5.2-6, 2.5.2-7, 2.5.2-8, 2.5.3-2, 2.5.4-1, 2.5.4-2, 2.5.4-3, 2.5.4-4, 2.5.4-5, 2.5.4-6, 2.5.4-7, 2.5.4-8, 2.5.4-11, 2.5.4-12, 17.1-2

Responses to RAIs 2.5.2-9, 2.5.4-8 (c), 2.5.4-9, 2.5.4-10, and 2.5.5-1 will be submitted at a later date. In addition, part of the response to RAI 2.5.4-1 involves proprietary information that will be submitted by separate letter.

It is our intent to revise the North Anna ESP application to reflect our responses to these and other RAIs to support issuance of the NRC staff's draft safety and environmental evaluations scheduled for later this year. Planned changes to the application are identified following the response to each RAI.

If you have any questions or require additional information, please contact Mr. Joseph D. Hegner at 804-273-2770.

Very truly yours,

Eugene S. Grecheck
Vice President-Nuclear Support Services

A001

Enclosure: 1. Response to NRC RAI Letter No. 5

Commitments made in this letter:

1. Revise North Anna ESP application to reflect RAI responses.
2. Submit proprietary portion of RAI 2.5.4-11 response separately.

cc: (with enclosure)

U. S. Nuclear Regulatory Commission, Region II
Sam Nunn Atlanta Federal Center
61 Forsyth Street, SW
Suite 23T85
Atlanta, Georgia 30303

Mr. Mike Scott
U. S. Nuclear Regulatory Commission
Washington, D.C. 20555

Mr. M. T. Widmann
NRC Senior Resident Inspector
North Anna Power Station

Serial No. 04-347
Docket No. 52-008
Response to 6/1/04 RAI Letter No. 5

COMMONWEALTH OF VIRGINIA

COUNTY OF HENRICO

The foregoing document was acknowledged before me, in and for the County and Commonwealth aforesaid, today by Eugene S. Grecheck, who is Vice President, Nuclear Support Services, of Dominion Nuclear North Anna, LLC. He has affirmed before me that he is duly authorized to execute and file the foregoing document on behalf of Dominion Nuclear North Anna, LLC, and that the statements in the document are true to the best of his knowledge and belief.

Acknowledged before me this 5th day of August, 2004

My Commission expires: 3/31/08

Maggie McCleese
Notary Public

(SEAL)

Enclosure 1

Response to NRC RAI Letter No. 5

RAI 2.5.1-5 (6/1/04 NRC Letter)

SSAR Subsection 2.5.1.1.4 describes the Mountain Run and Kelly's Ford scarps along the Mountain Run fault zone and states that field and aerial reconnaissance did not reveal any geologic or geomorphic features indicative of potential Quaternary activity along the Mountain Run fault zone. Please describe the relevant physiographic features associated with these two scarps and the evidence that led to the conclusion that "the scarp most likely formed due to erosion, as southeastward-migrating streams impinge against more resistant rocks of the Mountain Run fault zone."

Response

The Mountain Run fault zone strikes northeast and is located along the eastern margin of the Culpeper Basin (Figure 1), approximately 18 miles northwest of the North Anna ESP site. (Figures are located at the end of this RAI response.) Two pronounced northwest-facing scarps occur along the fault zone, including the 1-mile long Kelly's Ford scarp located directly northeast of the Rappahannock River, and the 7-mile long Mountain Run scarp located along the southeast margin of the linear Mountain Run drainage (Figure 1).

As described in SSAR Section 2.5.1.1.4, reconnaissance-level field and aerial evaluation of the Mountain Run fault zone revealed that this structure lacks topographic and geomorphic expression of Quaternary activity. Inspection of 1:24,000 scale topographic maps shows that the steeper portions of the Mountain Run scarp on the southeast side of the valley correlate with the areas where the Mountain Run (creek) is impinging on the scarp. In addition, the northwest side of the narrow Mountain Run valley is steepest where the stream is impinging on that side of the valley. The reconnaissance observations and topographic analysis form the basis of the conclusion in the SSAR that the Mountain Run and Kelly's Ford scarps most likely were created by fluvial erosion and not tectonic displacement of the earth's surface.

This response presents cross sections across the Mountain Run and Kelly's Ford scarps to further document the observations presented in the SSAR. In addition, cross sections are presented across a Pliocene colluvial deposit overlying the Mountain Run fault zone to document the absence of Quaternary faulting.

1. Preparation of Cross Sections

Nine geologic cross sections were prepared to document topography and geologic contacts, including fault contacts, across and adjacent to the Mountain Run fault zone, which includes the Mountain Run fault and subparallel proximal faults as mapped by Mixon et al. (2000) (see Figure 1 for cross section locations). The topography along each cross section was taken from 7.5-minute USGS topographic quadrangles (Germanna Bridge; Unionville) with 10 ft contour intervals. Faults, geologic units, and

geologic contacts from 1:100,000-scale geologic mapping by Mixon et al. (2000) were plotted on the topographic profiles primarily to show the spatial association of geologic contacts with topographic and geomorphic features, and are not intended to show subsurface geologic conditions. Thus, these cross sections are more accurately referred to as geologic profiles. Geologic units crossed by the profiles include: Paleozoic metamorphic rocks of the Piedmont province, Triassic sedimentary rocks and Jurassic diabase intrusions in the Culpeper Basin; late Neogene to Quaternary colluvial deposits; and Quaternary fluvial deposits (Figure 2). For the purposes of this response, surficial deposits are shown on the profiles as a veneer with uncertain thickness; bedrock geologic units are shown with vertical contacts to the base of the section. The nine profiles are labeled A through I on Figure 1, and are presented in Figures 3 through 11.

2. Analysis of Profiles

The northern two profiles (profiles A and B on Figure 1) cross the Mountain Run fault zone north and south, respectively, of the point where the east-flowing Rappahannock River exits the Culpeper Basin. Profile A (Figure 3) crosses the Kelly's Ford scarp, which is a prominent northwest-facing scarp in Paleozoic bedrock on the southeast side of the Marsh Run drainage, just northeast of its confluence with the Rappahannock River. Profile B (Figure 4) crosses the Mountain Run fault zone and Mountain Run creek southwest of the Rappahannock River. Both profiles document northwest-facing slope breaks on the southeast sides of the valleys that contain Marsh Run and Mountain Run; however, there is no consistent association of these slope breaks with faults within the Mountain Run fault zone. Whereas the Kelly's Ford scarp is adjacent to the buried trace of the Mountain Run fault (Figure 3), the pronounced bedrock scarp on the southeastern margin of Mountain Run valley is located about 3000 ft southeast of the mapped trace of the Mountain Run fault (Figure 4). If the Kelly's Ford scarp in Profile A formed by repeated late Cenozoic west-side-down surface rupture on the Mountain Run fault, then we would reasonably expect to see a similar scarp or geomorphic expression of movement along the fault approximately two miles on strike to the south at Profile B. Instead of being consistently associated with the fault, however, the northwest-facing scarps in both profiles are associated with incised drainages that are preferentially eroding the southeast valley walls, creating asymmetric valley profiles. We interpret that the Kelly's Ford scarp and northwest-facing scarp that forms the eastern valley wall of Mountain Run are products of fluvial erosion, not late Cenozoic fault activity.

The central group of four profiles (profiles C, D, E and F on Figures 5-8, respectively) all cross the Mountain Run fault zone where it is buried by late Neogene colluvial deposits (i.e., "QTc" on Figure 1) that mantle a broad, 5000-ft- to 6000-ft-long northwest facing slope, which drops gently from the Piedmont province into the eastern Culpeper Basin between Mountain Run creek and the Rapidan River (Figure 1). The Mountain Run fault zone generally is mapped by Mixon et al. (2000) in the central to eastern part of this slope. The fault zone is not located at the base of the slope and thus the slope

itself is not created or controlled by the fault. Profiles C through F document the absence of laterally continuous 50-ft to 100-ft-high northwest-facing scarps (i.e., features comparable to the Kelly's Ford scarp) along this slope or in the late Neogene colluvial deposits that cover the Mountain Run fault zone (Figures 5-8).

Profiles D through F reveal that the broad, northwest-facing slope between the Piedmont province and Culpeper Basin is interrupted by short reaches with steeper gradients. Inspection of the Germanna Bridge 7.5-minute topographic map indicates that the steeper slope reaches are associated with ephemeral streams that are incised into, and dissect, the originally smooth slope. For example, the gradient of the NW-facing slope in Profile D increases abruptly west of the Mountain Run fault zone (approximately at horizontal distance 5900 ft; Figure 6). The increased gradient is directly associated with the valley of an ephemeral stream that is incised in the broad slope, and which is obliquely intersected by the profile. In Figure 6 we show an interpreted reconstruction of the northwest-facing slope as a smooth surface prior to incision, and the incised valley can be seen as an asymmetric convexity in the topographic profile below the reconstructed smooth surface. Another incised stream valley impinges on Profile D at horizontal distance 1800 ft. Here, the profile of the incised valley is more symmetric because the stream and valley intersect the profile at a higher angle.

Similarly, two short, relatively steep reaches of slope occur at horizontal distances of 5600 ft and 6600 ft on Profile E (Figure 7). Although one of the steep reaches is located within the Mountain Run fault zone, neither reach is associated with a mapped fault trace (Figure 7). Examination of the adjacent topography on the Germanna Bridge 7.5-minute quadrangle map shows that both steep reaches of the slope are associated with the headwaters of incised, ephemeral drainages that obliquely intersect Profile E. As in Profile D, we show an interpreted reconstruction of the NW-facing slope prior to incision of these drainages as a smooth surface (Figure 7). Fluvial dissection of the slope is more obvious on Profile F (Figure 8), where ephemeral streams cross the profile at higher angles and have incised obvious convex valleys below the originally smooth, contiguous slope surface.

Based on the relations shown on Profiles C through F, we conclude that the broad northwest-facing slope between the Piedmont province and Culpeper Basin is non-tectonic, and that there is no laterally continuous scarp on the slope, or in the late Neogene colluvium, consistent with repeated late Cenozoic surface rupture on faults of the Mountain Run fault zone. Short reaches of slope with higher gradients on profiles D through F are due to fluvial incision of the originally smooth, contiguous slope surface by ephemeral streams, and are not tectonic in origin.

The southern three profiles G, H, and I (Figures 9-11) cross the Mountain Run valley southwest of the Rapidan River (Figure 1). The profiles clearly document that fluvial incision, rather than tectonic movement, has created relatively steep bedrock escarpments along the margins of Mountain Run valley. At Profile G (Figure 1),

Mountain Run valley is distinctly asymmetric with a steeper southeastern valley wall (Figure 9). The stream presently hugs the southeastern valley wall, and the valley geometry indicates that Mountain Run has preferentially undercut the southeastern margin of the valley during late Cenozoic incision. In contrast, Profile H (Figure 10), which is located about two miles southwest of Profile G (Figure 1), reveals a more symmetric valley. Here, Mountain Run flows through the center of the valley, and there are modest bedrock escarpments along both sides of the valley. Moving southwest from Profile H, the valley profile becomes asymmetric again, with Mountain Run flowing adjacent to the steeper northwestern valley wall (Profile I, Figure 11). The asymmetry of Mountain Run valley in Profile I indicates that the stream preferentially undercut the northwestern valley wall during incision. We conclude that the reversal in valley asymmetry and creation of both northwest- and southeast-facing bedrock scarps along the valley margins is due to fluvial erosion. This reversal in valley asymmetry is not consistent with late Cenozoic, northwest-side-down displacement along the Mountain Run fault zone.

3. Summary and Conclusions

From northeast to southwest, the profiles presented in Figures 3 through 11 document the following geomorphic and geologic relations:

- There is no consistent expression of a scarp along the Mountain Run fault in the vicinity of the Rappahannock River. The northwest-facing Kelly's Ford scarp is similar to a northwest-facing scarp along the southeastern valley margin of Mountain Run; both scarps were formed by streams that preferentially undercut the southeastern valley walls, creating asymmetric valley profiles.

- There is no northwest-facing scarp associated with the Mountain Run fault zone between the Rappahannock and Rapidan rivers. Undeformed late Neogene colluvial deposits bury the Mountain Run fault zone in this region, demonstrating the absence of Quaternary fault activity.

- The northwest-facing "Mountain Run" scarp southwest of the Rapidan River alternates with a southeast-facing scarp on the opposite side of Mountain Run valley; both sets of scarps have formed by the stream impinging on the edge of the valley.

These relations support the conclusion presented in the SSAR that the Mountain Run and Kelly's Ford scarps are fluvial features and were not created by late Cenozoic tectonic displacement along the Mountain Run fault zone. The Mountain Run fault zone is overlain by undeformed late Neogene colluvial deposits and thus has not experienced Quaternary surface fault rupture.

References

Mixon, R.B., Pavlides, L., Powars, D.S., Froelich, A.J., Weems, R.E., Schindler, J.S., Newell, W.L., Edwards, L.E., and Ward, L.W., 2000, Geologic map of the Fredericksburg 30' x 60' Quadrangle, Virginia and Maryland: United States Geological Survey Geologic Investigations Series Map I-2607.

Application Revision

None.

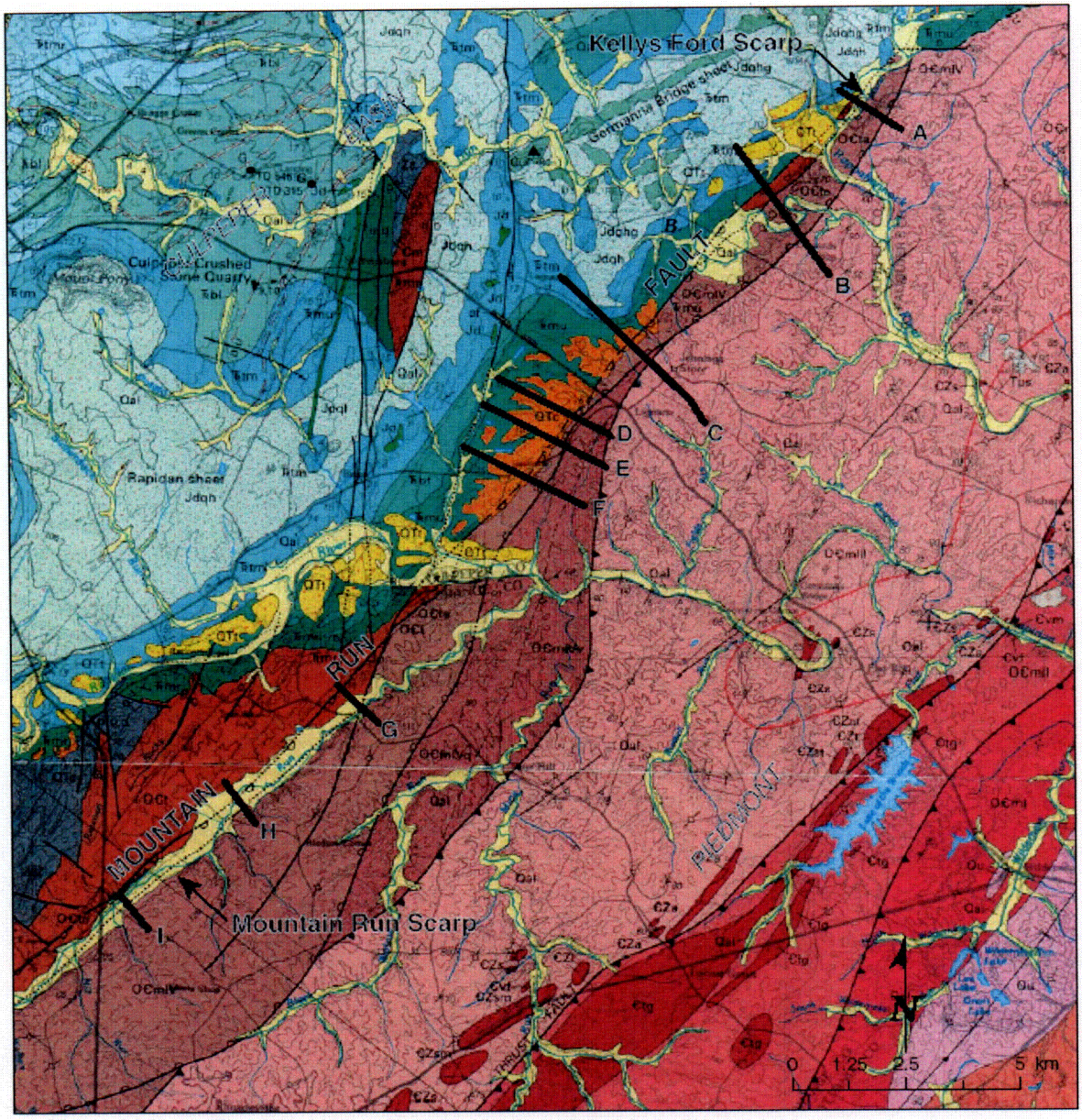

Figure 1. Geologic map of the Mountain Run Fault Zone (taken from Mixon et al., 2000). Profiles constructed across the fault, and illustrated in Figures 3-11, are indicated by black lines labeled A-I.

C01

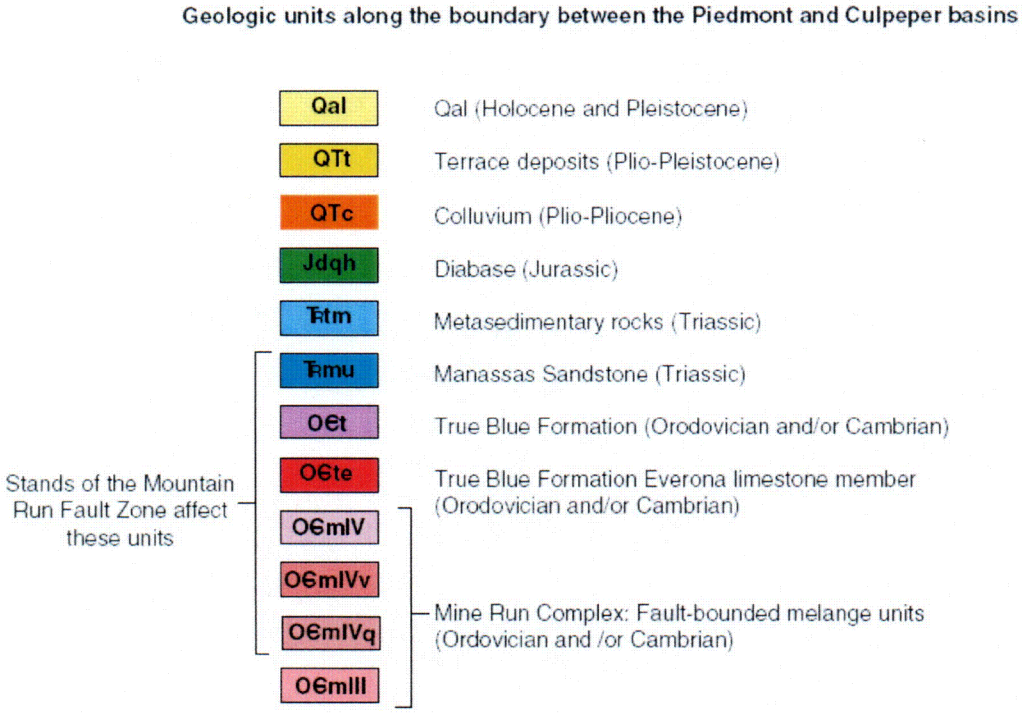

Figure 2. Geologic map units of Mixon et al. (2000) crossed by Profiles A through I (Figures 3-11; see text for discussion).

C02

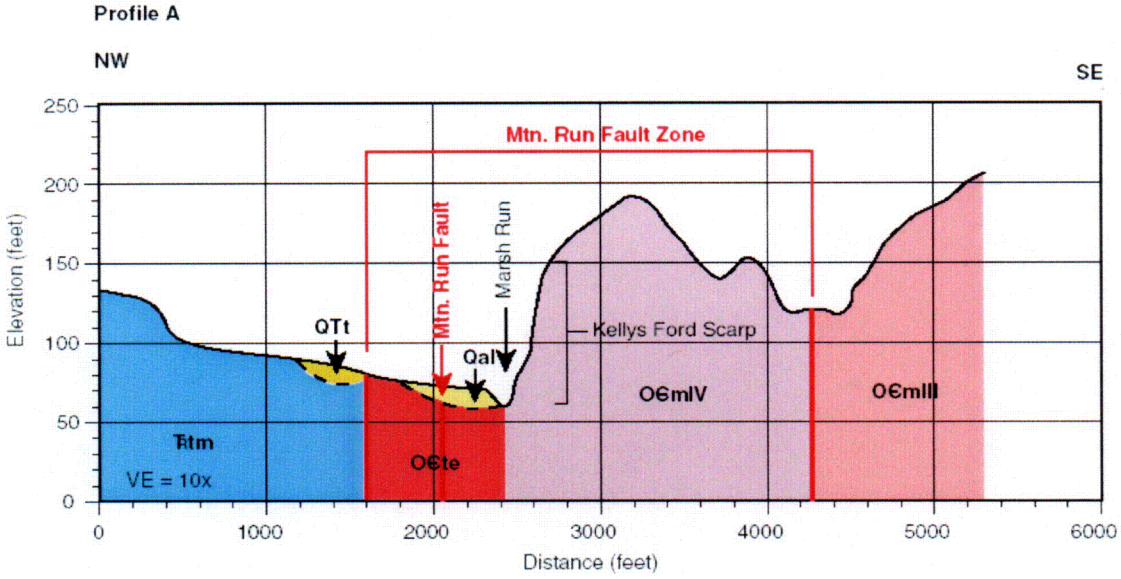

Figure 3. Profile A (see Figure 1 for profile location. Geology from Mixon et al. (2000).

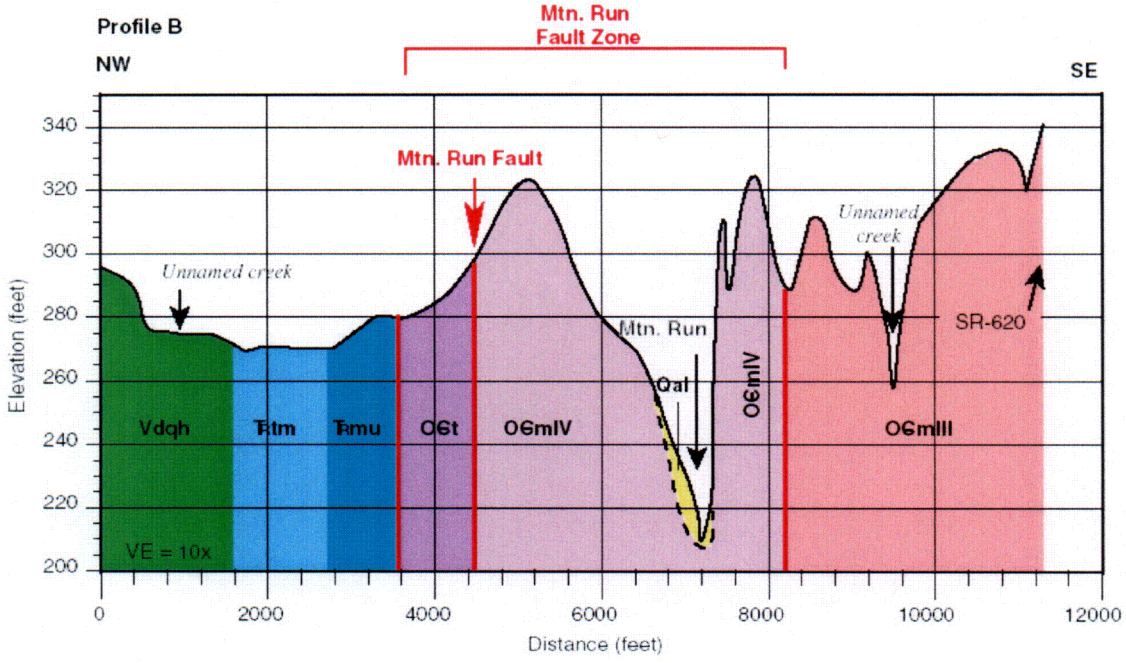

Figure 4. Profile B (see Figure 1 for location). Geology from Mixon et al. (2000).

C03

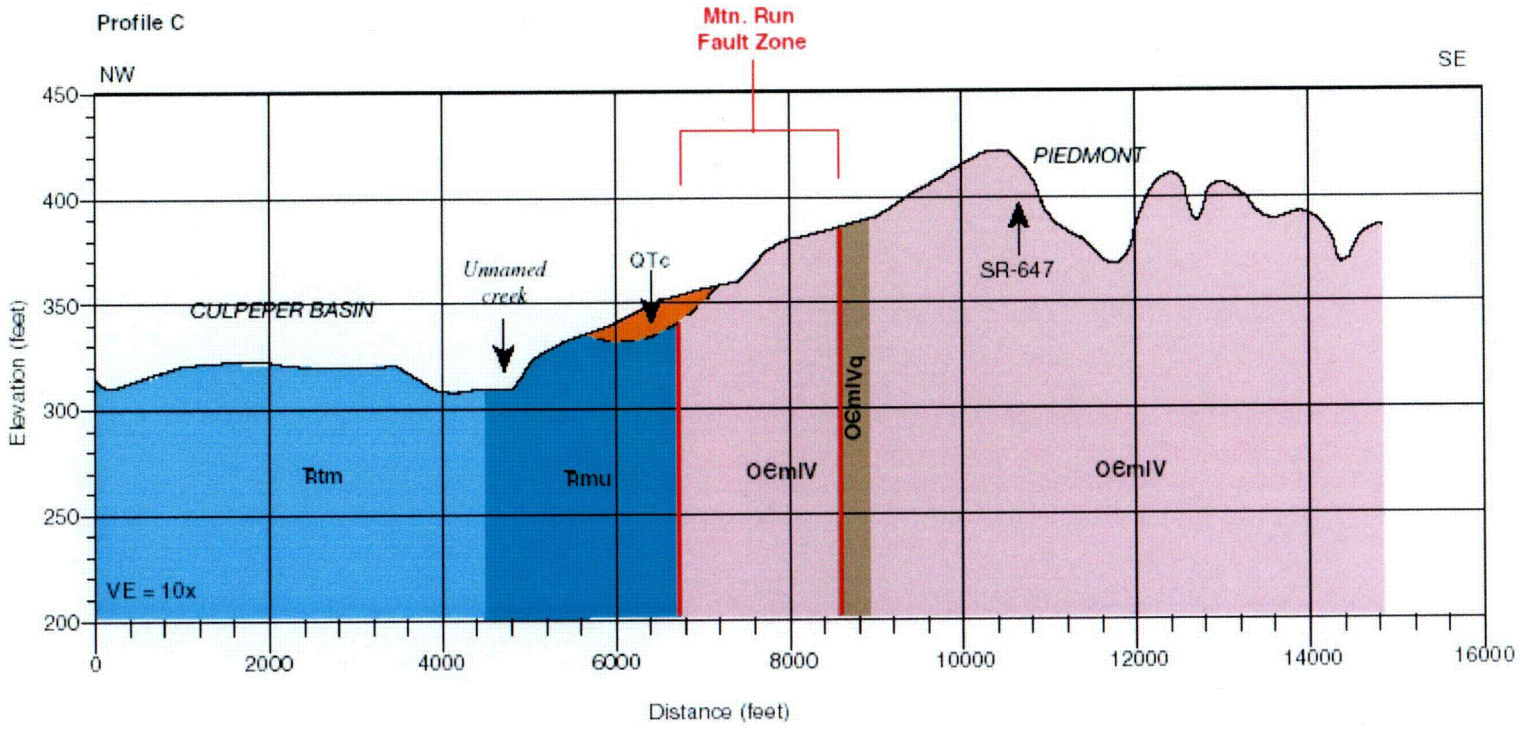

Figure 5. Profile C (see Figure 1 for location). Geology from Mixon et al. (2000).

C04

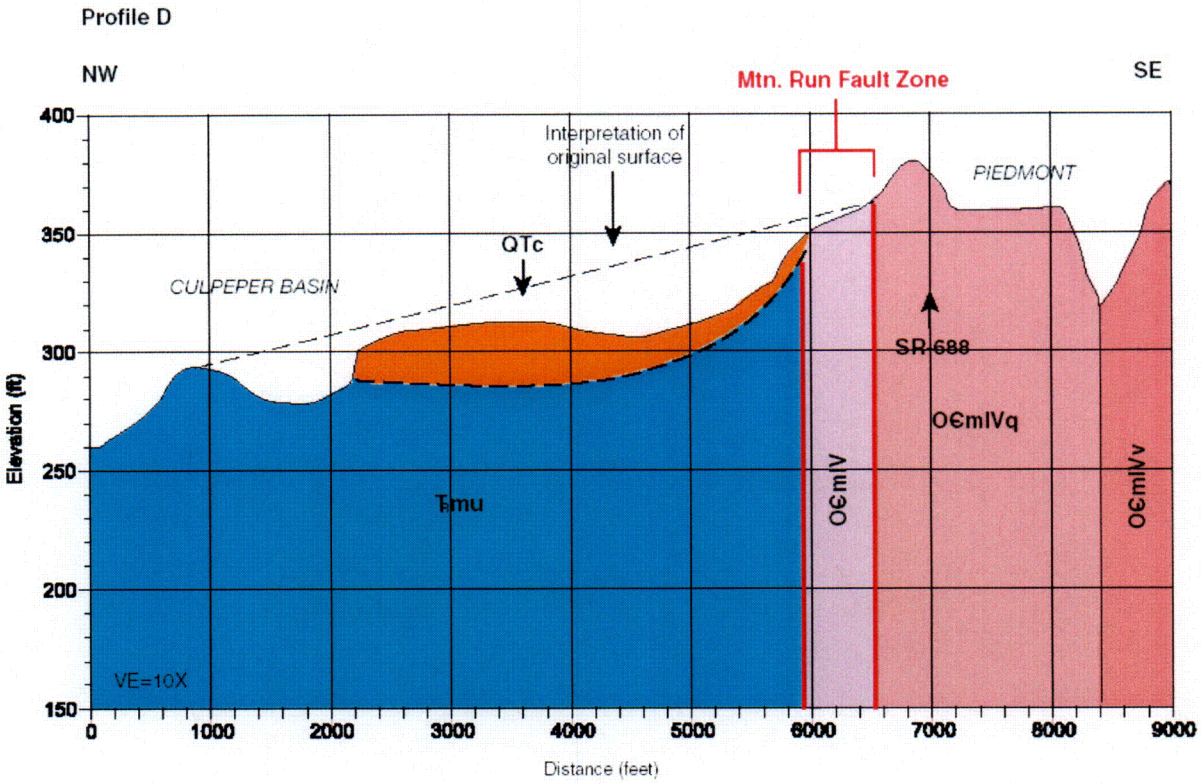

Figure 6. Profile D (see Figure 1 for location). Geology from Mixon et al. (2000). Dashed line shows interpretation of original undissected slope from the Piedmont to Culpeper Basin.

C05

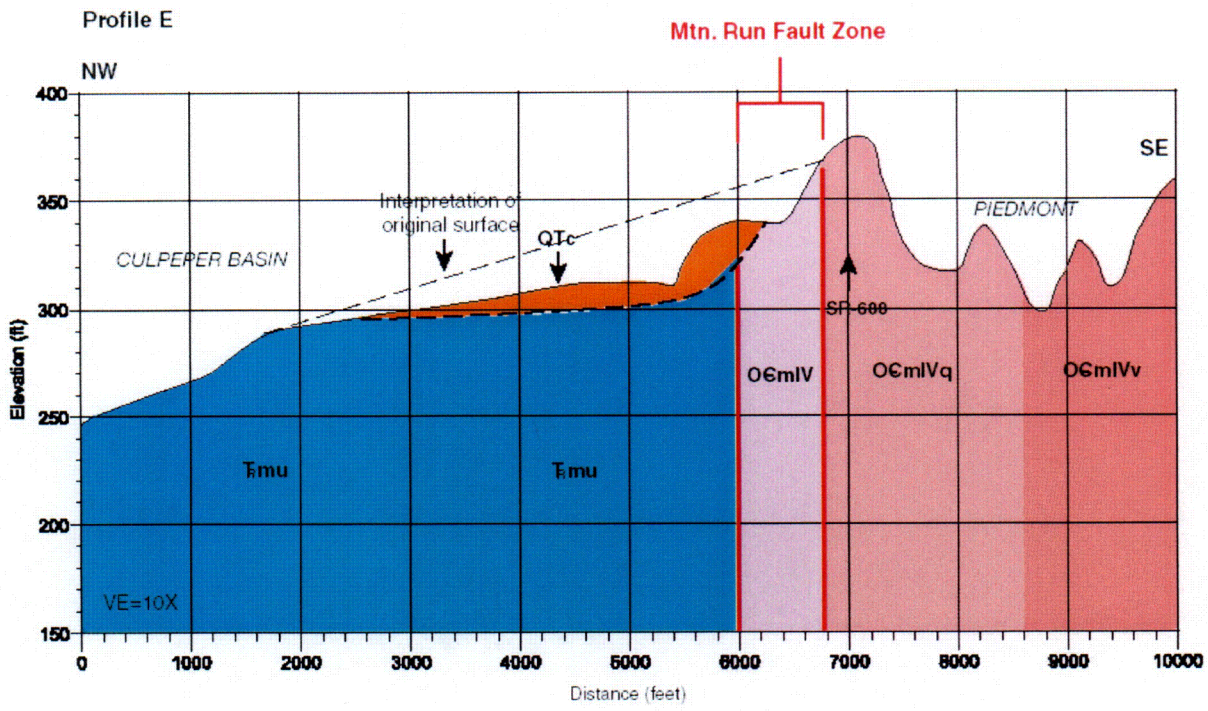

Figure 7. Profile E (see Figure 1 for location). Geology from Mixon et al. (2000). Dashed line shows interpretation of original undissected slope from the Piedmont to Culpeper Basin.

C06

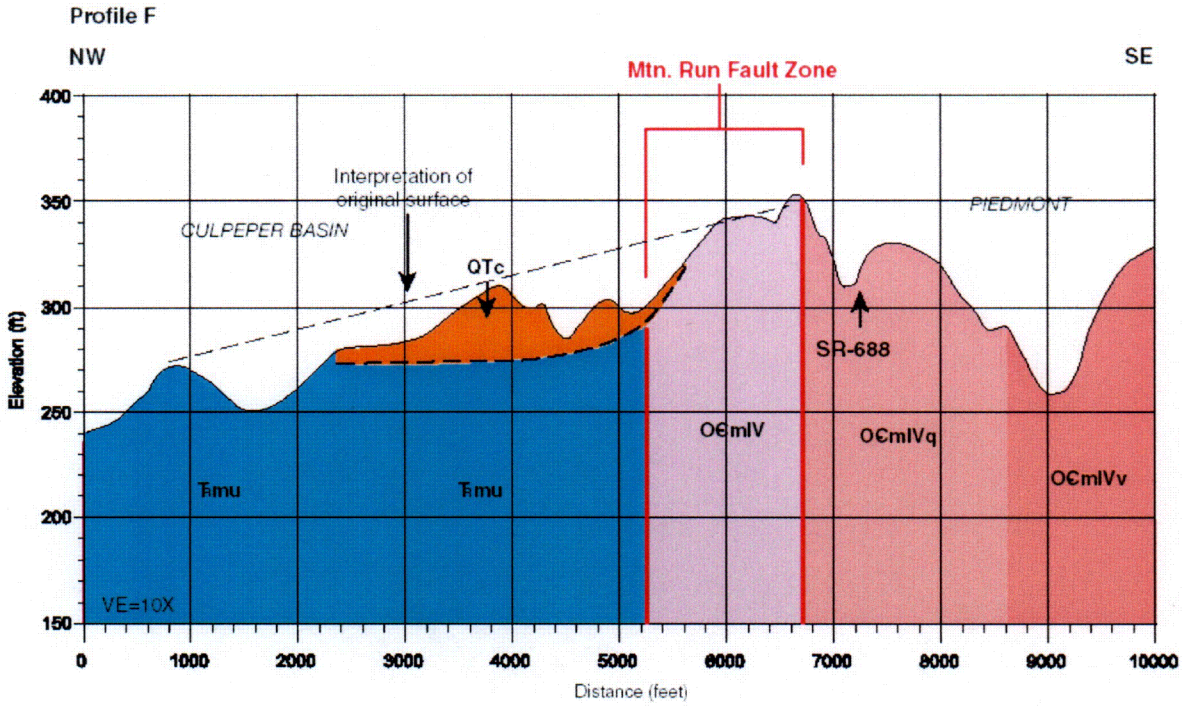

Figure 8. Profile F (see Figure 1 for location). Geology from Mixon et al. (2000). Dashed line shows interpretation of original undissected slope from the Piedmont to Culpeper Basin.

C07

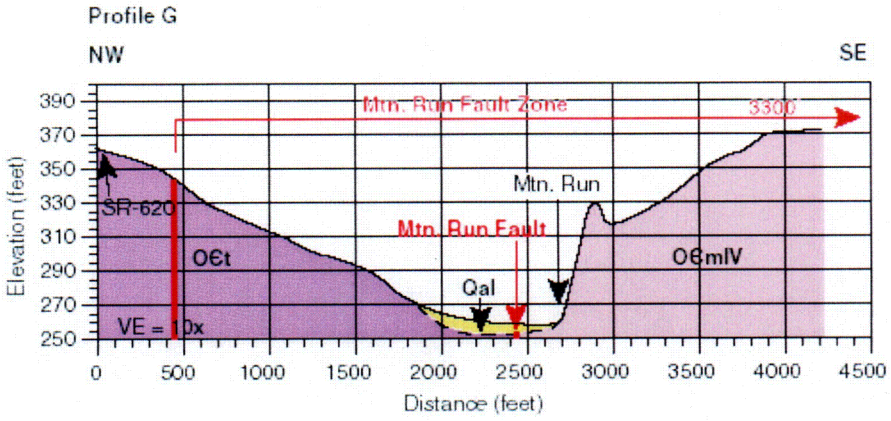

Figure 9. Profile G (see Figure 1 for profile location). Geology from Mixon et al. (2000).

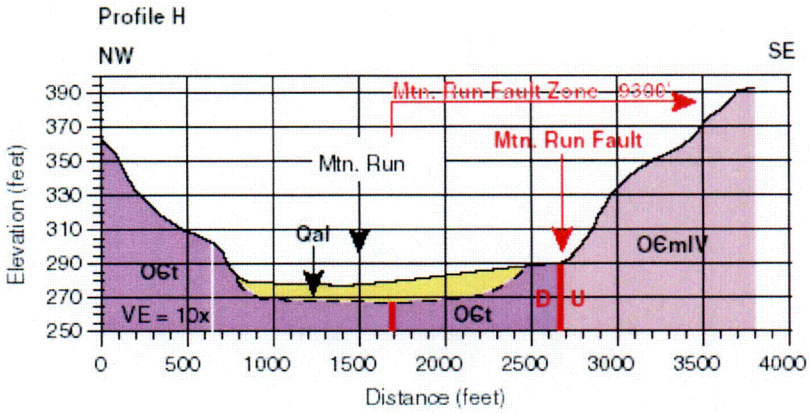

Figure 10. Profile H (see profile across the Mountain Run Fault. See Figure 1 for profile location. Geology from Mixon et al. (2000).

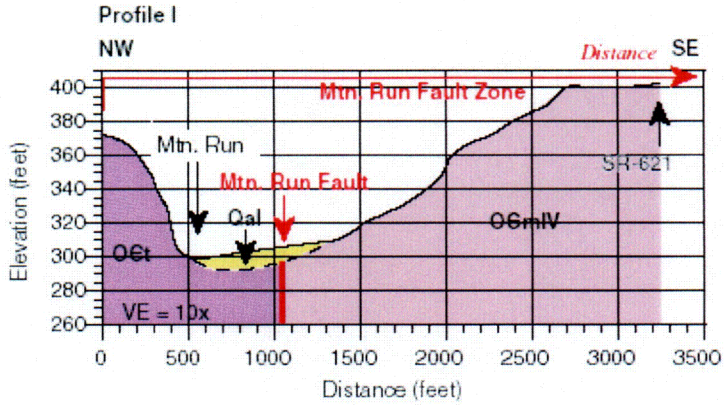

Figure 11. Profile I (see Figure 1 for profile location). Geology from Mixon et al. (2000).

C08

RAI 2.5.1-6 (NRC 6/1/04 Letter)

SSAR Subsection 2.5.1.1.4 states that the Stafford fault system is not a capable tectonic source. Please elaborate on the evidence gathered from field observations and aerial reconnaissance that support this conclusion with regard to the Dumfries, Fall Hill, Hazel Run, and Brooke faults.

Response

The conclusion that the Stafford fault system is not a capable tectonic source is based on review of existing literature, discussion with researchers familiar with the area (e.g., R.B. Mixon), aerial and field reconnaissance, and geomorphic analysis of upland surfaces capped by Neogene marine deposits, and Pliocene and Quaternary fluvial terraces of the Rappahannock River at Fredericksburg. These surfaces are not visibly deformed across mapped traces of the Stafford fault system. This response presents structure contour maps and topographic profiles across these geomorphic surfaces to supplement the aerial and field observations presented in the SSAR. In the following discussion, a brief description of the Stafford fault system is first presented, followed by our field observations and analysis of late Cenozoic deposits and geomorphic surfaces that overlie the Stafford fault system, and which we believe document the absence of post-Pliocene faulting along these structures.

1. The Stafford Fault System

The 42-mile-long Stafford fault system consists of a series of northeast-striking, northwest-dipping, high-angle reverse faults including, from northwest to southeast, the Dumfries, Fall Hill, Hazel Run, and Brooke faults (Figures 1 and 2). (Figures are located at the end of this RAI response.) An unnamed fault southeast of the Hazel Run fault and south-southwest of the city of Fredericksburg has a similar strike to the faults of the Stafford system (Figure 1). For convenience, the latter structure is referred to as the "Unnamed fault" in this response. Although the Unnamed fault is not usually referred to as part of the Stafford system, we evaluate it in this response because it has a similar strike to recognized faults of the Stafford system. The individual faults of the Stafford system are 10 to 25 miles long, and exhibit a left-stepping pattern. Horizontal slickensides found on the Dumfries fault zone suggest a component of dextral shear on the fault system (Mixon et al., 2000). In the vicinity of Fredericksburg, the Stafford fault system coincides with the Fall Line and a northeast-trending reach of the Potomac River.

Slip on the Stafford fault system during the Mesozoic and Tertiary is documented by displacement of Ordovician bedrock over lower Cretaceous bedrock along the Dumfries fault zone and abrupt thinning of the Paleocene Aquia Formation across multiple strands of the fault system (Mixon et al., 2000). Minor late Cenozoic activity of the fault system is documented by an interpreted 11-inch displacement of the base of a Pliocene terrace along the Rappahannock River by the Fall Hill fault (Mixon and Newell, 1978;

Mixon et al., 2000), and an 18-inch displacement of upland gravels of Neogene age on the Hazel Run fault (Mixon and Newell, 1978). Assuming that this deformation occurred in the past 2 my, the long-term average late Cenozoic separation rate on the faults is about 0.00015 mm/yr to 0.00023 mm/yr.

2. Geomorphic Analysis

As requested in the RAI, this response provides additional detail and documentation of our reconnaissance field observations and geomorphic analyses presented in SSAR Section 2.5.1.1.4. In particular, our geomorphic analyses and field observations included an evaluation of Pliocene and Miocene marine deposits (Sections 2.1 and 2.2, respectively) and late Pliocene and Quaternary fluvial terraces (Section 2.3) that overlie the Stafford fault system in the vicinity of Fredericksburg, Virginia.

2.1 Contours of Pliocene Unit "Tps"

As mapped by Mixon et al. (2000), all strands of the Stafford fault system except the Dumfries fault are overlain by a Pliocene-age, marginal-marine sand known as "Tps". Unit Tps ranges from 0 to 60 ft in thickness (Mixon et al., 2000), and it caps upland surfaces bordering the Rappahannock River valley (Figure 1). Because the Tps unit was deposited as the ancestral Atlantic shoreline retreated eastward in Pliocene time, the Tps sand most likely mantled a pre-existing shallow submarine topography, and the original upper depositional surface probably exhibited very low relief. Significant post-Tps movement on branches of the Stafford fault system would deform this surface and most likely create southeast-facing scarps discernable as gradients in the present elevation of Tps remnants overlying the faults.

To evaluate post-Pliocene activity of the Stafford system, we constructed a structure contour map of the Tps unit in the vicinity of the Rappahannock River. As shown on Figure 1, the Tps unit is extensively preserved in this region. The 1:100,000-scale geologic mapping of the Tps unit by Mixon et al. (2000) was transferred to USGS 7.5 minute topographic maps with 10-foot contour intervals (Fredericksburg, Spotsylvania, Guinea, Rappahannock Academy, Salem Church and Passapatanzy). From these maps, elevations along summit surfaces and ridge tops underlain by the Tps unit were identified as shown in Figure 1. These surfaces and ridge crests have experienced less erosional denudation than Tps remnants in interfluves between second- and third-order streams, and thus are most likely to reflect the original topography on the depositional surface of the Tps unit.

The selected elevations (Figure 1) were initially contoured using ArcGIS Spatial Analyst (Figure 3). After inspecting the ArcGIS-generated contours, the elevation data were recontoured by hand, using geological judgment to smooth the contours in areas with little or no data, such as the Rappahannock River valley, and disregarding isolated outliers. The resulting refined contour map is presented in Figure 4.

The major feature visible in the contours on the Tps unit is a broad NW-SE-trending trough approximately centered on the modern Rappahannock River valley. Based on the elevations of the Tps unit NE and SW of the Rappahannock River, minimum relief across this trough is about 20 ft to 30 ft. If this represents original relief on the upper surface of the Tps unit, then the "trough" may originally have been a submarine channel fed by the Pliocene Rappahannock River draining the Piedmont.

Most significantly for our conclusion that the Stafford fault system is not a capable tectonic source, the Tps contours cross the Stafford fault system at moderate to high angles, and are not deflected across the fault system. The major gradients in the contoured Tps surface are not parallel to fault dip, as would be expected if the fault system had been active since Tps deposition. The only area on the map where the Tps contours are subparallel to the Stafford system is at the southern end of the Fall Hill fault. Close inspection of the map shows, however, that this deflection in the contours is not confined to the fault, but rather is part of an apparent east-west-trending "trough" that is located directly north of and subparallel to Hazel Run creek. We interpret that this "trough" represents original relief on the Tps surface, possibly associated with a submarine valley that was tributary to the larger NW-SE trough in the Tps surface centered on the modern Rappahannock River valley, discussed above. We conclude that the deflections in the contours at the southern end of the Fall Hill fault are associated with this "trough", and are not tectonic in origin. Aside from the very southern end of the Fall Hill fault, the Tps contours elsewhere cross the structure at a moderate angle and are not deflected.

In general, the steepest gradient in the upper Tps surface is expressed by the 240 to 280 ft contours, and it occurs northwest of the Fall Hill fault, which is the westernmost fault of the Stafford system at the latitude of Fredericksburg (Figure 4). South of the Fall Hill fault, contours of the Tps surface trend NW-SE, and they define a low gradient toward the northeast. In contrast, the surface of the Tps unit northwest of the Fall Hill fault strikes NE-SW, subparallel to the Stafford system, and dips southeast at a higher gradient than the northeast slope of the Tps surface southeast of the Fall Hill fault. The increase in slope of the Tps surface occurs west of the Fall Hill fault, and thus is not created by relative northwest-side-up movement on the fault. The increase in gradient is spatially associated with the Fall Zone at Fredericksburg (see discussion in Section 3 below).

Based on these observations, we conclude that the upper surface of the Pliocene Tps unit has not been measurably deformed by cumulative down-to-the-southeast movement along the Fall Hill, Hazel Run, Brooke faults of the Stafford system south-southwest of Fredericksburg, nor by the Unnamed fault. These conclusions are consistent with the observations of Mixon et al. (2000) that post-Pliocene displacements on the Fall Hill and Brooke faults are less than 0.5 m (Section 1), which are too small to be resolved by this method.

Because we are contouring surface elevations of the highest erosional remnants of the Tps unit, rather than a well-defined stratigraphic contact, our maximum uncertainty that the elevations represent an originally contiguous, isochronous datum is equal to the thickness of the Tps unit (i.e., about 60 ft; Mixon et al., 2000). The true uncertainty probably is less than 60 ft, because the maximum relief on the contoured Tps unit in the vicinity of the Rappahannock River (Figure 4) is about 80 ft, which is greater than the stratigraphic thickness of the unit, and thus implies that at least some of the observed relief is either depositional and/or tectonic in origin. Locally, the relief on the Tps unit across the Rappahannock River valley is only about 30 ft (Figure 4). Although we interpret this to be original depositional relief on the top of the Tps unit, it is possible that it represents post depositional (post-Pliocene) erosional relief. If this is correct, then it suggests that the maximum uncertainty that the contoured elevations represent the upper depositional surface of the Tps unit is closer to 30 ft than 60 ft, when evaluating areas comparable in scale to the Rappahannock River valley.

We can use these estimates of uncertainty in the contoured elevations to estimate the resolution of this technique in terms of long-term vertical separation rate. If the maximum uncertainty in the contoured elevations is 60 ft, and if the upper depositional surface of the Tps unit is about 2.5 million years old, then we cannot identify faults with long-term average vertical separation rates of 0.0073 mm/yr or less. For a maximum uncertainty in the contoured elevations of 30 ft, our resolution of long-term average vertical separation rate is 0.0036 mm/yr or less.

2.2 Profile of the Miocene Calvert Formation Across the Dumfries Fault Zone

A profile of the upper surface of the Miocene Calvert Formation was constructed across the Dumfries fault zone, which lies northwest of the other strands of the Stafford system and is not overlain by the Pliocene Tps unit (Section 2.1). The middle and lower Miocene Calvert Formation is a fine-grained marine deposit capping the ridge that forms the interfluve between Potomac Creek and Accokeek Creek, approximately 7 miles north of Fredericksburg (Mixon et al., 2000) (Figure 2A). The Calvert Formation crosses the Dumfries fault zone and extends continuously for about 1 mile to the east and west of the mapped fault trace. The profile in Figure 2B shows the modern topography along the profile, and the projected elevations of the highest surfaces directly adjacent to the profile that are underlain by the Calvert Formation. We assume that these surfaces represent remnants of the original upper depositional surface of the Calvert Formation. The elevations of these high remnants define a surface with a uniform low gradient toward the east (Figure 2B) that is not deflected or offset across the trace of the Dumfries fault zone. We conclude that the profile documents absence of middle Miocene and younger activity on the Dumfries fault zone within the resolution of the topographic data used to construct the profile (estimated to be about + 5 ft).

2.3 Pliocene and Quaternary Terraces of the Rappahannock River

Mixon et al. (2000) mapped the Hazel Run fault and Unnamed fault as underlying Pliocene and Quaternary terraces of the Rappahannock River at Fredericksburg (Figure 1). We constructed topographic profiles of the terraces to document field evaluations presented in SSAR Section 2.5.1.1.4 that the terrace surfaces are not deformed by these faults. To construct the profiles, the geologic mapping of Mixon et al. (2000) was first transferred to a 7.5-minute topographic map (Figure 5). Specific landforms associated with the map units were identified. From oldest to youngest, these terrace units include:

> Tm, Moorings unit (Upper Pliocene): Fluvial terrace deposits of the Rappahannock River (3-9 m thick); altitude of depositional surface ranges from 140 ft to 155 ft (Mixon et al., 2000).
>
> Qcc, Charles City Formation (lower Pleistocene): Fluvial terrace deposits; ranges in altitude from 80 ft to 95 ft in the Fredericksburg area (Mixon et al., 2000).
>
> Qc, Chuckatuck Formation (middle Pleistocene): Fluvial terrace deposits inset well below the base of the Charles City Formation; ranges in altitude from 60 ft to 70 ft (Mixon et al., 2000).
>
> Qtu, Tabb Formation, undivided (upper Pleistocene): Deposits of low fluvial terraces ranging in altitude from 10 to 20 ft; associated with cut-and-fill episodes during Sangamon and post-Sangamon time (Mixon et al., 2000).

The topography in and around Fredericksburg reveals minor non-tectonic relief on some of the terrace surfaces. For example, the Qcc map unit, which is generally at an elevation of 80 ft, includes some higher surface remnants at 90 ft elevation. Similarly, the mapped Qc unit is associated with what appear to be different surfaces at elevations of 60 ft and 70 ft. The surfaces appear to be separated by breaks in topography that generally parallel the Rappahannock River. We speculate that the Qcc and Oc map units of Mixon et al. (2000) include multiple terrace surfaces, with younger terraces inset topographically below older terraces. The interpreted terrace surfaces within the map units of Mixon et al. (2000) are delineated on Figure 5. Note that this interpretation differs in minor detail from the mapping of Mixon et al. (2000) in Figure 1.

A series of topographic profiles were drawn across the landforms associated with the Tm, Qcc and Qc map units (Figures 6 through 9; see Figure 5 for profile locations). We did not profile the Qtu terrace because we observed during field reconnaissance that it floods annually, and thus any scarps are unlikely to be preserved on the surface. The traces of the Unnamed fault and Hazel Run fault were transferred to the profiles based on the mapping of Mixon et al. (2000). As shown on Figures 6 through 9, there are no scarps or anomalous breaks in topography on the terrace surfaces associated with the

mapped fault traces. We conclude that the profiles document the absence of Quaternary vertical offset of the terrace surfaces above the buried traces of the Unnamed fault and the Hazel Run fault, within the resolution of the topographic data on the maps (about ± 5 ft).

Where preserved and topographically well defined, terrace risers between the late Cenozoic terrace surfaces at Fredericksburg constrain horizontal displacements. For example, the riser between the terrace tread of the Qc2 terrace and the tread of the Tm surface extends across the Hazel Run fault at a high angle and is not visibly offset or deflected by lateral movement on the fault (Figure 5). Although the riser itself has been dissected by erosion, the base of the riser, which forms the southwestern edge of the tread of the Qc2 terrace, is a well-preserved, generally linear NW-trending feature that is not deflected across the fault. Similarly, the riser between the Qsh and Qtu terrace treads crosses the Hazel Run fault and is not noticeably deflected or offset. We conclude that these relations document the absence of Quaternary horizontal displacement on the Hazel Run fault, in addition to the absence of vertical offset documented by the topographic profiles (i.e., Figures 6, 8, and 9).

3. Discussion

Although the Tps structure contour map (Figure 4) and profiles of Neogene and Quaternary surfaces document the absence of post-Pliocene movement on the Stafford fault system, the gradient in the Tps surface northwest of the Fall Hill fault suggests that epeirogenic uplift or tilting may have occurred west of the Stafford system. Assuming that the higher gradient in the Tps unit northwest of the Fall Hill fault does not reflect original depositional relief, then the trend of the Tps contours indicates up-to-the-northwest tilting along a NE-SW-trending axis that is approximately coincident with the Fall Zone on the Rappahannock River. These relations are consistent with modest late Cenozoic uplift of the Piedmont relative to the Coastal Plain, accommodated by tilting or flexure along the Fall Zone. The Pliocene Moorings Unit terrace west of Fredericksburg and directly adjacent to the Fall Zone (Figure 6) has a slightly higher eastward gradient than the younger Qcc and Qc terraces (Figures 7 and 8, respectively), which also may be the result of modest late Cenozoic eastward tilting.

This interpretation is consistent with stratigraphic and structural relations along the western margin of the Atlantic Coastal Plain north of Fredericksburg. Pazzaglia and Gardner (1994) presented longitudinal profiles of a well-preserved sequence of fluvial terraces flanking the lower Susquehanna River in Delaware and Maryland that document progressive fluvial incision of the Piedmont since at least middle Miocene. Miocene terraces presently stand about 100 m above the Susquehanna River, suggesting a maximum incision rate of about 0.009 mm/yr (8.7 m/m.y.; Pazzaglia and Gardner, 1994). Correlation of these terraces with stratigraphic contacts in sediments of the Coastal Plain to the east indicates progressive subsidence of the Coastal Plain during the same period of time. The transition between coeval Neogene incision and deposition is centered on the Fall Line (Pazzaglia and Gardner, 1994).

Pazzaglia and Gardner (1994) used a simple numerical model to test the hypothesis that epeirogenic uplift of the Appalachian Piedmont (assumed to drive Neogene incision of the Susquehanna River), and subsidence of the Coastal Plain are isostatic responses of the lithosphere to erosion and sedimentation, respectively. In the model, erosional denudation and sedimentation are treated as unloading and loading of lithosphere in isostatic equilibrium. The response to imposition of these loads is uplift and subsidence, respectively, modified by the elastic flexural strength of the lithosphere. The longitudinal profiles and gradients of deformed surfaces across transitional zones like the Fall Line are sensitive to the elastic parameters of the model.

Pazzaglia and Gardner (1994) found that Neogene to Quaternary erosional relief can be explained by erosionally driven isostatic uplift of the Piedmont and depositionally driven subsidence of the Coastal Plain, provided that: (1) both denudation and sedimentation rates are on the order of about 10 m/m.y.; (2) the elastic thickness of the lithosphere is about 40 km; and (3) the flexural rigidity of the lithosphere is about 4×10^{23} N-m. They note that these values are consistent with estimates of these parameters determined by independent studies. The Fall Zone is reproduced in the models as the hinge between the uplifting and subsiding regions. The main process that drives uplift in the model is isostatic response of the lithosphere to denudation; Pazzaglia and Gardner (1994) note that an elastic "peripheral bulge" effect from depositional loading east of the Fall zone accounts for only 20% of the total uplift 100 km west of the Fall Zone. Similarly, Pazzaglia and Gardner (1994) find that the denudation rate is the controlling factor on uplift rate.

The model of Pazzaglia and Gardner (1994) potentially explains the increased gradient of the Tps unit northwest of the Stafford fault system, and the higher gradient of the Pliocene Tm terrace at Fredericksburg relative to the younger Quaternary terraces. The mechanical process inferred to be driving this deformation is similar to isostatic rebound of the lithosphere following retreat of Pleistocene continental glaciers. The very small displacements (less than 0.5 m) of Pliocene deposits along the Fall Hill and Hazel Run faults near Fredericksburg reported by previous workers may be related to elastic flexure of the lithosphere along the Fall Line, rather than seismogenic faulting.

4. Summary and Conclusions

The data presented in Section 2 of this response support the conclusions in the SSAR of no Quaternary activity on the Stafford fault system. Very small displacements of Pliocene deposits along the Fall Hill and Hazel Run faults previously observed may represent minor adjustments associated with slow, erosionally and depositionally driven flexure of the lithosphere along the Fall Line, as proposed by Pazzaglia and Gardner (1994) for the Susquehanna River area north of Fredericksburg.

References

Mixon, R. B., and W. L. Newell, 1978, The Faulted Coastal Plain Margin at Fredericksburg, Virginia: Tenth Annual Virginia Geology Field Conference, October 1978.

Mixon, R.B., Pavlides, L., Powars, D.S., Froelich, A.J., Weems, R.E., Schindler, J.S., Newell, W.L., Edwards, L.E., and Ward, L.W., 2000, Geologic map of the Fredericksburg 30' x 60' Quadrangle, Virginia and Maryland: United States Geological Survey Geologic Investigations Series Map I-2607.

Pazzaglia, F.J., and Gardner, T.W., 1994, Late Cenozoic flexural deformation of the middle U.S. Atlantic passive margin: Journal of Geophysical Research, v. 99, p. 12,143-12,157.

Application Revision

None.

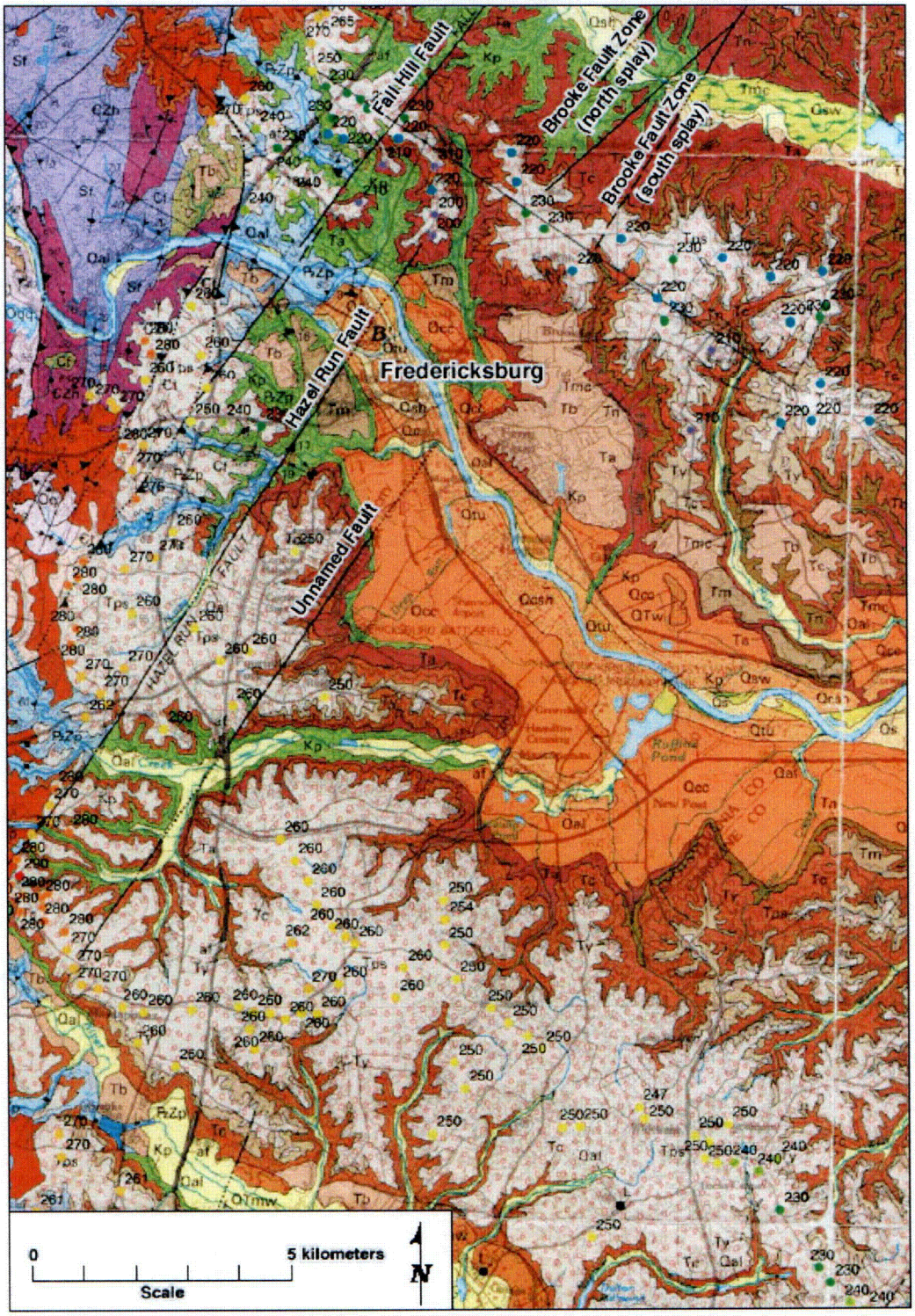

Figure 1. Part of the geologic map of Mixon et al. (2000) near Fredericksburg, Virginia, showing selected elevations of summit surfaces and ridge tops underlain by the Pliocene Tps unit (pinkish colored unit with open-circle pattern). Elevations were picked from 7.5-minute USGS topographic maps and entered into a GIS database, which was subsequently used to develop the contour maps in Figures 3 and 4. See text for details.

C09

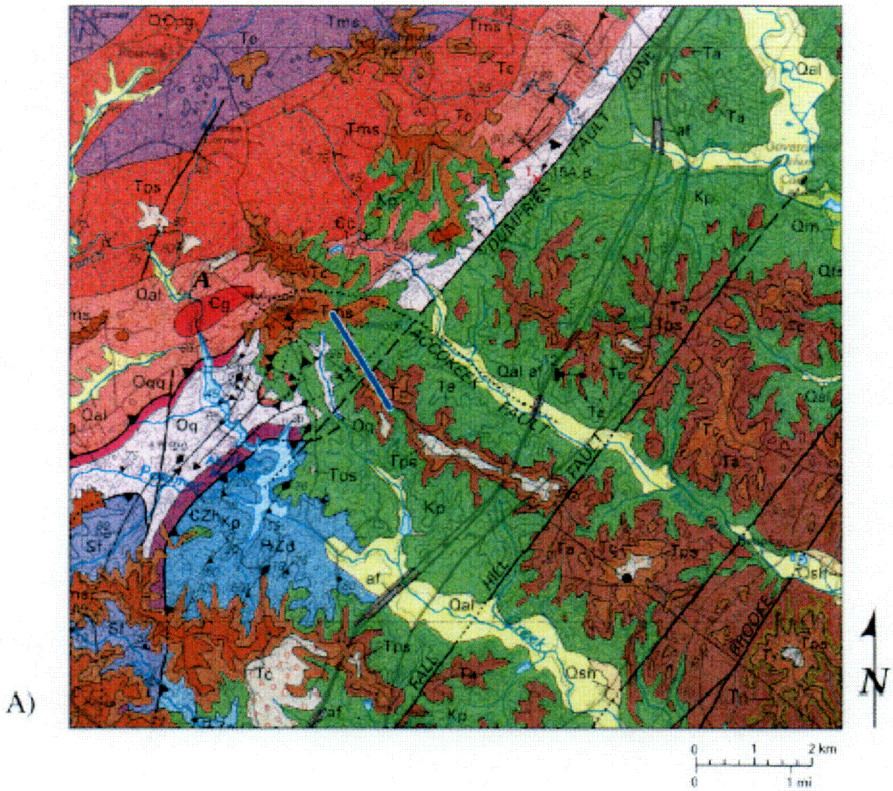

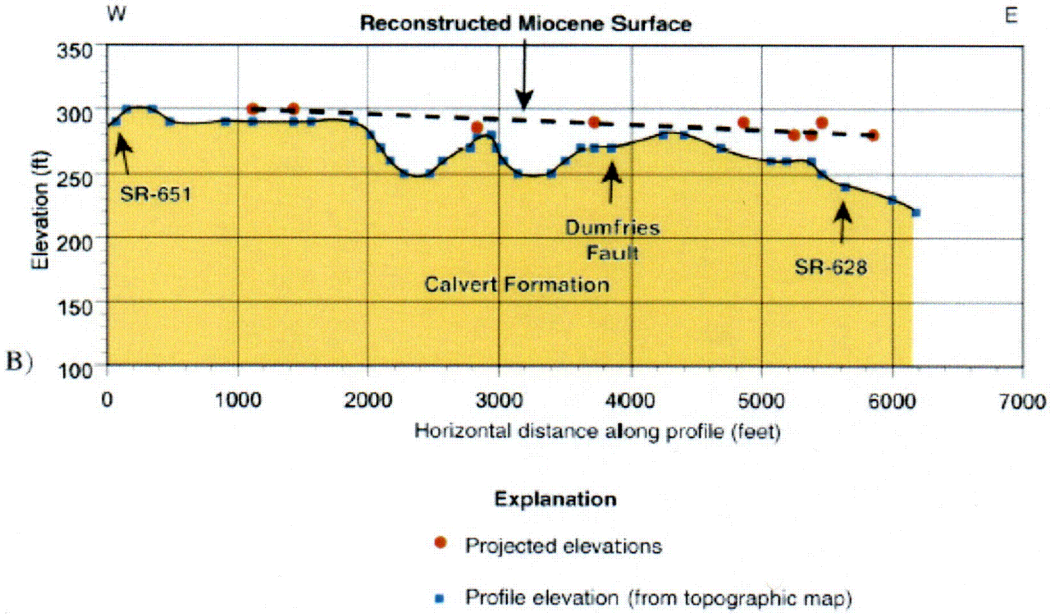

Figure 2. Profile of the Calvert Formation (Tc) across the Dumfries Fault. A) Profile location (blue line) and local geology from Mixon et al. (2000). B) Topographic profile points (blue squares) with elevations of upper summit surface underlain by the Calvert Formation (red dots) projected onto the profile. Dashed line shows reconstructed Miocene surface. Note uniform gradient of reconstructed Miocene surface across the Dumfries Fault.

C10

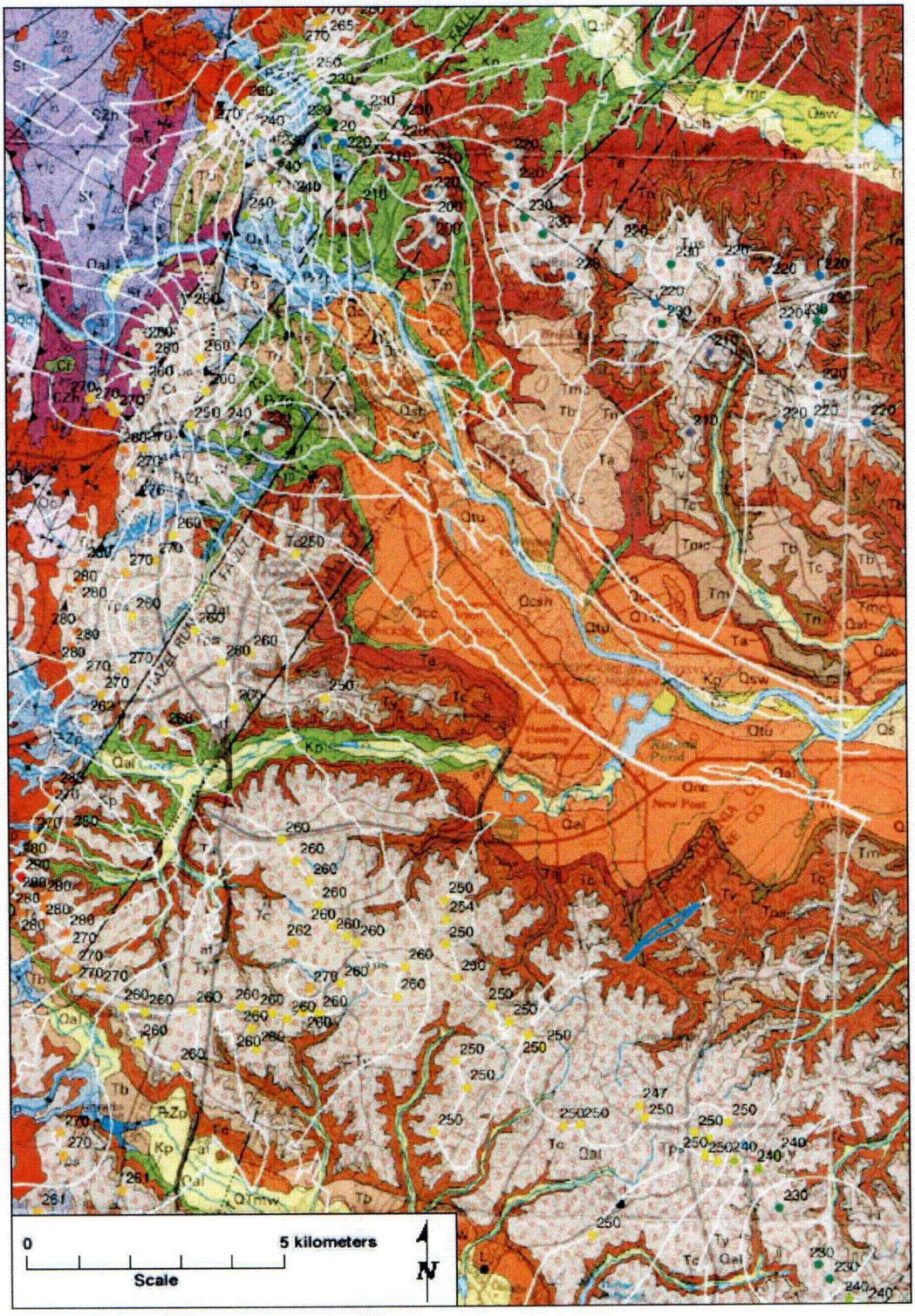

Figure 3. Structure contour map of the upper surface of the Pliocene Tps unit in the vicinity of Fredericksburg, Virginia (geologic base from Mixon et al. 2000). Contours (5 ft interval) were generated by ArcView Spatial Analyst. See text for additional discussion.

C11

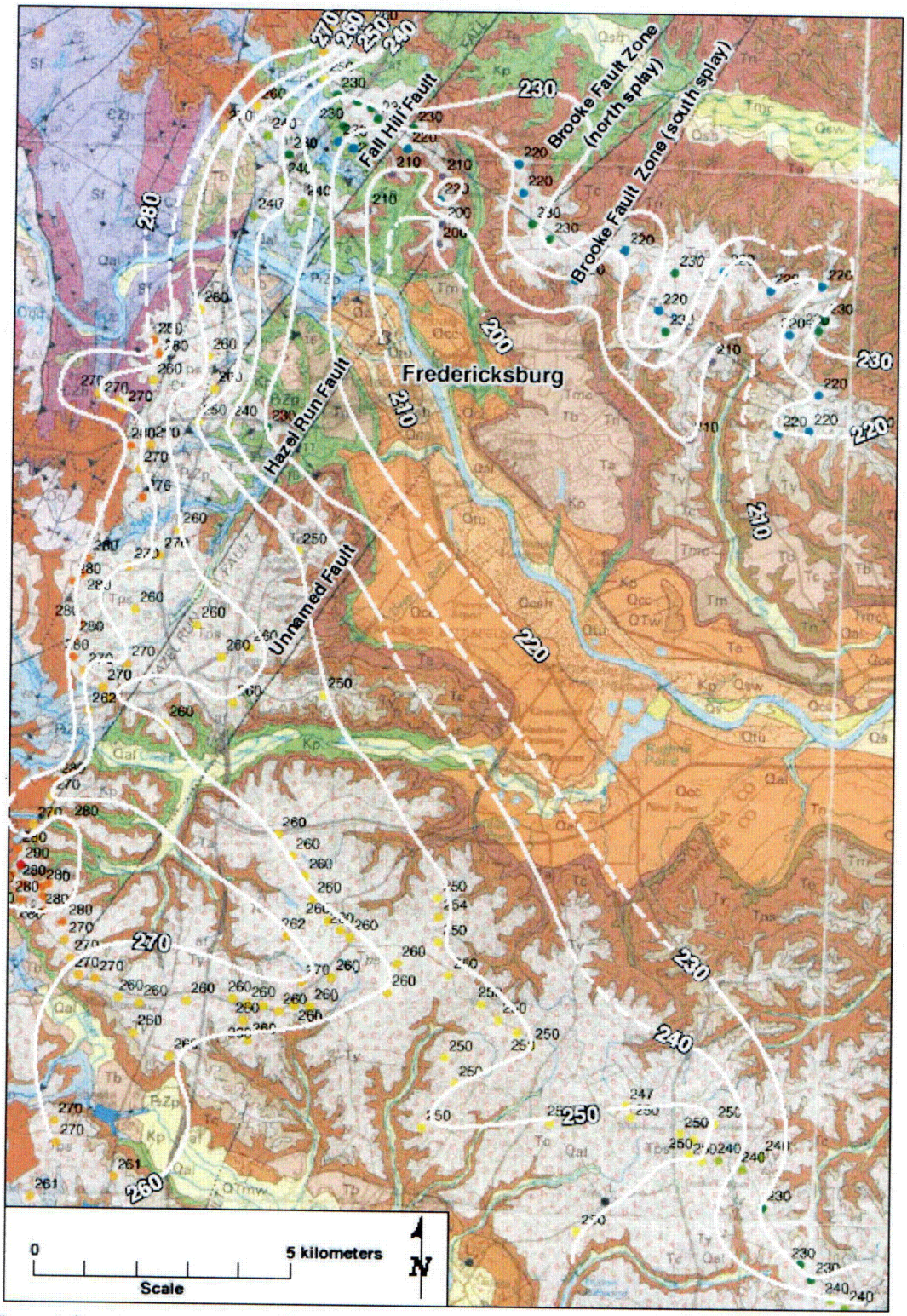

Figure 4. Structure contour map of the upper surface of the Pliocene Tps unit in the vicinity of Fredericksburg, Virginia (geologic base from Mixon et al. 2000). Contours (10 ft interval) were hand-modified from machine-generated contours in Figure 3. See text for additional discussion.

C 12

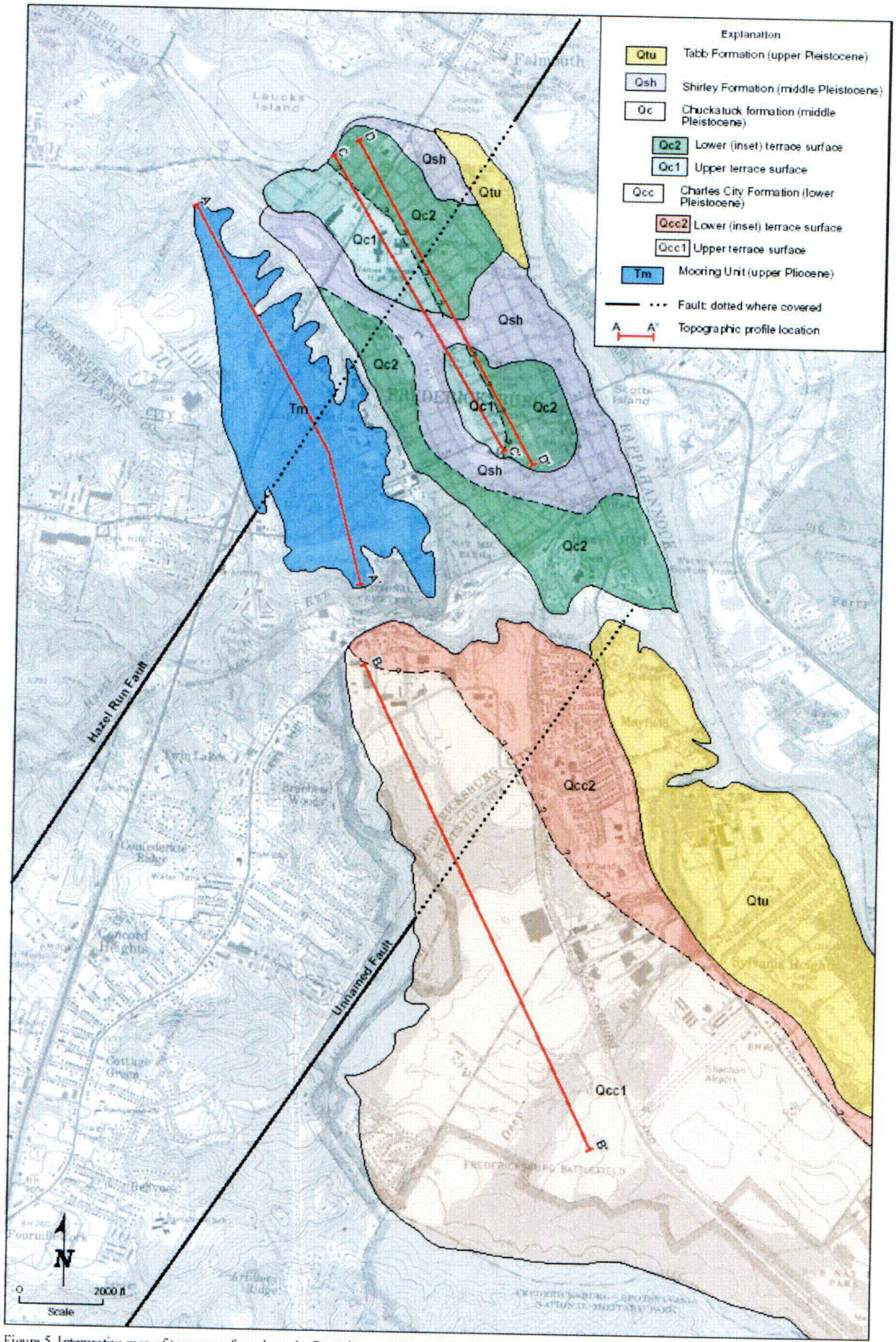

Figure 5. Interpretive map of terrace surface along the Rappahannock River at Fredericksburg, Va. (southwest bank). Geology from Mixon et al. (2000) Fredericksburg quadrangle, modified to reflect interpretation of multiple terrace levels within the Qc and Qcc units (see text for discussion). Red lines show location of topographic profiles (Figures 6 through 9).

C 13

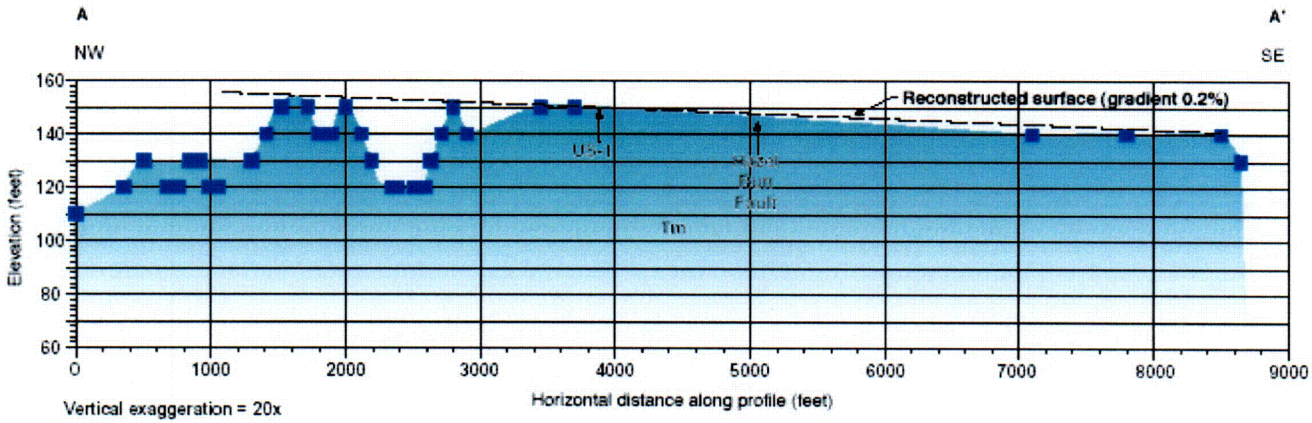

Figure 6. Profile of the surface of the Moorings Unit (Tm). See Figure 5 for location. Blue squares represent points where profile crosses a contour interval on the topographic base map. Geology from Mixon et al. (2000).

C 14

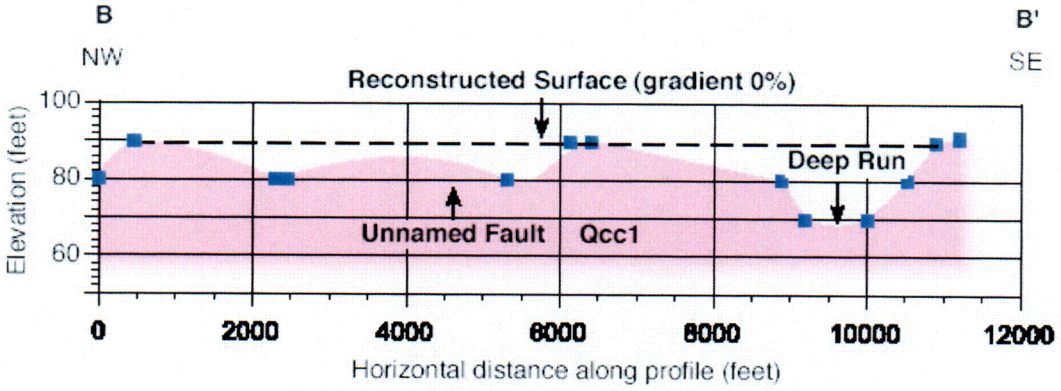

Figure 7. Profile of the surface of the Charles City Formation (Qcc). See Figure 5 for location. Blue squares represent points where profile crosses a contour interval on the topographic base map. Geology from Mixon et al. (2000).

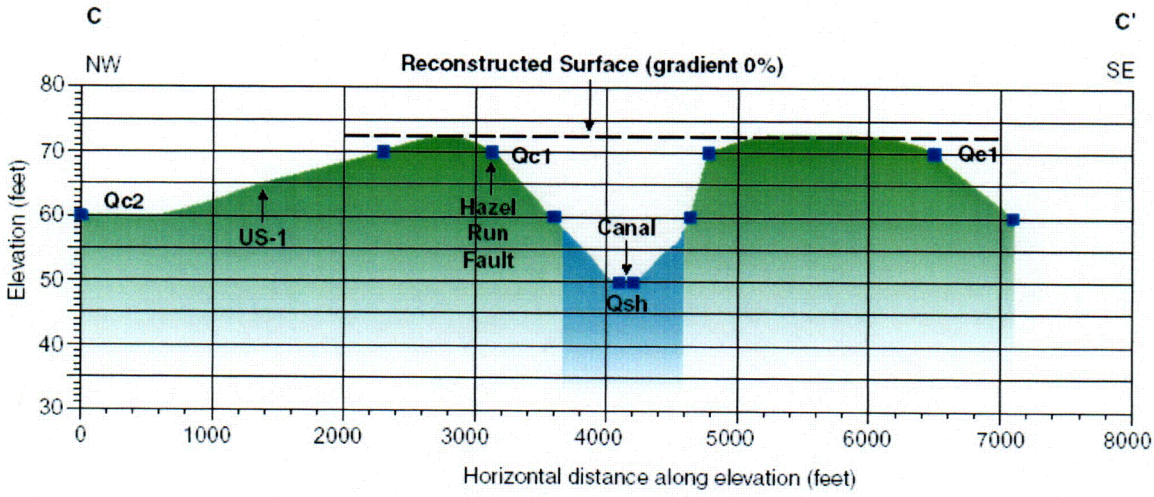

Figure 8. Profile of the surface of the Chuckatuck Formation (Qc). See Figure 5 for location. Blue squares represent points where profile crosses a contour interval on the topographic base map. Geology from Mixon et al. (2000).

C15

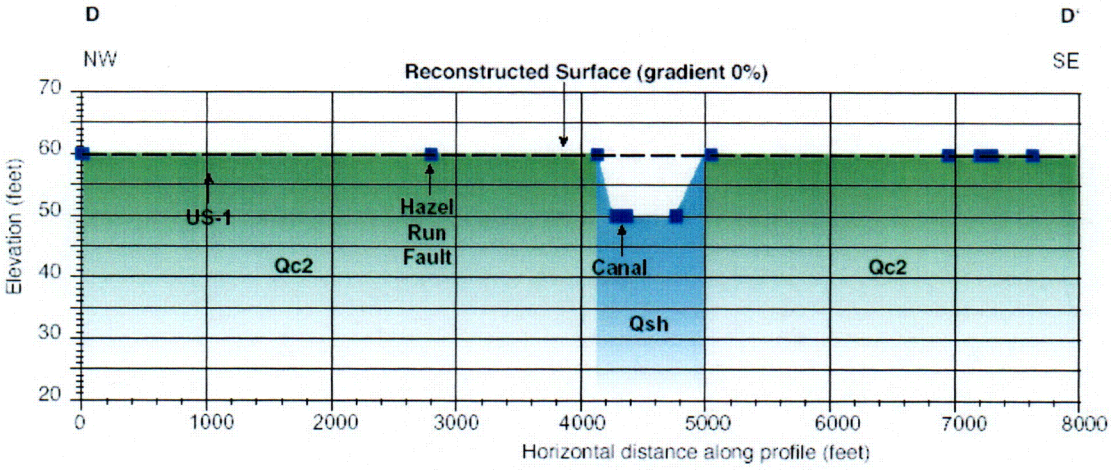

Figure 9. Profile of the surface of the Chuckatuck Formation (Qc). See Figure 5 for location. Blue squares represent points where profile crosses a contour interval on the topographic base map. Geology from Mixon et al. (2000).

C16

RAI 2.5.2-5 (NRC 6/1/04 Letter)

SSAR Subsection 2.5.2.6.3 summarizes the use of new data to revise the recurrence interval and source geometry for the Charleston seismic source zone. Page 2-2-248 of the application states:

> The southern segment of the ECFS [East Coast Fault System] was used as an alternative source geometry for the sensitivity analysis. In this approach, the southern segment was assumed to be active with a characteristic magnitude with a mean recurrence interval of 550 years.

RAI 2.5.2-5 Part a)

a) Please explain the rationale for the designation of the southern segment of the ECFS as an "alternative" source geometry for the Charleston seismic source zone.

Response to Part a)

Marple and Talwani (2000) describe the East Coast fault system (ECFS) as a ~ 600-kilometer long, north-northeast-trending buried fault system in the Coastal Plain extending from South Carolina to Virginia. They divide the ECFS into three segments: the southern, central, and northeast segments. The southern segment is characterized by Marple and Talwani (2000) as having the strongest evidence for existence. They state that the southern segment "traverses the epicentral area of the 1886 Charleston, South Carolina, earthquake and lies west of paleoliquefaction sites along the outer South Carolina Coastal Plain; thus, the fault system could be the source of the Charleston earthquake" (Marple and Talwani (2000), p. 200).

The southern segment is interpreted by Marple and Talwani (1993 and 2000) to be ~ 200 kilometers long, 10- to 15-kilometers wide, and to be characterized by a zone of river anomalies and association with the Woodstock fault. Earlier, Talwani (1982) interpreted the intersection of the north-northeast-trending Woodstock fault and the northwest-trending Ashley River fault as the probable seismogenic source of the 1886 Charleston event. Marple and Talwani (2000) state that "The Woodstock fault, which represents the southern end of the East Coast fault system, is an oblique right-lateral strike-slip fault dipping steeply to the west-northwest."

In preparation of the SSAR, an independent evaluation of the evidence presented by Marple and Talwani (2000) for the northern segment of the ECFS was performed. As concluded in both the SSAR and in the response to RAI 2.5.1-2, the northern segment of the ECFS probably does not exist or has a very low probability of activity if it does exist. If the northern ECFS exists, a very low activity rate is required for this feature to fall below the threshold of geomorphic, geologic, and seismologic detection.

Although we believe that the southern segment of the ECFS also probably does not exist, we did not perform a similar independent evaluation of the evidence presented by Marple and Talwani (2000) for the southern segment of the ECFS. Rather, we performed a sensitivity analysis conservatively assuming that the southern segment may, in fact, exist and be active and that it is the seismogenic source of the Charleston 1886 event. In this sensitivity analysis, we characterize the southern segment of the ECFS as active (with a probability of activity of 1.0) with a characteristic earthquake ranging in maximum magnitude from M6.6 to M7.5 and mean recurrence interval of 550 years (adopted from the USGS characterization of the Charleston source zone, Frankel et al, 2002).

In the sensitivity analysis, the characteristic earthquake is allowed to initiate anywhere along the southern segment of the ECFS. The geometry of the southern segment is a linear source zone that extends north-northeast beyond the northern limit of the areal source zones defined by the EPRI SOG Earth Science Teams for the Charleston source zone. Thus, the geometry of the southern segment of the ECFS represents a new, alternative geometry for the Charleston source zone. The southern segment of the ECFS also was included as an alternative source geometry for the Charleston source zone in the recent 2002 USGS source model (Frankel et al., 2002). Our rationale for including this alternative source geometry in the sensitivity analysis was to evaluate whether or not the southern segment of the ECFS could produce a significant increase to hazard at the North Anna site, and, if so, would require further investigation to better constrain it's probability of existence, probability of activity, maximum magnitude and recurrence rate.

In performing the sensitivity analysis, it is important to note that no changes were made to the EPRI SOG characterization of the Charleston source zone. The hazard calculated from the characteristic earthquake on the southern segment of the ECFS was evaluated independently and additatively to conservatively assess the maximum possible change to hazard at the North Anna ESP site from this newly postulated source. The alternative source geometry of the southern segment of the ECFS was used in the sensitivity analysis as a conservative depiction of the Charleston source zone that would allow the source zone to extend farther to the north and, thereby, closer to the North Anna site. In providing this alternative source geometry we fully characterize the potential hazard to the North Anna site associated with Marple and Talwani's (2000) postulated existence of the southern segment of the ECFS.

RAI 2.5.2-5 Part b)

b) Please provide a logic tree, similar to SSAR Figure 2.5-35, that covers all of the source models for the Charleston seismic source, including the weights for maximum magnitudes and recurrence intervals as well as the probabilities of activity for each of the models.

Response to Part b)

Figure 1 shows a logic tree illustrating how the Charleston seismic source was modeled for seismic hazard sensitivity calculations.

As explained in SSAR Section 2.5.2.2.1, the original EPRI seismic hazard study implemented a screening criterion for each Earth Science Team and each site. For a given team, all sources whose combined hazard was less than 1 percent of the total hazard for that team were not considered to contribute significantly to the hazard for that site and were excluded from the hazard analysis.

For five of the six EPRI Earth Science Teams (Bechtel, Dames & Moore, Law Engineering, Rondout, and Weston Geophysical), the original representation of the Charleston source did not contribute significantly to the seismic hazard at North Anna, as reported in SSAR Tables 2.5-5 through 2.5-9. Thus the original representation of the Charleston source was not used for these teams in the seismic hazard calculations. In the seismic hazard sensitivity calculations for the SSAR, the ECFS-S fault was used for each of these five teams to represent the hazard of a large-magnitude earthquake in the Charleston area. The magnitudes, weights, and recurrence interval used for the ECFS-S fault are shown in SSAR Figure 2.5-35.

For the sixth EPRI Earth Science Team (Woodward-Clyde Consultants, WCC), two alternative original representations of the Charleston source did contribute significantly to the seismic hazard at North Anna, as reported in SSAR Table 2.5-10. Therefore WCC sources 29 and 29A were included in the seismic hazard sensitivity calculations for North Anna. Weights for maximum magnitudes m_{max} (on the m_b scale), recurrence intervals, and probabilities of activity for these two sources are shown in the Table 1. For this table, the recurrence interval of each m_{max} value was calculated assuming that the largest value of m_{max} applied.

For the Woodward-Clyde team, in addition to these sources 29 and 29A, the ECFS-S fault was added to the WCC source model to represent the hazard of a large-magnitude earthquake in the Charleston area with a recurrence interval of 550 years. The magnitudes, weights, and recurrence interval used for the ECFS-S fault are shown in SSAR Figure 2.5-35.

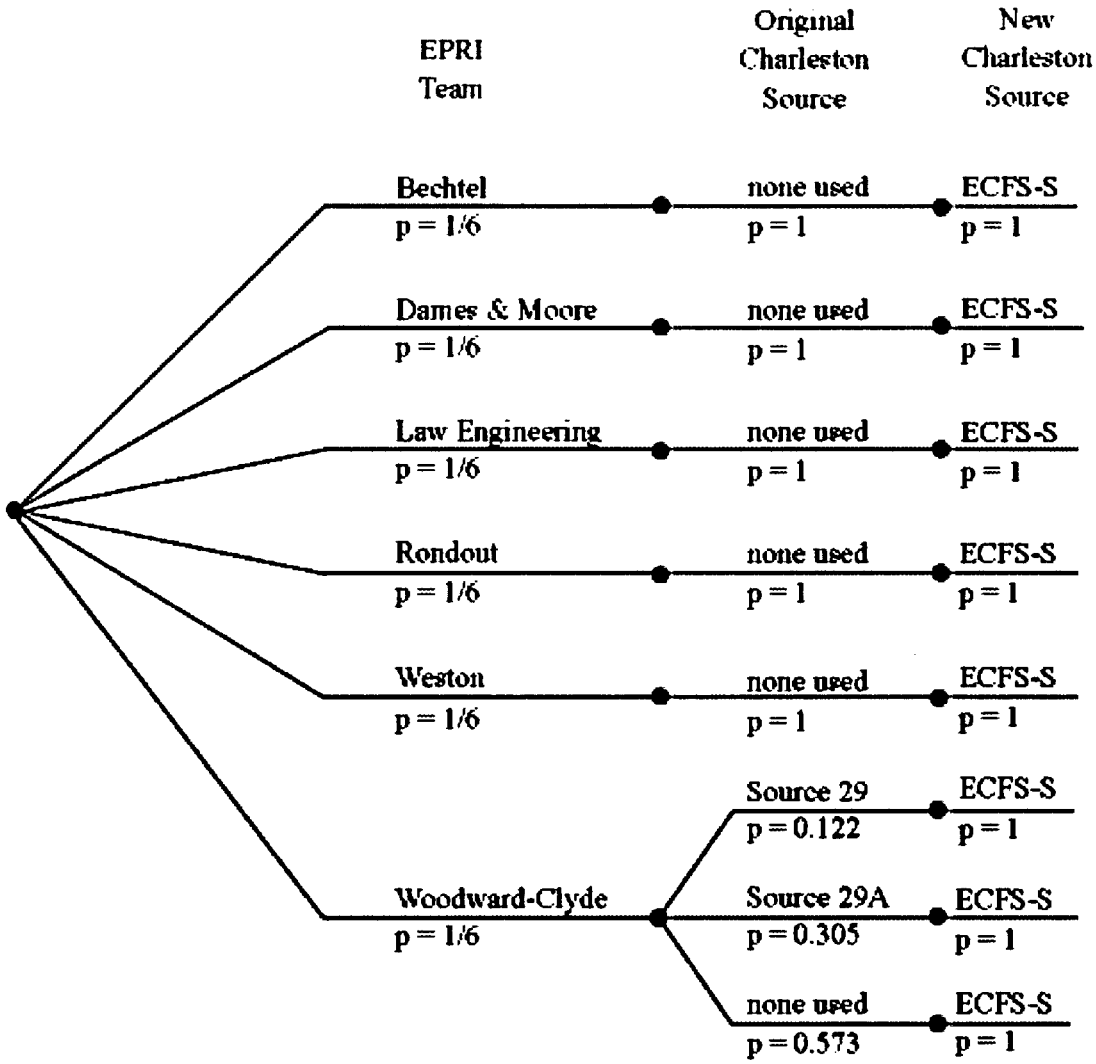

Figure 1. Logic tree for sources used to represent Charleston area earthquakes.

Table 1. Parameters and weights for Woodward-Clyde Sources 29 and 29A

WCC source	Prob. activity	m_{max}	wt. on m_{max}	Recur. interval, yrs
Source 29	0.122	6.7	0.33	2,119
		7.0	0.34	5,349
		7.4	0.33	∞
Source 29A	0.305	6.7	0.33	3,241
		7.0	0.34	8,181
		7.4	0.33	∞

References

Frankel, A. D., M. D. Petersen, C. S. Mueller, K. M. Haller, R. L. Wheeler, E. V. Leyendecker, R. L. Wesson, S. C. Harmsen, C. H. Cramer, D. M. Perkins, and K. S. Rukstales. Documentation for the 2002 Update of the National Seismic Hazard Maps, U.S. Geological Survey Open-File Report 02-420, 2002, (Reference 127 of SSAR Section 2.5).

Marple, R.T., and Talwani, P., 2000, Evidence for a buried fault system in the Coastal Plain of the Carolinas and Virginia-implications for neotectonics in the southeastern United States: Geological Society of America Bulletin, v. 112, p. 200-220, (Reference 74 of SSAR Section 2.5).

Talwani, P., 1982, An internally consistent pattern of seismicity near Charleston, South Carolina: Geology, v. 10, pp. 655-658

Application Revision

None.

RAI 2.5.2-6 (NRC 6/1/04 Letter)

SSAR Figures 2.5-44 and 2.5-45 provide mean and median hazard curves for 1 Hz and 10 Hz spectral acceleration. Please provide the 15th and 85th percentile hazard curves for both 1 and 10 Hz spectral acceleration. In addition, please provide the mean, median, 15th, and 85th percentile hazard curves for both 2.5 and 5 Hz spectral acceleration.

Response

The mean, median, 15th, and 85th percentile hazard curves for 1 Hz, 2.5 Hz, 5 Hz, and 10 Hz spectral acceleration are shown in Figures 1 through 4, respectively. (Figures are located at the end of this RAI response.) Note that SSAR Figures 2.5-44 and 2.5-45 compare seismic hazard with the 1989 and 2003 EPRI ground motion equations without the inclusion of seismic hazard from the ECFS-S fault, whereas Figures 1 through 4 include seismic hazard from the ECFS-S fault. The median 1 Hz curve in Figure 1 matches the "Original+ECFS-S, median" hazard curve in SSAR Figure 2.5-40. The mean 1 Hz curve in Figure 1 matches the "Original+ECFS-S, mean" hazard curve in SSAR Figure 2.5-41. The median 10 Hz curve in Figure 4 matches the "Original+ECFS-S, median" hazard curve in SSAR Figure 2.5-42. The mean 10 Hz curve in Figure 4 matches the "Original+ECFS-S, mean" hazard curve in SSAR Figure 2.5-43.

Application Revision

None.

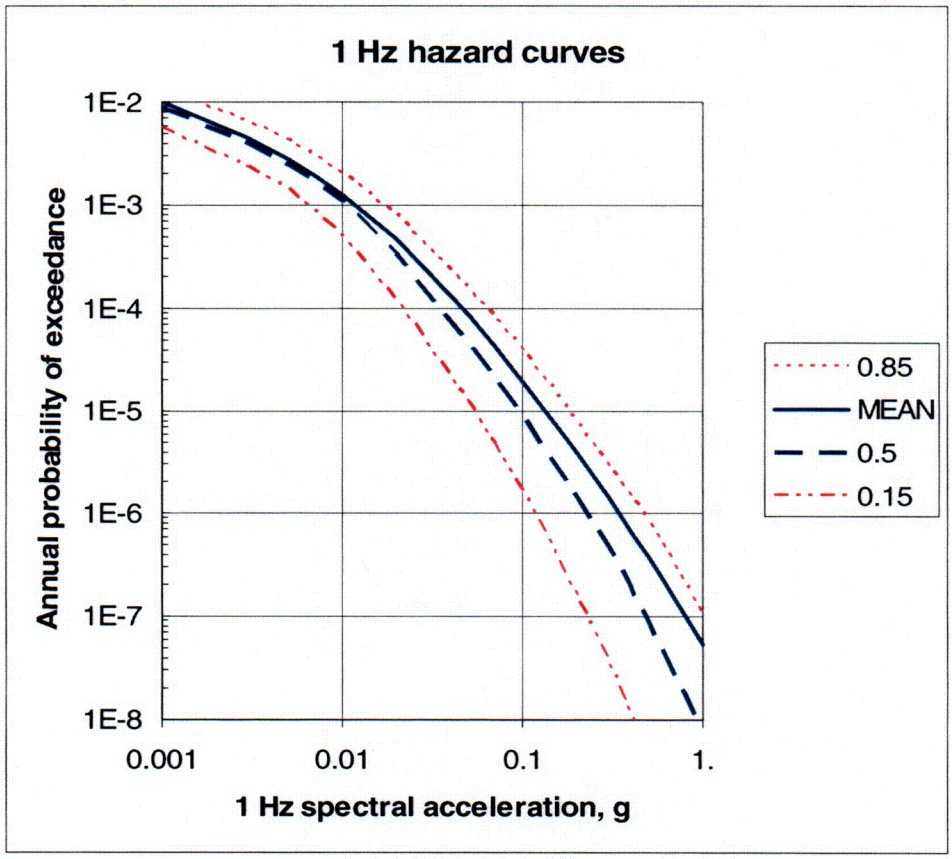

Figure 1. Hazard curves for 1 Hz spectral acceleration.

C17

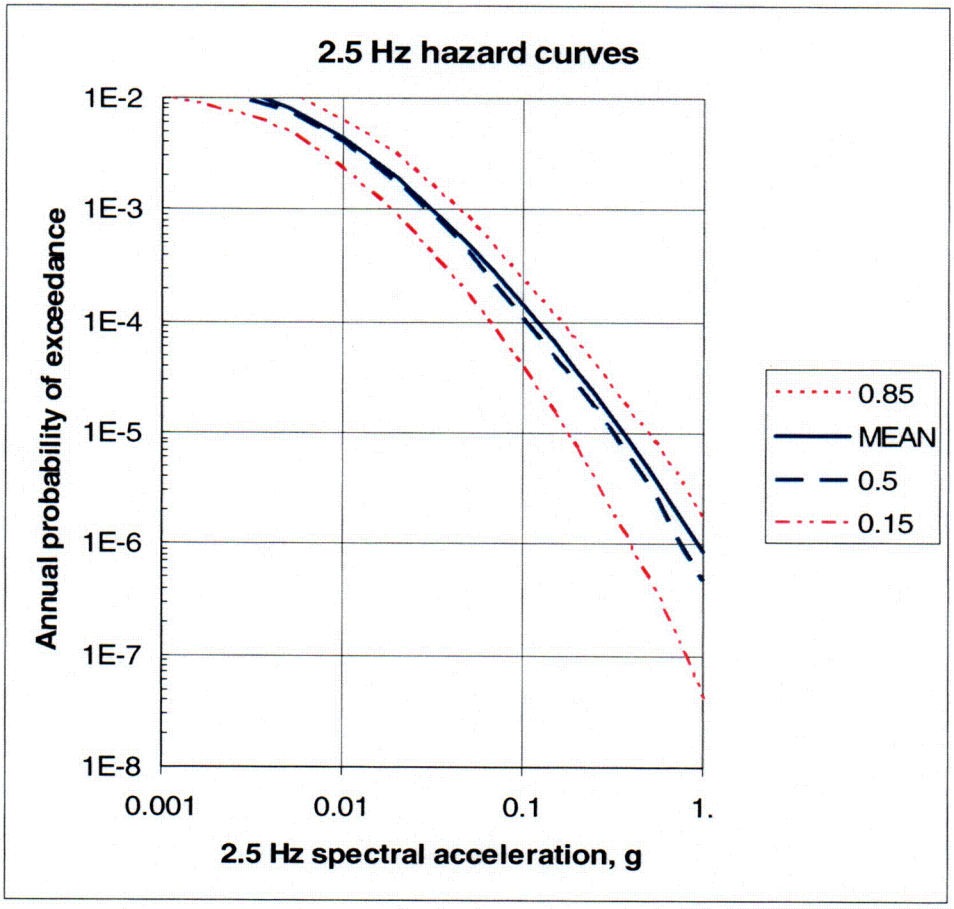

Figure 2. Hazard curves for 2.5 Hz spectral acceleration.

C18

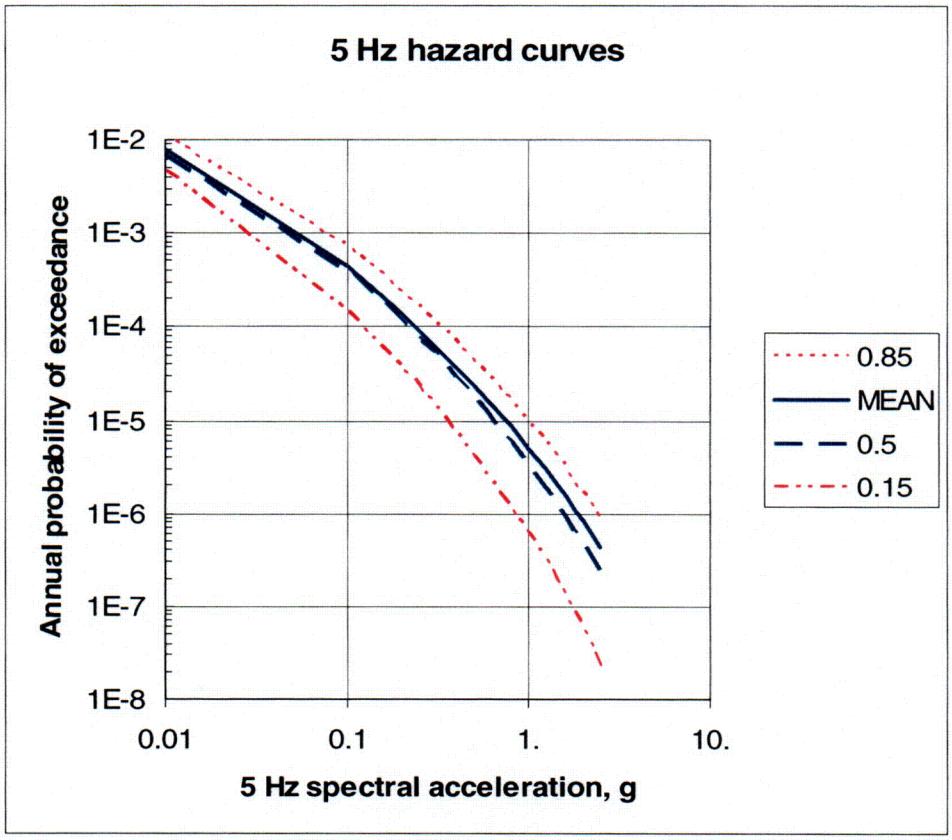

Figure 3. Hazard curves for 5 Hz spectral acceleration.

C19

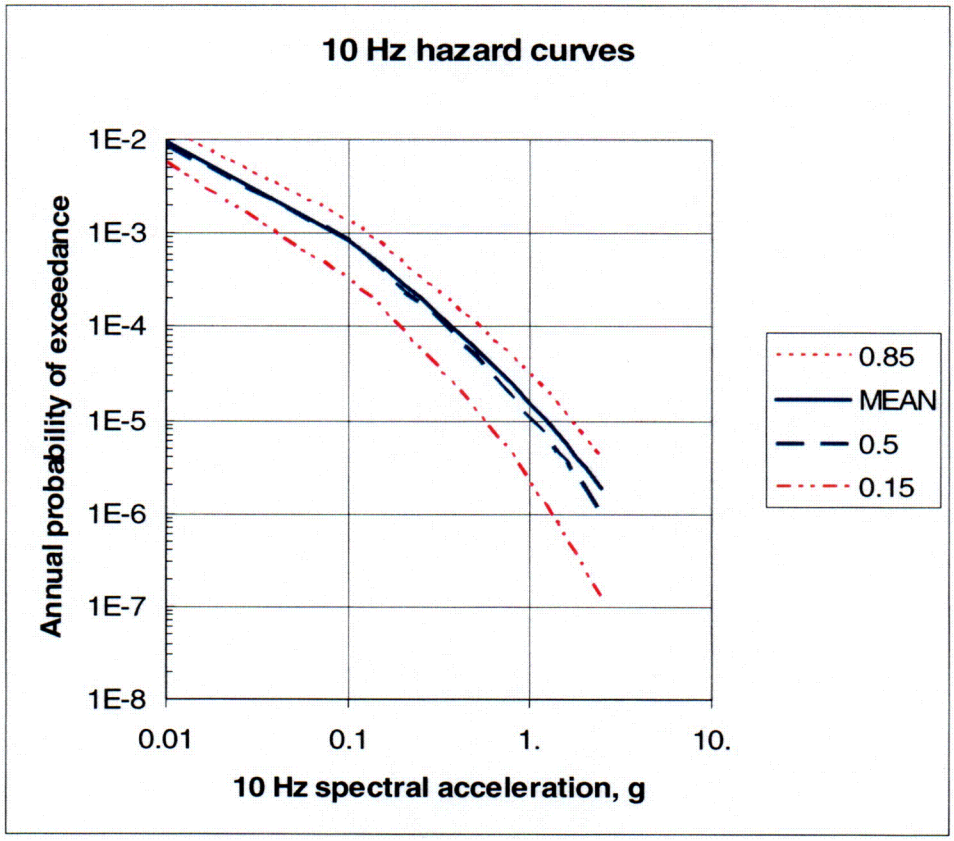

Figure 4. Hazard curves for 10 Hz spectral acceleration.

C20

RAI 2.5.2-7 (NRC 6/1/04 Letter)

Table 2.5-11 in SSAR Section 2.5.2 shows that several of the Electric Power Research Institute (EPRI) teams used a probability of activity less than 1.0 for the Central Virginia Seismic Zone (CVSZ). For each of the EPRI teams, please describe how the modern and historical seismicity of the CVSZ is distributed among either a specific source zone or a background source zone.

Response

The six EPRI teams modeled the CVSZ as described below.

Bechtel team. The Bechtel team defined source E to represent the CVSZ and assigned it a probability of activity (P_a) of 0.35. For the scenario when source E is not active (with probability 0.65), background source BZ5 represents seismicity in the central Virginia region and adjacent areas of the eastern U.S. Following the EPRI methodology, the Bechtel team used three smoothing options to estimate seismicity parameters for source BZ5. (In the EPRI project, "low smoothing" meant that seismicity rates were estimated in a degree cell using only the historical seismicity in that degree cell, with slight averaging with adjacent cells. "High smoothing" meant that seismicity rates were estimated in a degree cell by averaging with *all* degree cells in that source.) Two of Bechtel's smoothing options (with weight 2/3) assumed low spatial smoothing on the seismicity rate. This low spatial smoothing captured the high historical seismicity in the CVSZ, relative to other parts of source BZ5. The third smoothing option (with weight 1/3) assumed a constant seismicity rate throughout source BZ5.

Dames and Moore team. The Dames and Moore team defined source 40 to represent the CVSZ, and assigned this source P_a=1.0.

Law Engineering team. The Law Engineering team did not delineate a source representing the CVSZ, but defined sources representing mafic plutons in the CVSZ area (sources M19 through M24). The seismicity parameters of these pluton sources were calculated from seismicity in a one-degree region around each source, assigning 70% of this seismicity to the pluton sources and the remaining 30% seismicity to a large regional source. The mafic pluton sources were assigned P_a=0.43. For the scenario when the mafic pluton sources were not active (with probability 0.57), seismicity in the central Virginia region was assigned to an Eastern Piedmont background source (source 107), to an Eastern Basement source (source 17), and to an Eastern Basement background source (source 217). Each of these three sources used a high spatial smoothing assumption to calculate activity rates for degree cells within the seismic source.

Rondout team. The Rondout team defined source 29 to represent the CVSZ, and assigned this source P_a=1.0.

Weston Geophysical team. The Weston Geophysical team defined source 22 to represent the CVSZ and assigned it a probability of activity (P_a) of 0.82. For the scenario when source 22 is not active (with probability 0.18), background source 104 was used to represent seismicity in the CVSZ region. Various configurations of background source 104 were used, depending on other regional sources that were active, and the seismicity rates for degree cells in these configurations of background source 104 were generally estimated using a constant spatial rate assumption.

Woodward-Clyde team. The Woodward-Clyde team defined three sources to represent seismicity in the central Virginia region: source 26 (the Central Virginia Gravity Saddle, P_a=0.434), source 27 (the State Farm Complex, P_a=0.474), and source 28 (the Richmond Basin, P_a=0.092). The last of these is a small source that contributed less than 1% of the total hazard for the 1989 EPRI study, and therefore was not included in the EPRI hazard calculations or in those for the North Anna ESP. For the scenario when sources 26 and 27 were not active (with probability 0.092), a local background source represented local seismicity in the central Virginia region. This local background source used low spatial smoothing on the seismicity rate, thereby retaining the concentration of historical seismicity in the CVSZ.

Application Revision

None.

RAI 2.5.2-8 (NRC 6/1/04 Letter)

SSAR Subsection 2.5.2.5 provides a list of the subsurface materials at the ESP site. Please describe how these site-specific materials were factored into the determination of the SSE ground motion spectrum. Please describe the subsurface model in terms of layer thicknesses and engineering properties (e.g., density, shear wave velocity, damping ratio) and describe how the variability of each of these properties was accounted for in the site characterization of the ground motion.

Response

The SSE spectrum is calculated using the EPRI 2003 ground motion models. For the North Anna ESP site, the selected SSE directly incorporates the hard rock foundation assumption of the EPRI 2003 ground motion models (a shear-wave velocity of 2.8 km/s or about 9,200 ft/s). The containment (reactor) building and primary supporting safety-related structures would be founded on sound bedrock, either Zone IV or Zone III-IV materials (see SSAR Section 2.5.2.5) for which this shear-wave velocity is a good approximation. Therefore, site-specific materials are factored into the determination of the SSE by recognizing that the hazard analysis performed to develop the SSE uses attenuation relations that are directly applicable to specific subsurface conditions at the North Anna site.

Some safety-related structures (for example, the diesel generator building) may be founded on Zone III weathered rock, Zone IIB saprolite, or improved Zone IIA saprolite. No safety-related structures would be founded on unimproved Zone IIA or Zone I material. (See also response to RAI 2.5.4-11).

Characterization of site-specific subsurface materials (including definition of the zones) is detailed in SSAR Section 2.5.4.2.2. If the final plant layout requires that SSE ground motions be calculated for foundation conditions other than hard rock, these SSE ground motions will be developed to take into account these site-specific conditions. For example, USNRC NUREG/CR-6728 recommends methods for developing ground motion spectra on soil that are consistent (in terms of seismic hazard) with spectra on rock. This is appropriate at the COL stage when the final plant layout has been determined and site-specific materials above the parent bedrock have been characterized.

Application Revision

None.

RAI 2.5.3-2 (NRC 6/1/04 Letter)

SSAR Subsection 2.5.3.2.2 states that aerial reconnaissance, field reconnaissance, and air photo interpretation did not reveal evidence for the southwestward continuation of unnamed fault "a" beyond the ESP site as mapped by Pavlides (Reference 36), which was compiled onto the map of Mixon and others (Reference 66). Please provide support for this conclusion by describing (1) the map relations shown by Pavlides and Mixon and others that implied the extension of unnamed fault "a" beyond the ESP site, (2) the field observations that raise questions about the map relations, and (3) information on the adjacent geologic sheet, suggested as an alternative interpretation, that does not call for the extension of unnamed fault "a" beyond the ESP site.

Response

1. Map Relations That Imply Extension of Unnamed Fault "a" Beyond the ESP Site

Fault "a" is the unnamed bedrock fault identified in 1973 during the foundation excavation for abandoned units 3 and 4 at the North Anna site. The fault was mapped by Dames and Moore (1973) for a distance of about 3000 feet in the site vicinity based on their field mapping and correlation of the fault in foundation excavations and three trenches. The fault was not observed in the foundation excavations for existing units 1 and 2 directly along projection to the northeast, thus limiting its mapped extent to the northeast at that time. Subsequent to the Dames and Moore (1973) investigation, Pavlides (1989, 1990, 1994, and 1995) mapped the fault for a total distance of about 7 miles, extending about 2 miles to the northeast and about 5 miles to the southwest of the site (Figure 1). Pavlides does not provide an explanation or basis for mapping the fault other than the observed stratigraphic and structural relationships shown on his maps. This mapped location of the fault was then compiled onto the Fredericksburg 30' x 60' Quadrangle by Mixon and others (2000) (Figures 1 and 2).

As shown on Figure 2, fault "a" is mapped within the Cambrian Ta River metamorphic suite near the site. Pavlides does not map any offset stratigraphic contacts in the Lake Anna area to support the mapped location of the fault. To the southwest, Pavlides interprets the fault to cross the contact between the Ta River metamorphic suite and the Carboniferous Falmouth intrusive suite and between the Falmouth intrusive suite and the Ordovician Quantico Formation. On all four Pavlides maps (1989, 1990, 1994, and 1995), these contacts are not shown to be offset. However, on the compilation map by Mixon et al. (2000), these contacts are shown to be offset in a right lateral sense. Under close inspection of the original mapping by Pavlides (1980, 1990) compared to the compilation map by Mixon et al (2000), the apparent offsets in the stratigraphic contacts shown by Mixon et al (2000) appear to be a compilation error. The apparent offsets shown on the Mixon et al (2000) map are within the line weight of the contacts shown on the Pavlides (1990) map. In addition, the apparent right lateral offset of the Falmouth intrusive suite is opposite to the sense of movement as shown for other faults

with a similar northeast trend in the region, such as the Sturgeon Creek fault directly to the west (Figure 2). Unfortunately, Pavlides is deceased and the basis for his mapping of fault "a" and whether or not the margin of the Falmouth intrusive contact is displaced is not known. Neither Pavlides (1980, 1990) or Mixon et al (2000) describe fault "a" or any stratigraphic, structural, or geomorphic evidence that would support the existence of fault "a" other than the possible offset contacts noted above.

2. Field Observations That Raise Questions About the Map Relations

During preparation of the SSAR, we performed aerial reconnaissance, field reconnaissance and air photo interpretation of fault "a" (described in the response to RAI 2.5.3-1). Based on these studies, we did not observe any stratigraphic, structural or geomorphic evidence that would support the existence of fault "a" beyond the mapped extent of the fault at the site shown by Dames and Moore (1973). There are no scarps, tonal lineaments, topographic lineaments, vegetation lineaments, or springs along the mapped fault trace. Fault "a" appears to be a minor bedrock shear within the Ta River metamorphic suite. In the site investigations described by Dames and Moore (1973), the expression of fault "a" changes significantly across the site between trenches 1 and 2 and trench 3, suggesting that the small minor fault likely dies out along strike. It is very unlikely that such a minor fault or bedrock shear could be recognized or mapped over a significant distance without a significant number of exposures. The Ta River metamorphic suite contains interbedded quartzite veins as mapped by Marr (2002) on the Richmond quadrangle to the south (Figure 2) and likely contains numerous small, minor bedrock faults and shears, such as fault "a" exposed at the site.

Based on field reconnaissance and air photo interpretation, fault "a" as mapped by Pavlides (1990) and Mixon et al (2000) traverses an area that is nearly devoid of any exposures of bedrock or weathered bedrock (i.e., saprolite). Based on the absence of exposures, it is impossible to confirm the presence or absence of a fault in this terrain. In one of the few road cut exposures along the mapped fault trace, at Centreville southwest of the site (Figure 1), there is no evidence of a fault zone within weathered bedrock (i.e., saprolite) across the fault trace.

Based on our field reconnaissance, a Miocene pediment surface with a veneer of gravel is preserved in the site area. The pediment surface may be a former marine abrasion platform cut across bedrock in the site area. Remnants of this Miocene surface are preserved locally on many of the hilltops and ridge tops in the site area, but have only been mapped by Mixon et al (2000) to the east where the deposits are more extensive and laterally continuous. Although we did not map these Miocene surface remnants in detail across the site area, there is no observed geomorphic expression of fault "a" across this surface where preserved, and there is no apparent vertical separation of the Miocene surface across the fault trace as it is mapped by Mixon et al (2000).

Mapping of bedrock geology is difficult in saprolitic terrain with very few exposures. Bedrock float in the site area is composed primarily of quartz rich stringers that appear

to form the only natural outcrops within the site. The quartz-rich stringers weather much more slowly than the more mafic-rich metamorphic rocks. No macroscopic differences were observed between quartz-rich float collected from areas mapped by Pavlides as the Falmouth intrusive suite and the Ta River metamorphic suite. Based on our field reconnaissance, we cannot distinguish between the Ta River metamorphic suite and the Falmouth intrusive suite, certainly not to the resolution required to map an offset of the intrusive contact along fault "a". Similarly, there are no exposures of the contact between the Falmouth intrusive suite and the Quantico Formation in the area of fault "a". Mapping between these two units is based on float within the saprolitic soil and on sparse road cut and natural exposures. The resolution of this mapping is not sufficient to identify the minor offset of the stratigraphic contact as shown by Mixon et al (2000).

3. Information on Adjacent Geologic Sheet That Does Not Call for the Extension of Unnamed Fault "a" Beyond the ESP site

The map contact between the Fredericksburg quadrangle mapped by Mixon et al (2000) and the Richmond quadrangle mapped by Marr (2002) occurs directly south of the southern end of the mapped location of fault "a" (Figure 2). Mixon et al (2000) show fault "a" terminating southward within the Quantico formation. Marr (2002) does not show a corresponding fault along the southwestern projection of fault "a". In addition, several other features mapped at the southern edge of the Fredericksburg quadrangle by Mixon et al (2000), such as the Falmouth intrusive suite and the Sturgeon Creek fault, are not shown on the adjacent Richmond sheet (Marr, 2002). Marr published his map after Pavlides (1980, 1990) and Mixon et al (2000) published their maps of the Fredericksburg quadrangle and, therefore, had the opportunity to verify and include these features on his map, but he did not. Based on our field reconnaissance and air photo interpretation, we concur with Marr (2002) that the Ta River metamorphic suite contains lenses of quartzite within the more mafic metamorphic rock, as opposed to the recognition and differentiation of distinct intrusive complexes as shown by Pavlides (1990) and Mixon et al. (2000). If the interpretation of the Ta River metamorphic suite by Marr is correct, then the existence and offset of the Falmouth intrusive complex along fault "a" as shown by Pavlides (1990) and Mixon et al (2000) is not correct.

4. Summary

The existence of fault "a" as shown by Mixon et al (2000) cannot be confirmed based on air photo interpretation or field reconnaissance. There are no stratigraphic, structural or geomorphic features along the fault trace that would suggest the presence of a fault. As shown by Mixon et al (2000), fault "a" is interpreted to offset the margin of the Falmouth intrusive suite southwest of the site (Figure 2). However, subsequent bedrock mapping by Marr (2002) on the adjacent Richmond quadrangle does not show the existence of the Falmouth intrusive suite, and thus calls into question the apparent offset of this unit by fault "a". In our opinion, fault "a" is a minor bedrock fault or shear that was identified in the foundation excavation for abandoned units 3 and 4 at the North Anna site, and that likely does not have significant lateral continuity either to the northeast or to the

southwest from the site. Geologic investigation of the fault by Dames and Moore (1973) documents the absence of Quaternary activity on the fault. Dames and Moore (1973) map the fault extending for a distance of about 3000 feet, but even within this distance the fault changes expression within bedrock and its lateral continuity is not certain.

References

Dames and Moore, 1973, Supplemental geologic data, North Anna Power Station, Proposed units 3 and 4, Louisa County, Virginia, Virginia Electric Power Company Report.

Marr, J. D., Jr., 2002, Geologic map of the western portion of the Richmond 30 x 60 Minute Quadrangle, Virginia, Virginia Division of Mineral Resources, Publication 165.

Mixon, R.B., L. Pavlides, D.S. Powars, A.J. Froelich, R.E. Weems, J.S. Schindler, W.L. Newell, L.E. Edwards, and L.W. Ward, 2000, Geologic map of the Fredericksburg 30' x 60' quadrangle, Virginia and Maryland, U.S. Geological Survey, Geologic Investigations Series Map I-2607.

Pavlides, L., 1989, Early Paleozoic composite mélange terrane, central Appalachian Piedmont, Virginia and Maryland; Its origin and tectonic history; Geological Society of America, Special Paper 228.

Pavlides, L., 1990, Geology of part of the northern Virginia Piedmont, U.S. Geological Survey Open-File Report 90-548, 1:100,000 scale.

Pavlides, L., 1994, Early Paleozoic alkalic and calc-alkalic plutonism and associated contact metamorphism, central Virginia Piedmont; U. S. Geological Survey Professional Paper 1529.

Pavlides, L., 1995, Piedmont geology of the Stafford, Storck, Salem Church, and Fredericksburg Quadrangles, Stafford, Fauquier and Spotsylvania Counties, Virginia; U. S. Geological Survey Open-File Report 577.

Application Revision

None.

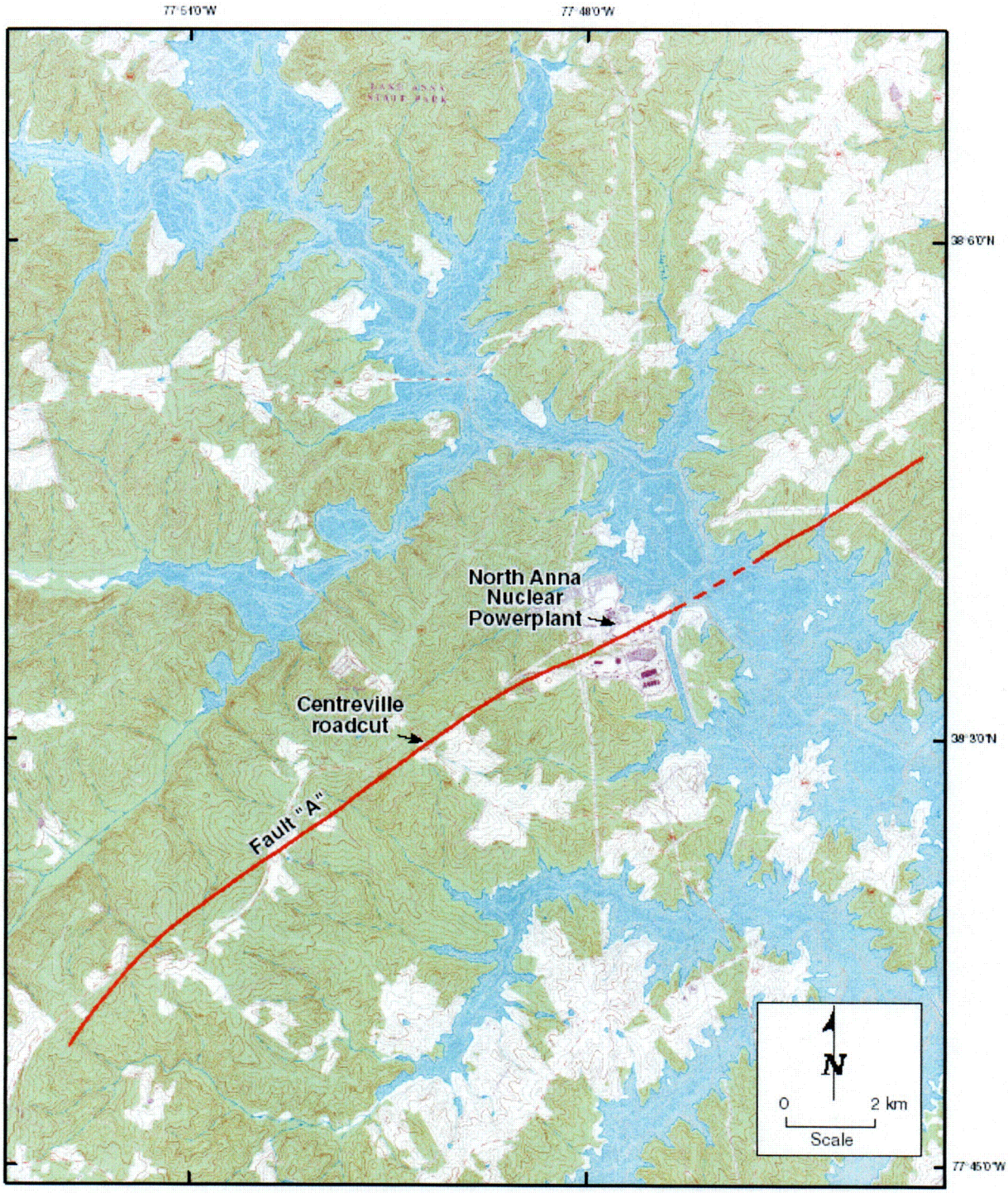

Figure 1. Topographic map of the site location with Fault "A" as located by Mixon et al. 2000. Lake Anna West 7.5-minute USGS quadrangle base map reduced to 1:60,000 scale, contour interval is 10 feet.

C 21

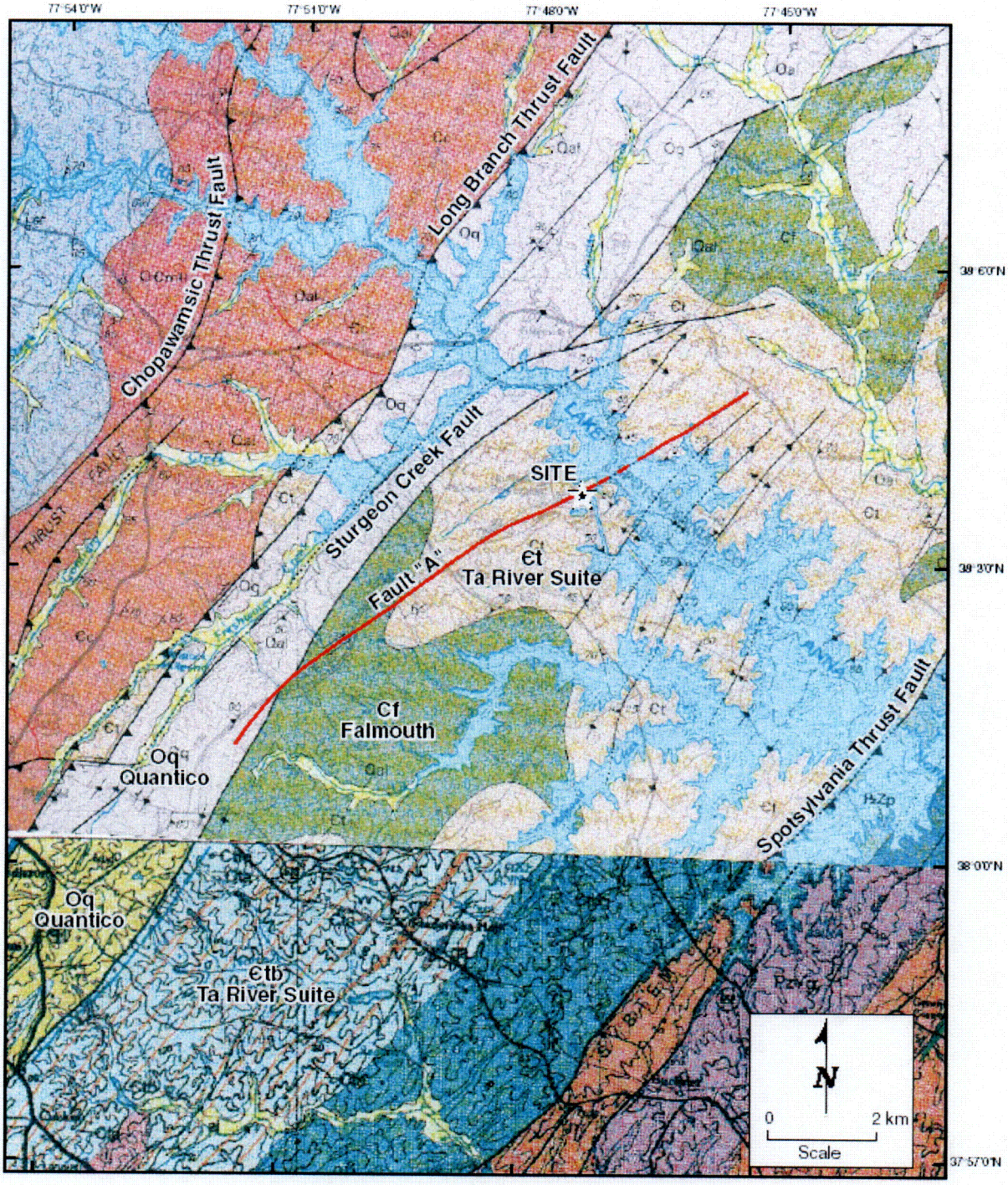

Figure 2. Geologic map of the site area with Fault "A" highlighted. Geology taken from Mixon et al. (2000) Fredericksburg 100k quadrangle and Marr (2002) western portion of Richmond 100k quadrangle.

C22

RAI 2.5.4-1 (NRC 6/1/04 Letter)

SSAR Section 2.5.4 states that additional structure-specific exploration and testing would be performed during detailed engineering and would be described in the combined license (COL) application. Regulatory Guide 1.132 recommends borings at 100 ft spacings for major structures. Please provide the basis (especially given the documented presence of severely weathered, fractured and jointed intervals in the Zone III-IV and Zone IV rock) for concluding that the subsurface conditions in the southwest part of the ESP footprint (an area roughly 1000 ft by 500 ft, in which there have apparently been no borings) do not materially differ from conditions in the adjacent areas where borings have been drilled.

Response

The North Anna site is underlain by a consistent geologic profile (bedrock of the Ta River Metamorphic Suite), as described in SSAR Section 2.5.1.2.3 and illustrated in SSAR Figures 2.5.4-11 (plan view) and 2.5.4-17 (section). This rock extends to a depth of several thousand feet. The soils that overlie this bedrock are the results of in-situ weathering of the rock, and range from saprolites with up to 50 percent of the core stone remaining, to a veneer of residual soils with all structure of the parent rock lost. This profile is described in SSAR Section 2.5.4.2.2, that is:

Zone I	Residual clays and clay silts – all structures of parent rock are lost.
Zone IIA	Saprolite – core stone less than 10 percent of volume of overall mass.
Zone IIB	Saprolite – core stone 10 to 50 percent of volume of the overall mass.
Zone III	Weathered rock – core stone more than 50 percent of volume of the overall mass.
Zone IV	Parent rock – slightly weathered to fresh rock below zone of isolated core stones.

The materials overlying the parent Zone IV rock represent a continuously more pronounced form of in-place weathering. An additional zone, termed Zone III-IV, has been adopted to represent this slightly to moderately weathered rock.

The 145 borings performed throughout the North Anna site (including 7 for the ESP subsurface investigation) indicated a consistent overall subsurface profile, with expected variations in the thickness of the various strata.

The anticipated soil and rock profile in the roughly 1,000 feet x 500 feet area referenced in the RAI is discussed in the next paragraphs.

Soil Profile

As noted previously, all of the natural soils onsite are residual materials derived from in-situ weathering of the underlying bedrock. These soils consist almost entirely of the Zone II saprolites – less than 1 percent of the soils encountered in the borings were Zone I residual soils. The existing topography in the 1,000 feet by 500 feet area is gently rolling, ranging from about Elevation 300 to 330 feet, very typical of the site topography. Excavation to the proposed plant elevation at Elevation 271 feet would be through the Zone II saprolites, although bedrock could be encountered at some locations above Elevation 271 feet, as described below.

Bedrock Profile

The bedrock in the 1,000 feet by 500 feet area is described in SSAR Figure 2.5-18 as an interbedded hornblende gneiss, biotite granite gneiss and granite gneiss. The top of bedrock at the site is generally gently sloping, as shown on the two subsurface profiles on SSAR Figures 2.5-57 and 2.5-58, with steepest slopes in the 12 to 15% range. (Vertical exaggeration on these figures is approximately 5 and 2.5, respectively.)

The 1,000 feet by 500 feet area has borings on all sides, all showing similar and consistent conditions. Table 1 summarizes these borings, with their direction relative to the 1,000 feet by 500 feet area. In addition to the tabulated information, two observation wells were drilled for the ESP investigation, close to the referenced area, with OW-842 on the western edge of the area, and OW-847 about 350 feet south of the area. These wells were terminated in dense or very stiff Zone IIA soils at Elevations 284 feet and 266 feet, respectively.

Table 1. Borings Adjacent to 1,000 feet x 500 feet area

Investigation	Direction	Zone III-IV or IV Bedrock		
		Number of Borings To Rock	Top of Rock Elevation (feet)	
			Range	Median
Units 1 and 2	Northeast	44	201-298	236
Units 3 and 4 *	Northeast	38	190-266	234
SWR	East	7	216-234	221
ISFSI	South	0	**	**
ESP, B-801, 802 & 805	Northeast	3	229-263	232
ESP, B-803 & 804	North	2	244-287	266
ESP, B-806 & 807	Northwest	2	254-288	271

* Most of the abandoned Units 3 and 4 borings were drilled from plant grade at Elevation 271 feet, and so the median values are lower since bedrock had already been excavated at some of the boring locations.
** Borings only advanced into Zone III weathered rock.

From the information given in Table 1, it is reasonable to expect that the top of rock elevations in the referenced 1000 feet by 500 feet area will fall within the tabulated top of rock ranges for the surrounding borings. The overlying soils will be the residual materials found universally throughout the site. If any weathered, fractured, and/or jointed intervals are found in the rock directly beneath safety related structures in this area, they would be removed or treated, as described in the response to RAI 2.5.4-2.

Application Revision

None.

RAI 2.5.4-2 (NRC 6/1/04 Letter)

SSAR Subsection 2.5.4.1 (Geologic Features) references SSAR Section 2.5.1.2.3 (Site Area Stratigraphy), which states that borings drilled for the ESP application revealed severely weathered, fractured and jointed intervals in the Zone III-IV and Zone IV rock. Section 2.5.1.2.3 further states that these severely weathered fracture zones were encountered in four of the seven borings drilled for the ESP application.

RAI 2.5.4-2 Part a)

a) Please describe the extent of similar severely weathered fracture zones, if any, that were observed during the site investigation performed for the abandoned Units 3 and 4.

Response to Part a)

Table 1 summarizes the zones where very poor quality rock, defined as having a Rock Quality Designation (RQD) of 0 – 25% according to Peck et al. (1974), were cored in the investigation for abandoned Units 3 and 4. This level of RQD can be anticipated in zones that are weathered, fractured, and jointed. Table 1 divides the RQD into 0-10% and 11-25% columns. The 0-10% column reflects the severely fractured zones.

Table 1. Zones of Rock Quality Designation 0-25% for Abandoned Units 3 and 4

Boring	RQD (0-10% range)	Depth, feet/Elevation, feet	RQD (11-25% range)	Depth, feet/Elevation, feet
B-602	9	22-30/255-247	25	36-39/241-238
B-607	0	43-45/227-225		
B-615			16	43-45/227-225
B-616	0	54-59/217-212		
	0	61-63/210-208		
B-618	0	34-36/236-234		
B-624	0	12-15/259-256	25	83-93/188-178
	0	114-119/157-152		
	0	120-122/151-149	25	136-140/135-131
B-626	8	8-13/264-259		
	0	44-48/228-224		
	0	62-70/210-202	15	70-74/202-198
	0	74-83/198-189		
B-627			23	49-51/222-220
	0	76-79/195-192		
B-628	0	29-31/242-240		

Table 1. Zones of Rock Quality Designation 0-25% for Abandoned Units 3 and 4				
Boring	RQD (0-10% range)	Depth, feet/Elevation, feet	RQD (11-25% range)	Depth, feet/Elevation, feet
B-633	0	57-59/227-225		
B-635	6	50-51/225-224		
B-637			23	56-66/215-205
B-638	9	40-50/228-218		
B-639	0	56-57/218-217		
	0	60-61/214-213		
B-643			21	65-69/205-201
B-644	1	26-50/245-221		
B-645	0	5-6/266-265	17	20-27/251-244

Note that the rock thicknesses for many of the RQD = 0 intervals in Table 1 are in the 1 to 2-foot thick range. This is similar to the situation noted in the 4 ESP borings referenced in the RAI, where the fracture zones range in thickness from 0.5 to 1 feet.

RAI 2.5.4-2 Part b)

b) Please describe the impact of the existence of the severely weathered fracture zones on the suitability of the site to host safety-related structures.

Response to Part b)

SSAR Section 2.5.1.2.3 states:

> Severely weathered fracture zones were encountered in Zone III-IV rock at varying depths, ranging from about 11 feet (El. 260) to 81 feet (El. 211) below the ground surface. These fracture zones were encountered in four of the borings (B-802, B-803, B-805, and B-806) and ranged in thickness from about 0.5 to 1-foot thick.

SSAR Section 2.5.4.10.1 states:

> The Zone III-IV and Zone IV bedrock have design unconfined compressive strengths of 4 ksi (576 ksf) and 12 ksi (1728 ksf), respectively (SSAR Table 2.5-45). Allowable bearing capacities of these materials are much higher than any applied structure bearing pressure. If excavation during construction reveals any weathered or fractured zones at foundation level, such zones would be overexcavated and replaced with lean concrete. The allowable values of the bearing capacity of 80 ksf and 160 ksf for Zone III-IV and Zone IV rock, respectively, are presumptive values based on various building codes for moderately weathered to fresh foliated rock.

As noted in these SSAR sections, any weathered or fractured zone encountered at foundation level would be excavated and replaced with lean concrete. If such zones exist below sound rock beneath the foundation, they would have no impact on the stability of the foundation, since these zones are typically only 0.5 to 1-foot thick, and are confined within an unfractured rock mass with strengths of 4,000 to 12,000 psi (compared to the maximum foundation pressure of just over 100 psi). The foundation itself would consist of a large, thick, highly-reinforced concrete mat that is so stiff that it cannot locally yield.

Multiple borings would be performed at each structure location once the building locations are chosen as part of detailed engineering. These borings would identify whether there are any thicker fracture zones beneath the foundation than those encountered in the ESP borings and in the abandoned Units 3 and 4 borings. If any thicker zones are found, analysis would be performed to identify their impact on foundation stability. If they are close enough to the foundation to potentially impact stability, they would be excavated and replaced with lean concrete.

References

Peck, R. B., W. E. Hanson, and T. H. Thornburn. *Foundation Engineering,* Second Edition, John Wiley and Sons, Inc., New York, 1974 (Reference 182 of SSAR Section 2.5).

Application Revision

None.

RAI 2.5.4-3 (NRC 6/1/04 Letter)

SSAR Section 2.5.4.2 (Properties of Subsurface Materials) provides the results of the extensive field and laboratory tests that were performed earlier for the abandoned Units 3 and 4, the service water reservoir (SWR), and the independent spent fuel storage installation (ISFSI) facilities at North Anna Power Station. Please discuss how the results of the site investigations for the SWR and the ISFSI, which are located away from the abandoned Units 3 and 4, were integrated with those of the ESP borings in characterizing the subsurface materials at the ESP site.

Response

The results of the site investigations for the SWR and the ISFSI were integrated into the site characterization of the ESP area in the following manner:

- As noted in the response to RAI 2.5.4-1, some of the SWR borings are closer to the southeast portion of the 500 feet by 1,000 feet area referred to in that RAI than any of the other borings. Similarly, some of the ISFSI borings are as close to the southwest portion of the 500 feet by 1,000 feet area as any of the other borings. Thus, the SWR and ISFSI borings can reasonably be used to help characterize the ESP area.

- All of the borings that were performed at the North Anna site prior to the ESP borings showed the same general subsurface profile, with consistent geology, i.e., Zones I through IV as described in SSAR Section 2.5.4.2.2 and the response to RAI 2.5.4-1. This included the SWR and the ISFSI borings. As expected, the ESP borings also fit into the general subsurface profile. This was one reason for including ESP borings B-806 and B-807. Although these borings were performed for non-safety related structures (i.e., the plant cooling towers), they illustrate that the same general subsurface profile extends well to the west of any previous exploration points.

In summary, the North Anna site has a consistent geology and has displayed a very consistent subsurface profile, with expected variations in the thickness of the various strata overlying bedrock. The SWR and ISFSI borings, although located away from abandoned Units 3 and 4, are closer or as close to the ESP area as any other borings, and disclosed the same profile, thus adding to the overall confidence level in the subsurface consistency.

Application Revision

None.

RAI 2.5.4-4 (NRC 6/1/04 Letter)

Table 2.5-29 in SSAR Section 2.5.4 compares the total thicknesses of the soil layers sampled at the locations of Units 1 and 2, abandoned Units 3 and 4, the ISFSI, the SWR, and the ESP site. Table 2.5-29 shows that the total thickness of all the soil layers sampled at the ESP site is only 105 ft, whereas the total thicknesses of soil layers sampled at the other sites mentioned range from 451 ft for the ISFSI to 2204 ft for Units 1 and 2. Please explain how the total thickness of soil layers sampled at the ESP site is sufficient to characterize the soil conditions there.

Response

The soils at the North Anna site have been very well characterized by the 138 borings previously performed. The in-situ soils in all of the borings showed the same general subsurface soil profile, i.e., Zones I, IIA and IIB as described in SSAR Section 2.5.4.2.2 and the response to RAI 2.5.4-1. Subsurface profiles shown on SSAR Figures 2.5-57 and 2.5-58 demonstrate these zones as typically found at the ESP site. One of the primary purposes of the 7 ESP borings was to show that the soil (and rock) profiles in each of the borings fit within the general subsurface profile. The results of the borings did indeed demonstrate this. The cone penetrometer tests and geophysical tests performed for the ESP also gave the same conclusion.

The 105 feet referred to in SSAR Table 2.5-29 is the total thickness of Zone IIA saprolite sampled in the 7 borings. The Zone IIA saprolite is the dominant soil type at the North Anna site. The thickness per boring ranged from 0 to 31 feet. In some cases, the small thickness of Zone IIA saprolite is the result of excavation for the existing or abandoned units at the site, e.g., the B-802 location (3 feet of Zone IIA saprolite) had about 40 feet of soil excavated for the original construction, and B-801 (zero Zone IIA saprolite) is at the location of the abandoned Unit 3 excavation. SSAR Table 2.5-29 shows that the constituents of the Zone IIA saprolite are in line with the constituents found in the previous borings.

As noted in SSAR Section 2.5.4: "The additional field and laboratory investigations performed for the ESP were intended to confirm the already large volume of geotechnical data developed for the existing units and the abandoned Units 3 and 4 within the ESP site area. Additional structure-specific exploration and testing would be performed during detailed engineering and would be described in the COL application." The main purpose of the structure-specific borings from the soils aspect would be to verify the thickness of the soil strata at the structure location.

Application Revision

None.

RAI 2.5.4-5 (NRC 6/1/04 Letter)

With regard to Table 2.5-45 (Summary of Geotechnical Engineering Properties) in SSAR Section 2.5.4:

RAI 2.5.4-5 Part a)

a) Please explain why no shear wave velocities are given for Zone IIB saprolite and for Zones III and III-IV weathered rock.

Response to Part a)

SSAR Table 2.5-45 gives average shear wave velocity values for Zones IIB, III, and III-IV, but does not provide a range of values. There are both average values and a range of values provided for Zone IIA and Zone IV. The reason the values were presented this way in SSAR Table 2.5-45 was that there were a range of measured and computed values of shear wave velocity for Zones IIA and IV, but there were much fewer values for Zones IIB, III, and III-IV, as explained in the following paragraphs. Additions, however, have been made in the revision to SSAR Table 2.5-45 at the end of this RAI response.

SSAR Figure 2.5-62 (a) illustrates the 600 to 1,350 feet/second range of shear wave velocity values for Zone IIA saprolite – values from a cross-hole seismic test and two CPT down-hole seismic tests performed as part of the ESP investigation, and average shear wave velocity values from the investigation for Units 1 and 2.

SSAR Section 2.5.4.4.1 describes a 4,000 to 8,000 feet/second range of shear wave velocity values for Zone IV bedrock. For the Units 1 and 2 investigation, shear wave velocities were measured with a Birdwell 3-D velocity recorder and from cross-hole seismic tests. Cross-hole seismic and down-hole seismic tests were performed in the Zone IV bedrock as part of the ESP investigation.

Zone IIB saprolite occurs much less frequently than the Zone IIA saprolite, and there are correspondingly less shear wave velocity measurements in the Zone IIB saprolite. No shear wave velocity values were attributed to the Zone IIB saprolite in the Units 1&2 investigations. For the ESP investigation, the CPT-825 down-hole seismic test was interpreted as penetrating about 10 feet of Zone IIB saprolite, and gave a shear wave velocity measurement of about 1,650 feet/second. Using a different approach, the Zone IIB shear wave velocity was computed from the high strain modulus values given in SSAR Table 2.5-45 using the relationship between high and low strain modulus given in SSAR Figure 2.5-63. The resulting computed shear wave velocity value was 1,574 feet/second. The average shear wave velocity value of 1,600 feet/second given in SSAR Table 2.5-45 was selected based on the 1,650 and 1,574 feet/second values. The 1,574 to 1,650 feet/second range was not included in SSAR Table 2.5-45 since it was considered that including such a narrow range would provide an optimistic assessment of the actual range. A note has been added in the revision to SSAR Table 2.5-45 stating that there is no range of values available for the Zone IIB saprolite.

As with the Zone IIB saprolite, the CPT-825 down-hole seismic test provides the only field measurement of shear wave velocity in the Zone III weathered rock. As shown in SSAR Figure 2.5-62 (a), shear wave velocities of 1,650 and 2,440 feet/second were measured in the upper and lower portions of the Zone III stratum. Using the same approach adopted for Zone IIB, the Zone III shear wave velocity was also computed from the high strain modulus values given in SSAR Table 2.5-45 using the relationship between high and low strain modulus given in SSAR Figure 2.5-63. The resulting computed shear wave velocity value was 2,000 feet/second. Since this was close to the median of the field shear wave velocity measurements, it was adopted as the average shear wave velocity value in SSAR Table 2.5-45. A range of 1,500 to 2,500 feet/second is added for the Zone III weathered rock in the revision to SSAR Table 2.5-45.

There were several measured shear wave velocities for Zone III-IV. In boring B-104 performed for Units 1 and 2, measured shear wave velocity in Zone III-IV ranged from 3,000 to 4,500 feet/second (Birdwell 3-D velocity recorder). In the ESP down-hole seismic test, the measured shear wave velocities in Zone III-IV near boring B-802 were 1,482, 3,435 and 5,278 feet/second. The shear wave velocity computed from the shear modulus derived from the rock strength was 3,366 feet/second. These values are the basis for the average value of 3,300 feet/second in SSAR Table 2.5-45. A range of 2,500 to 4,500 feet/second is added for the Zone III-IV rock in the revision to SSAR Table 2.5-45.

RAI 2.5.4-5 Part b)

b) Please provide the range of standard penetration test (SPT) values separately for coarse-grained and fine-grained soil zone IIA, along with the depths of the soils at which the N-values were obtained.

Response to Part b)

Table 1 (located at the end of this RAI response) provides the standard penetration test (SPT) values for coarse-grained and fine-grained Zone IIA saprolites from all the site borings. Note that Dames and Moore used their "Dames and Moore Sampler" on many occasions, especially in the Units 1 and 2 investigation. Since the blowcount from the Dames and Moore sampler cannot be directly correlated with the SPT blowcount, the Dames and Moore blowcounts are not included in Table 1.

Coarse-grained soils in the table are poorly graded gravels (GP), poorly graded sands (SP), silty sands (SM), and clayey sands (SC). Fine-grained soils are low and high plasticity silts (ML and MH) and low and high plasticity clays (CL and CH).

SPT N-values were obtained for 397 samples of coarse-grained Zone IIA saprolites. Range was 4 to 1,260 blows/foot. (1,260 blows/foot is extrapolated from 210 blows for 2 inches.) The median N-value was 33 blows/foot.

SPT N-values were obtained for 200 samples of fine-grained Zone IIA saprolites. Range was 6 to 171 blows/foot. (171 is extrapolated from 50 blows for 3.5 inches.) The median N-value was 19 blows/foot.

Application Revision

For the Description "Shear wave velocity range, ft/sec," revise SSAR Table 2.5-45 for Stratums IIB, III, and III-IV to read as follows:

Description	IIB	III	III-IV
Shear and compression wave velocity			
Shear wave velocity range, ft/sec	No range available	1,500 to 2,500	2,500 to 4,500

Table 1. Standard penetration test values for coarse-grained and fine-grained Zone IIA saprolites					
		Coarse –Grained Zone IIA		Fine-Grained Zone IIA	
Study	Boring Number	Depth, Ft	SPT N-Value, Blows/ft	Depth, Ft	SPT N-Value, Blows/ft
Units 1&2	B-1	2	27		
		5	24		
		11	50		
		15	138		
		20	194/6 in.		
		25	225/6 in.		
		30	250/5 in.		
Units 1&2	B-10	2	40		
		5	17		
		11	62		
		15	151		
		21	207		
		25	210/2 in.		
		31	205/8 in.		
Units 1&2	B-27	2.5	17		
		11	16		
		21	55		
		31	107		
Units 1&2	B-43	5	89		
		11	140		
		16	106		
		21	69		
		26	81		
		31	87		
Units 1&2	B-50	5	4		
		11	4		
		21	4		
		25	7		
		31	9		
		36	10		
		41	10		
		46	17		
		51	65		
Units 1&2	B-103	11	29		
		21	28		
		31	22		
		41	52		

Table 1. Standard penetration test values for coarse-grained and fine-grained Zone IIA saprolites					
		Coarse –Grained Zone IIA		Fine-Grained Zone IIA	
Study	Boring Number	Depth, Ft	SPT N-Value, Blows/ft	Depth, Ft	SPT N-Value, Blows/ft
		51	60		
		61	119		
		71	277		
Units 1&2	B-105	11	6		
		21	7		
Units 3&4	B-601	6	16		
		21	25/3 in.		
Units 3&4	B-603	26	105		
		31	175		
Units 3&4	B-604			7	40
Units 3&4	B-605	15	35		
		20	54		
		25	123		
Units 3&4	B-606	5	18		
		10	26		
		15	70		
		20	70/6 in.		
Units 3&4	B-607	5	13		
		10	23		
		15	32		
		20	50/2 in.		
		25	50/3 in.		
Units 3&4	B-608	5	31		
		25	146		
		30	143		
Units 3&4	B-609	15	21	5	13
		25	17/3 in.	10	18
		30	70/6 in.		
Units 3&4	B-610	5	25		
		10	22		
		15	28		
		25	52		
		45	79		
		50	77		
		55	45/2 in.		
		60	78		
Units 3&4	B-611	7	20		
		21	15		
		34	33		

Table 1. Standard penetration test values for coarse-grained and fine-grained Zone IIA saprolites					
		Coarse –Grained Zone IIA		Fine-Grained Zone IIA	
Study	Boring Number	Depth, Ft	SPT N-Value, Blows/ft	Depth, Ft	SPT N-Value, Blows/ft
		41	59		
		46	100/5 in.		
Units 3&4	B-612	10	13		
Units 3&4	B-613	5	34		
		10	15		
		15	21		
		20	25		
		25	34		
		30	30		
		40	90		
Units 3&4	B-614	5	23		
		10	23		
		15	20		
		20	18		
		30	33		
Units 3&4	B-615	5	12		
		10	17		
		15	40		
		20	44		
Units 3&4	B-616	5	22	10	9
		15	31	20	24
				25	45
Units 3&4	B-617	5	26		
		10	28		
		15	94		
		20	64		
		25	108		
		30	57/6 in.		
		35	68/6 in.		
Units 3&4	B-618	5	14		
		10	24		
		20	40		
		25	32		
		30	44		
Units 3&4	B-619	5	65		
		10	110		
Units 3&4	B-620	5	40		
Units 3&4	B-622	5	41		
		10	210		

Table 1. Standard penetration test values for coarse-grained and fine-grained Zone IIA saprolites					
		Coarse –Grained Zone IIA		Fine-Grained Zone IIA	
Study	Boring Number	Depth, Ft	SPT N-Value, Blows/ft	Depth, Ft	SPT N-Value, Blows/ft
		15	120/4 in.		
Units 3&4	B-623	5	170/4 in.		
		10	49		
Units 3&4	B-624	5	49		
		7	150		
Units 3&4	B-625	4	6		
Units 3&4	B-626	5	119		
Units 3&4	B-631	25	46		
		40	19		
		50	30		
		60	51		
		65	59		
		70	240		
		75	262		
Units 3&4	B-632	5	44		
		10	56		
		15	58/6 in.		
Units 3&4	B-634	5	25	10	23
		25	100	15	48
		30	65/5 in.	20	65
Units 3&4	B-636	5	15		
		10	25		
		15	70/2 in.		
		20	15/1.5 in.		
		25	100/6 in.		
Units 3&4	B-637	10	14		
		25	42		
		30	50/3 in.		
Units 3&4	B-638	5	116		
Units 3&4	B-639	25	40/3 in.		
		30	75/7 in.		
Units 3&4	B-640	5	22		
		10	41		
		15	29		
		20	22		
		25	59		
		30	156		
		35	101/5 in.		
		40	100/5 in.		

Table 1. Standard penetration test values for coarse-grained and fine-grained Zone IIA saprolites					
		Coarse –Grained Zone IIA		Fine-Grained Zone IIA	
Study	Boring Number	Depth, Ft	SPT N-Value, Blows/ft	Depth, Ft	SPT N-Value, Blows/ft
Units 3&4	B-641	5	19		
		10	24		
		15	25		
		20	16		
		25	22		
		30	31		
		35	45		
		40	63		
		45	70/3 in.		
		50	50/2 in.		
Units 3&4	B-642	5	19		
		10	25		
		15	26		
		20	21		
		40	47/6 in.		
		45	80		
		50	34		
Units 3&4	B-643	5	18		
		10	20		
		15	59		
		20	51		
		25	149		
		30	100/3 in.		
Units 3&4	B-646	10	25	15	25
		20	57		
		25	79		
		30	118		
		35	162		
		40	100/5 in.		
		45	20		
Units 3&4	B-647	5	13		
		10	23		
		15	44		
		20	69		
		25	50/3 in.		
SWR	P-10	3	24		
		10	43		
		15	142		
		20	20		

Table 1. Standard penetration test values for coarse-grained and fine-grained Zone IIA saprolites					
		Coarse –Grained Zone IIA		Fine-Grained Zone IIA	
Study	Boring Number	Depth, Ft	SPT N-Value, Blows/ft	Depth, Ft	SPT N-Value, Blows/ft
	P-11	21	23	16	16
		35	21	25	16
		40	13	30	16
		45	17		
SWR	P-12	11	18	5	17
		15	25		
		20	18		
SWR	P-16	40	19	35	18
		45	19		
		50	28		
		55	39		
		60	107		
		65	62		
SWR	P-17	65	45	35	18
				40	17
				45	17
				50	17
				55	22
				60	23
SWR	S1-1	45	17	15	26
		50	19	20	18
		55	27	25	22
		60	25	30	31
		65	24		
		70	56		
		75	80		
		80	100		
SWR	S1-2	7	15		
		10	18		
		15	33		
		20	94		
		25	33		
		30	100		
		35	100		
SWR	S1-3	10	47	5	31
		15	57		
		20	92		
		25	63		
		30	50		

Table 1. Standard penetration test values for coarse-grained and fine-grained Zone IIA saprolites					
		Coarse –Grained Zone IIA		Fine-Grained Zone IIA	
Study	Boring Number	Depth, Ft	SPT N-Value, Blows/ft	Depth, Ft	SPT N-Value, Blows/ft
		35	134		
		40	32		
		47	155		
SWR	SWR-1			1	15
				2.5	21
				4	21
				5.5	20
				7	14
				8.5	13
				10	18
				11.5	17
				13	17
				14.5	20
				16	16
				18	17
				19.5	20
				21	15
				24	21
				24.5	14
				26	12
				28	9
				31.5	16
				33	15
				34.5	22
				36	15
				37.5	15
				39	16
				40.5	20
				42	22
				43.5	24
SWR	SWR-2			1.5	16
				3	18
				4.5	24
				6	18
				7.5	13
				9	12
				10.5	16
				12	20
				13.5	17

Table 1. Standard penetration test values for coarse-grained and fine-grained Zone IIA saprolites					
		Coarse –Grained Zone IIA		Fine-Grained Zone IIA	
Study	Boring Number	Depth, Ft	SPT N-Value, Blows/ft	Depth, Ft	SPT N-Value, Blows/ft
				15	16
				16.5	16
				18	17
				19.5	18
				21	19
				22.5	20
				24	18
				25.5	22
				27	21
				28.5	11
				30	12
				31.5	11
				33	12
				34.5	13
				36	13
				37.5	14
				39	19
				40.5	20
				42	45
				43.5	55
				45	74
				46.5	84
				48	38
				49.5	46
SWR	SWR-3	7	15		
		10	16		
		15	13		
		20	55		
		25	12		
		30	25		
		35	17		
		40	29		
		45	33		
		50	45		
		55	41		
		60	51		
		65	45		
		70	91		
		75	75		

Table 1. Standard penetration test values for coarse-grained and fine-grained Zone IIA saprolites					
		Coarse –Grained Zone IIA		Fine-Grained Zone IIA	
Study	Boring Number	Depth, Ft	SPT N-Value, Blows/ft	Depth, Ft	SPT N-Value, Blows/ft
		80	131		
		85	100		
		90	142		
		95	138		
SWR	SWR-4	5	39		
		10	16	15	16
		20	17		
		25	19		
		30	27		
		35	18		
		40	29		
		45	19		
		50	24		
		55	38		
		60	31	65	40
		70	57		
		75	27		
		80	52		
		85	37		
		90	100		
		95	100		
		100	400		
SWR	SWR-5	25	15		
		30	22	35	16
		40	21		
		45	21		
		50	32		
		55	31		
		60	28		
		65	25		
		70	37		
		75	100		
		80	39		
		90	226		
SWR	SWR-6	35	21	15	21
		40	21	20	27
		45	26	25	22
		55	16	30	23
		65	19	50	22

Table 1. Standard penetration test values for coarse-grained and fine-grained Zone IIA saprolites					
		Coarse –Grained Zone IIA		Fine-Grained Zone IIA	
Study	Boring Number	Depth, Ft	SPT N-Value, Blows/ft	Depth, Ft	SPT N-Value, Blows/ft
		70	48	60	21
		75	100+		
		80	100+		
		85	100+		
		90	100+		
		95	100+		
		100	400		
SWR	SWR-7	35	16	15	17
		40	9	25	19
		50	15	30	24
		55	17	45	8
		60	19	75	26
		65	23		
		70	32	80	37
SWR	SWR-8	30	16	10	24
		35	19	15	15
		40	35	20	9
		45	25	25	10
		50	41		
		55	50		
		60	109		
		65	98		
		70	81		
SWR	SWR-9	20	10	15	12
		30	17	25	8
		35	17		
		40	60		
		45	68		
		50	274		
		55	50		
		60	75		
		65	163		
SWR	SWR-10	33	14	45	24
		35	21	47.5	37
		37.5	18	50	19
		40	16	52.5	26
		42.5	14	55	14
				57.5	25
				60	30

Table 1. Standard penetration test values for coarse-grained and fine-grained Zone IIA saprolites					
		Coarse –Grained Zone IIA		Fine-Grained Zone IIA	
Study	Boring Number	Depth, Ft	SPT N-Value, Blows/ft	Depth, Ft	SPT N-Value, Blows/ft
				62.5	36
SWR	SWR-11	33	300	17.5	17
		36	300	22.5	19
				28	48
SWR	SWR-13	40	21	30	22
				35	19
				45	25
				50	14
				55	13
				60	24
				65	31
				70	62
ISFSI	F-2	15	14	1	13
		20	18	4	20
		25	18	8	18
		30	22	10	18
		35	14		
		40	17		
		45	18		
		50	43		
		55	54		
		60	78		
ISFSI	F-4	10	15	1	25
		15	21	3	29
		20	16	4.5	19
		25	23	7	19
		29.5	50/5 in.		
ISFSI	F-5			1	25
				3	25
				4.5	18
				7	21
				10	9
				15	13
				20	9
				25	12
				30	14
				35	26
				40	31
				45	27

Table 1. Standard penetration test values for coarse-grained and fine-grained Zone IIA saprolites					
		Coarse –Grained Zone IIA		Fine-Grained Zone IIA	
Study	Boring Number	Depth, Ft	SPT N-Value, Blows/ft	Depth, Ft	SPT N-Value, Blows/ft
				50	44
				55	27
				60	40
ISFSI	F-6	30	17	1	19
		35	23	3	26
		40	80/9 in.	4.5	26
				7	26
				10	19
				15	14
				20	13
				25	13
ISFSI	F-7	65	54	1	19
		70	71	3	41
		75	50/3 in.	4.5	36
				7	27
				10	15
				15	10
				20	10
				25	10
				30	15
				35	15
				40	14
				45	17
				50	22
				55	36
				60	38
ISFSI	F-8	1	18	3	33
				4.5	29
				7	36
				10	17
				15	18
				20	25
				25	24
				30	16
ISFSI	F-9	1	17		
		3	25		
		4.5	23		
		7	24		
		10	16		

Table 1. Standard penetration test values for coarse-grained and fine-grained Zone IIA saprolites					
		Coarse –Grained Zone IIA		Fine-Grained Zone IIA	
Study	Boring Number	Depth, Ft	SPT N-Value, Blows/ft	Depth, Ft	SPT N-Value, Blows/ft
		15	14		
		20	12		
		25	7		
		30	14		
		35	21		
		40	26		
		45	52		
		50	56		
ISFSI	F-10	1	23		
		3	30		
		4.5	28		
		7	27		
		10	20		
		15	24		
		20	32		
		25	22		
		30	48		
		35	61		
		40	80		
		45	26		
ISFSI	F-11	25	61	1	43
				3	62
				4.5	41
				7	32
				10	38
				15	50/3.5 in.
				20	39
ESP	B-802	5	44		
ESP	B-803	1	12		
		5	31		
		7	14		
		10	22		
		12	13		
		15	23		
		20	18		
		25	31		
		30	30		
ESP	B-804	7	6	1	13
		9.5	5	2.5	13

Table 1. Standard penetration test values for coarse-grained and fine-grained Zone IIA saprolites					
		Coarse –Grained Zone IIA		Fine-Grained Zone IIA	
Study	Boring Number	Depth, Ft	SPT N-Value, Blows/ft	Depth, Ft	SPT N-Value, Blows/ft
		12	5	4.5	6
		14.5	9		
		19.5	24		
ESP	B-805	8.5	17	1	12
		11.5	25	3.5	20
		14.5	38	6	14
		19.5	34		
		24	100/8.5 in.		
		28.5	100/1 in.		
ESP	B-806	4	22		
		6.5	18		
ESP	B-807	23	22	1	12
		27.5	100	3	17
		32.5	80	5.5	15
		36.5	100/2.5 in.	8	12
				11	13
				13	13
				16	21

RAI 2.5.4-6 (NRC 6/1/04 Letter)

With regard to Table 2.5-44 (Summary of ESP Test Rest Results - Rock) in SSAR Section 2.5.4:

RAI 2.5.4-6 Part a)

a) Please explain why test results were not provided for the materials at several depths, for example, between depths 25 ft and 48 ft in boring B-801, between depths 21 ft and 44 ft, 46 ft to 66 ft, and 67 ft to 85 ft in boring B-802, and several depths in borings B-803 and B-806.

Response to Part a)

The containment (reactor) buildings for the new units would be founded on the Zone III-IV and/or Zone IV metamorphic gneiss bedrock at the North Anna site. Rock coring and testing performed on 23 cores from the Units 1 and 2 investigation gave unconfined compression strengths of the Zone III-IV and Zone IV rock ranging from 1.0 to 16.3 ksi with a median strength of 6.8 ksi, that is, rock strengths that were typical for this type of rock, and more than sufficient to support the maximum containment (reactor) building loads of about 0.1 ksi.

During logging of the rock cores in the field for the ESP investigation, it was apparent that the metamorphic rock was a strong material. (See, for example, the photos of the recovered cores from boring B-801 in SSAR Section 2.5.4 Appendix B, page 2.5.4B-31.) Sufficient tests were performed on the ESP cores to verify that the rock strengths were similar to or higher than those cores tested for Units 1 and 2. Rock coring and testing performed on 18 cores from the ESP investigation gave unconfined compression strengths of the Zone III-IV and Zone IV rock ranging from 2.7 to 28.4 ksi with a median strength of 18.4 ksi, generally higher than the Units 1 and 2 strengths.

In this situation where there are moderately strong or strong rocks, more important parameters from a structure stability standpoint are the recovery and the rock quality designation (RQD). (The RQDs are given as percentages for each core in the detailed rock coring logs in SSAR Section 2.5.4 Appendix B.) These parameters indicate the degree of recovery and fracturing of the core run. For bearing capacity on rock, it is more desirable to have a lower strength rock with high recovery and RQD than a strong rock with low recovery and RQD since the low strength rock has adequate strength to support the loads, whereas high strength rock with many fractures may be subject to local differential settlement.

The recovery and RQD values for the ESP site cores were typically higher than for the Units 1 and 2 investigation, although this could have been due to better coring equipment in the recent investigation.

The 18 ESP rock core tests were assigned on representative cores recovered from the borings. For example, all six 5-foot long core runs in boring B-801 had 100 percent

recovery and 100 percent RQD, with similar descriptions. Strength tests were made on sections of core taken from the top and bottom core runs, and gave very consistent results.

Similarly, the four tests on sections of core from B-802 were representative of the core recoveries and RQDs of the cores in that boring, and were taken at representative depths – 90% recovery and 72% RQD at 20.7 feet depth, 100% and 96% at 45.3 feet depth, 100% and 80% at 66.4 feet depth, and 100% and 92% at 85.6 feet depth. The median recovery and RQD in B-802 were 100% and 80%, respectively.

The same approach was applied to core testing in B-803 and B-806. Thus, although testing was not conducted within certain depth intervals, the field characterization coupled with the laboratory test results demonstrate the quality and consistency of the rock.

RAI 2.5.4-6 Part b)

b) Please explain why no test results were provided for boring B-807.

Response to Part b)

Boring B-807 is located in the ESP site cooling tower area. The cooling towers that would be located in this area would not serve a safety-related function. The cooling towers are relatively lightly-loaded structures (1 to 2 ksf or 0.007 to 0.014 ksi loading). They would be founded at plant elevation (Elevation 271 feet) or above on improved Zone IIA saprolite or Zone IIB saprolite, 15 to 20 feet above the underlying gneiss in B-807. The gneiss would not impact the performance of the cooling tower foundations. During detailed engineering, once the actual cooling tower locations are established, borings would be made to confirm the soil properties at that location and the depth and quality of the bedrock.

RAI 2.6.5-6 Part c)

c) Please discuss the significance of the relatively low value (4.43 ksi) of the unconfined compressive strength of the Zone IV rock in Boring B-805, as compared to the values for the Zone IV rock strengths in Borings B-802, 803, and 806 at similar depths, which are much higher (by a factor 2 to 6).

Response to Part c)

There is no significance from a foundation stability standpoint – 4.43 ksi puts the rock in the moderately strong classification, and is around the compressive strengths typical of reinforced concrete foundations (4,000 to 5,000 psi).

This core had 100% recovery and 92% RQD, with the RQD only slightly below the median value for Zone IV cores recovered in the ESP investigation. However, reference to the tested core (SSAR Section 2.5.4 Appendix B, page 2.5.4B-324) shows

the core failed in a clean diagonal break, not along the foliation plane but fairly close to it. The core is described as strongly foliated. The pictures of failed high strength cores (e.g., B-801, 24.1 to 24.8 feet depth, 27.21 ksi strength, SSAR Section 2.5.4 Appendix B, page 2.5.4B-325) show a failure along multiple planes, and these cores are generally described as weakly foliated. Other cores that are described as strongly foliated tend to have lower strengths than the very high strength weakly foliated materials. Thus, the lower strength is probably linked to strong foliation. It should be noted that failure along a predetermined plane can occur in an unconfined compression test, but not in the rock mass itself.

Application Revision

None.

RAI 2.5.4-7 (NRC 6/1/04 Letter)

SSAR Subsection 2.5.4.7.1 (Shear Wave Velocity Profile) states (on page 2.2-291) that some safety-related structures (excluding the reactors) may be founded on the Zone III weathered rock, Zone IIB saprolite, or Zone IIA saprolite. However subsection 2.5.1.2.6 (Site Engineering Geology Evaluation) of the SSAR states (on page 2.2-222) that Zone III is not a suitable material for safety-related plant structures. Please reconcile these two statements.

Response

The statement in SSAR Section 2.5.4.7.1 is correct—some safety-related structures (excluding the reactor containment building) may be founded on the Zone III weathered rock, Zone IIB saprolite, or improved Zone IIA saprolite. Note that SSAR Section 2.5.4.10.2 states that Zone IIA saprolite is unsuitable for the support of any safety-related structure without ground improvement. Ground improvement is discussed in SSAR Section 2.5.4.12.

The statement in SSAR Section 2.5.1.2.6 will be deleted because Zone III weathered rock is suitable under certain conditions. (See response to RAI 2.5.4-11.)

Application Revision

The 2nd paragraph under the heading "Rock" in SSAR Section 2.5.1.2.6 will be revised to delete the last sentence which reads: "These results indicate that Zone III is not a suitable bearing surface for the safety-related plant structures."

RAI 2.5.4-8 (NRC 6/1/04 Letter)

SSAR Subsection 2.5.4.7.2 (Variation of Shear Modulus and Damping with Strain) describes the shear modulus and damping ratio curves for Zone IIA saprolite (improved and unimproved), Zone IIB saprolite, and Zone III rock. With regard to this subsection:

RAI 2.5.4-8 Part a)

a) Please provide the basis for the selected modulus reduction curves for Zone IIA saprolite, Zone IIB saprolite, and Zone III weathered rock.

Response to Part a)

1. Introduction

EPRI (1993) comprehensively reviews much of the published literature on the topic of shear modulus reduction curves, including the work of Seed et al at the University of California, Berkeley, in the 1970s and 1980s. The SSAR design curves for shear modulus reduction with strain are based on the EPRI (1993) recommendations, wherever applicable.

EPRI (1993) indicates that the property most affecting the shape of the shear modulus versus strain curves is grain size. Exhibit 1 (from EPRI (1993)) shows typical ranges for different grain sizes. The coarser grained soils show greater reduction with increasing strain than the finer grained soils. At North Anna, the Zone IIA soils are classified as sands. However, the Zone IIA soils are also looked at as clays for comparison, since these soils do have some cohesive characteristics.

Although the Zone IIB saprolite contains relict structure of the parent rock, it does not appear to exhibit any of the cohesive characteristics noted in the Zone IIA saprolite. In fact, with up to 50 percent of core stone remaining intact, the Zone IIB saprolite required rock coring in some instances. It can be argued that the Zone IIB saprolite will behave more like a gravel or crushed stone than a sand.

Solid rock does not exhibit the strain softening characteristics of soil. Like steel and concrete, sound rock has essentially the same modulus (shear and elastic) throughout the strain range. The elastic modulus values computed from the stress-strain measurements (relatively high strain) on samples of sound rock core obtained during the ESP subsurface investigation were similar to those calculated from the ultra low strain cross-hole seismic tests. However, at some stage of weathering, rock becomes sufficiently decomposed to exhibit modulus attenuation. The Zone III moderately to severely weathered rock is considered to fall into this sufficiently weathered state. Unlike soils, relatively little research has been performed on weathered rock. Sun et al (1988) developed a shear modulus versus strain relationship for mudstone (a soft rock) with a shear wave velocity of 1,500 feet/sec. As would be expected, the attenuation at

the highest measured strain (about 0.5 percent) is only about 50 percent, compared to about 90 percent for sand, gravel and clay at that strain.

2. Zone IIA Saprolite

This saprolite is treated as a sand, but the sand curves are also compared with clay curves.

As noted above, EPRI (1993) indicates that the property most affecting the shape of the shear modulus versus strain curves is grain size. For sands, the second most influential property is the confining pressure. For clays, plasticity index plays a major role in determining the shape of the curves.

EPRI (1993) summarizes its recommendations for sands and clays in a series of 5 figures. These figures are included here as Exhibit 2. Each of these figures is reviewed below to see how it relates to the North Anna situation.

a. Page 1 of Exhibit 2. This shows modulus reduction as a function of reference strain. The "reference strain" is defined as τ_{max}/G_{max}, where τ_{max} is the "shear strength" of the soil. For sands, EPRI (1993) notes that the reference strain is typically about 0.1. Thus, the 0.1 reference strain curve is used as a starting point for the North Anna curve. This is plotted on Figure 1 as curve 1.

b. Pages 2 and 3 of Exhibit 2. These show the shear strain reduction curves as a function of vertical effective stress for dry and saturated sands, respectively. Groundwater table at the North Anna site generally varies from about 6 feet to 58 feet below ground surface. Assume groundwater level is at (1) 6 feet depth and (2) 30 feet depth, to see what difference is made to the shear modulus reduction curve.

For the Zone IIA saprolite, this zone is assumed to be 30 feet thick for computation purposes. Unit weight of soil is 125 pcf.

With water table at 6 feet, effective vertical stress at mid layer (15 feet) is:
$(6 \times 125) + (9 \times (125 - 62.4)) = 1{,}313$ psf.

With water table at 30 feet, effective vertical stress at mid layer (15 feet) is:
$15 \times 125 = 1{,}875$ psf.

The curves on Pages 2 and 3 of Exhibit 2 are spaced proportionally to the log of the effective vertical pressure. The effective vertical pressures of 1,313 psf and 1,875 psf for the dry sands were interpolated from the Exhibit 2, page 2 curves, and are plotted as curves 4 and 2, respectively, on Figure 1. There is minimal difference between the dry and submerged sand curves, and so the curves for the submerged sands are not plotted.

c. Page 4 of Exhibit 2. These curves are suitable for generic site response studies in Eastern North America, and cover the range from gravelly sands to low plasticity clays. A curve was interpolated for 10 to 40 feet depth for the North Anna sands. This curve is closer to the 20 to 50 feet curve than the 0 to 20 feet curve. It is plotted as curve 3 on Figure 1.

d. Page 5 of Exhibit 2. This shows modulus reduction curves for clays, demonstrating the variation with plasticity index. The cohesive portions of the Zone IIA saprolite are generally low plasticity. Curve 6 on Figure 1 is for a PI of 10. For PI = 30, the curve is close to curve 1 on Figure 1.

Curve 5 on Figure 1 is the average Seed and Idriss (1970) curve for sands that has been used in many SHAKE analyses.

The curves in Figure 1 fall into a fairly close group. The average curve is close to curves 3 and 4. This curve is plotted as curve 1 on SSAR Figure 2.5-63 and is the design curve for the Zone IIA saprolite. The curve is tabulated below.

Curve 1: Modulus Reduction Design Curve for Zone IIA Saprolite									
Cyclic Shear Strain, Percent	.0001	.000316	.001	.00316	.01	.0316	.1	.316	1
G/G_{max}	1	1	0.98	0.93	0.79	0.57	0.32	0.15	0.05

3. Zone IIB Saprolite

As noted in the introductory section, it can be argued that the Zone IIB saprolite will behave more like a gravel or crushed stone than a sand. EPRI (1993) points out that the reduction curves show greater reduction for coarser grained materials (Exhibit 1). However, EPRI (1993) does not contain specific recommendations for a gravel curve.

Seed et al (1984) provide a modulus reduction curve (included as Exhibit 3) that can be used for gravels, based on tests of four different gravels and crushed stone samples. This curve is tabulated below. The curve is plotted on SSAR Figure 2.5-63 as curve 2 and is the design curve for the Zone IIB saprolite. This curve has a somewhat higher reduction than the curve proposed by Rollins et al (1998).

Curve 2: Modulus Reduction Design Curve for Zone IIB Saprolite									
Cyclic Shear Strain, Percent	.0001	.000316	.001	.00316	.01	.0316	.1	.316	1
G/G_{max}	1	0.96	0.86	0.72	0.54	0.36	0.20	0.10	0.05

4. Zone III Weathered Rock

As noted in the introductory section, Sun et al (1988) developed a shear modulus versus strain for mudstone (a soft rock) with a shear wave velocity of 1,500 feet/sec

(included as Exhibit 4). As would be expected, the attenuation at the highest measured strain (about 0.5 percent) is only about 50 percent, compared to about 90 percent for sand, gravel and clay at that strain. The Zone III weathered rock has a shear wave velocity of 2,000 feet/sec. Thus, the SSAR Reference 169 mudstone curve is used for shear modulus input in the soil/rock column amplification/attenuation analysis for the Zone III weathered rock. This curve is tabulated below. The curve is plotted on SSAR Figure 2.5-63 as curve 3 and is the design curve for the Zone III weathered rock. (Note that this curve is close to the highly plastic clay curve in Exhibit 2, page 5, with PI = 70).

Curve 3: Modulus Reduction Design Curve for Zone III Weathered Rock									
Cyclic Shear Strain, Percent	.0001	.000316	.001	.00316	.01	.0316	.1	.316	1
G/G_{max}	1	1	1	1	1	0.97	0.85	0.61	0.32

Note that Sun et al (1988) gives only upper and lower bounds for the curve (see Exhibit 4). The tabulated curve plotted on SSAR Figure 2.5-63 is the average of the upper and lower bounds. Also, the Sun et al (1988) curve is only plotted as far as a strain of about 0.3%. The curve has been extrapolated to 1% shear strain in the table above, and on SSAR Figure 2.5-63.

RAI 2.5.4-8 Part b)

b) Please explain the basis for the selected damping ratio curves for Zone IIA saprolite, Zone IIB saprolite and Zone III weathered rock.

Response to Part b)

1. Introduction

For sands and clays, EPRI (1993) follows a similar course for damping as it did for shear modulus. Thus a similar process is followed for the Zone IIA saprolite damping as for the shear modulus. EPRI (1993) does not specifically address damping for gravel and soft rock. Sound rock will display some damping characteristics. However, this damping will not be dependent on the shear strain, i.e., it will exhibit a constant damping ratio.

2. Zone IIA Saprolite

EPRI (1993) summarizes its recommendations for sands and clays in a series of 5 figures. These figures are included here as Exhibit 5. Each of these figures is reviewed to see how it relates to the North Anna situation.

a. Page 1 of Exhibit 5. This shows damping ratio as a function of reference strain. The "reference strain" is defined as τ_{max}/G_{max}, where τ_{max} is the "shear strength" of the soil. For sands, SSAR Reference 170 notes that the reference strain is typically about 0.1. Thus, the 0.1 reference strain curve is used as a starting point for the North Anna curve. This is plotted on Figure 2 as curve 1.

b. Pages 2 and 3 of Exhibit 5. These show the damping ratio versus shear strain curves as a function of vertical effective stress for dry and saturated sands, respectively. Groundwater table generally varies from about 6 feet to 58 feet below ground surface. As in the shear modulus reduction curve computation, assume groundwater level is at (1) 6 feet depth and (2) 30 feet depth. This gives effective vertical pressures of 1,313 psf and 1,875 psf, respectively.

   The curves on Pages 2 and 3 of Exhibit 5 are spaced proportionally to the log of the effective vertical pressure. These were interpolated for effective vertical pressures of 1,313 psf and 1,875 psf for the dry sands and plotted as curves 2 and 3, respectively, on Figure 2. For the saturated sands, the curves are plotted as curves 4 and 5, respectively, on Figure 2.

c. Page 4 of Exhibit 5. These curves are suitable for generic site response studies in Eastern North America, and cover the range from gravelly sands to low plasticity clays. A curve was interpolated for 10 to 40 feet depth for the North Anna sands. This curve is closer to the 20 to 50 feet curve than the 0 to 20 feet curve. It is plotted as curve 6 on Figure 2.

d. Page 5 of Exhibit 5. This shows damping ratio versus shear strain curves for clays, demonstrating the variation with plasticity index. The cohesive portions of the Zone IIA saprolite are generally low plasticity. Curve 7 on Figure 2 is for a PI of 10.

   Curve 8 on Figure 2 is the average Seed et al (1970) curve for sands that has been used in many SHAKE analyses.

   The curves in Figure 2 fall into a fairly close group. The average curve is closest to curve 2. This average curve is plotted as curve 1 on SSAR Figure 2.5-64 and is the design curve for the Zone IIA saprolite. The curve is tabulated below.

Curve 1: Damping Ratio Versus Shear Strain Design Curve for Zone IIA Saprolite									
Cyclic Shear Strain, Percent	.0001	.000316	.001	.00316	.01	.0316	.1	.316	1
Damping Ratio	0.6	0.8	1.1	1.8	3.5	7.1	12.2	18.9	23.7

3. Zone IIB Saprolite

EPRI (1993) indicates that at intermediate and high strains, coarser cohesionless soils show greater values of damping with increasing strain than fine-grained, cohesive soils. At low strains, the picture is not clear. Seed et al (1984), on the other hand, concludes that damping ratios for gravels are very similar to those for sands. Referring to Figure 2, it can be seen that the Seed et al (1984) curve (curve 8) for sands has generally higher damping ratios than any of the EPRI (1993) curves. Thus, if the Seed et al (1984) sand curve is selected for the coarser grained Zone IIB saprolite, it will satisfy the Seed et al (1984) conclusion that the sand and gravel damping curves are similar (with the curves as defined in Seed et al (1984)), and also the EPRI (1993) observation that, at intermediate and higher strains, the coarser grained soils have higher damping values (comparing the Seed et al (1984) curve with the selected design curve for sands on SSAR Figure 2.5-64). At low strains of 0.0001% and 0.000316%, assume the Zone IIB saprolite design curve is the same as the Zone IIA saprolite design curve. This curve is plotted as curve 2 on SSAR Figure 2.5-64, and is the design curve for the Zone IIB saprolite. The curve is tabulated below. This curve is very similar to the curve proposed by Rollins et al (1998) at lower strains, and gives a higher damping ratio at higher strains.

Curve 2: Damping Ratio Versus Shear Strain Design Curve for Zone IIB Saprolite									
Cyclic Shear Strain, Percent	.0001	.000316	.001	.00316	.01	.0316	.1	.316	1
Damping Ratio	0.6	0.8	1.6	3.3	5.8	10.0	15.5	21.0	24.6

4. Zone III Weathered Rock

As noted in the introductory section, sound rock will have a constant damping ratio with strain, possibly in the 1 to 2 percent range. The Zone III weathered rock will display some variation with strain, but not to the extent of the saprolites discussed above. For the modulus reduction curve for the Zone III weathered rock, the mudstone curve in SSAR Reference 169 was used. Unfortunately, Sun et al (1988) makes no mention of an equivalent damping ratio versus strain curve. However, the relationship between the gravel, sand and weathered rock modulus reduction curves in SSAR Figure 2.5-63 can be used as a basis for deriving the damping ratio versus strain curves for the weathered rock.

SSAR Figure 2.5-63 shows no modulus reduction down to 0.01% strain. It is known that there is some damping at low strains for all materials. Assume that the weathered

rock has 0.6 damping ratio at 0.001% strain (same as the sand and gravel). Assume this damping ratio remains constant to 0.01% strain.

At 0.0316% strain, the weathered rock shear modulus had reduced by (1 – 0.97) = 0.03, while the sand (Zone IIA) had reduced by (1 – 0.57) = 0.43. The sand damping ratio is 7.1 at 0.0316% strain. Thus it could be assumed that the weathered rock damping ratio was (0.03/0.43) x 7.1 = 0.5. Since the damping ratio will not decrease with increasing strain, assume the 0.6 damping ratio adopted for the lower strain values.

At 0.1% strain, the weathered rock shear modulus had reduced by (1 – 0.85) = 0.15, while the sand (Zone IIA) had reduced by (1 – 0.32) = 0.68. The sand damping ratio is 12.2 at 0.1% strain. Thus it can be assumed that the weathered rock damping ratio was (0.15/0.68) x 12.2 = 2.7.

At 0.316% strain, the weathered rock shear modulus had reduced by (1 – 0.61) = 0.39, while the sand (Zone IIA) had reduced by (1 – 0.15) = 0.85. The sand damping ratio is 18.9 at 0.1% strain. Thus it can be assumed that the weathered rock damping ratio was (0.39/0.85) x 18.9 = 8.7.

At 1.0% strain, the weathered rock shear modulus had reduced by (1 – 0.32) = 0.68, while the sand (Zone IIA) had reduced by (1 – 0.05) = 0.95. The sand damping ratio is 23.7 at 0.1% strain. Thus it can be assumed that the weathered rock damping ratio was (0.68/0.95) x 23.7 = 17.0.

This curve is plotted as curve 3 on SSAR Figure 2.5-64, and is the design curve for the Zone III weathered rock. The curve is tabulated below. Note that this curve is fairly similar to the highly plastic clay (LL = 70) in Exhibit 5.

Curve 3: Damping Ratio Versus Shear Strain Design Curve for Zone III Weathered Rock									
Cyclic Shear Strain, Percent	.0001	.000316	.001	.00316	.01	.0316	.1	.316	1
Damping Ratio	0.6	0.6	0.6	0.6	0.6	0.6	2.7	8.7	17

RAI 2.5.4-8 Part c)

c) Please explain the use of a damping ratio of 2% for the Zone III-IV rock.

Response to Part c)

The response to Part c) will be provided by separate correspondence.

References

Guidelines for Determining Design Basis Ground Motions, Electric Power Research Institute (EPRI), Volumes 1-5, EPRI TR-102293, Palo Alto, CA, 1993 (Reference 170 of SSAR Section 2.5).

Sun, J. I., R. Golesorkhi, and H. B. Seed. Dynamic Moduli and Damping Ratios for Cohesive Soils, Report No. UCB/EERC-88/15, University of California, Berkeley, August 1988 (Reference 169 of SSAR Section 2.5).

Seed, H. B., and I. M. Idriss. Soil Moduli and Damping Factors for Dynamic Response Analyses, Report No. UCB/EERC-70/10, University of California, Berkeley, December 1970 (Reference 167 of SSAR Section 2.5).

Seed, H. B., R. T. Wong, I. M. Idriss, and K. Tokimatsu. Moduli and Damping Factors for Dynamic Analyses of Cohesionless Soils, Report No. UCB/EERC-84/14, University of California, Berkeley, September 1984 (Reference 168 of SSAR Section 2.5).

Rollins, K.M., M.D. Evans, N.D. Diehl, and W.D. Daily. "Shear Modulus and Damping Relationships for Gravels," ASCE Journal of Geotechnical and Environmental Engineering, Vol. 124, No. 5, May 1998.

Application Revision

None.

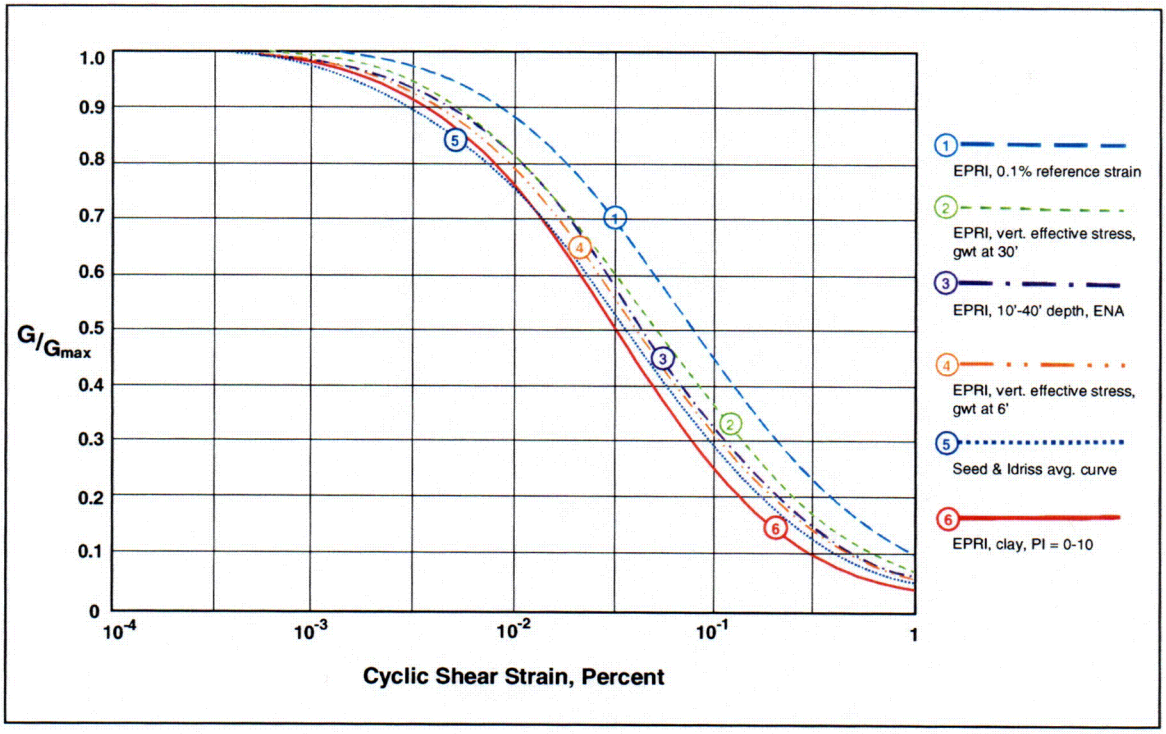

Figure 1. G/G_{max} versus Shear Strain Curves for Sands and Clay

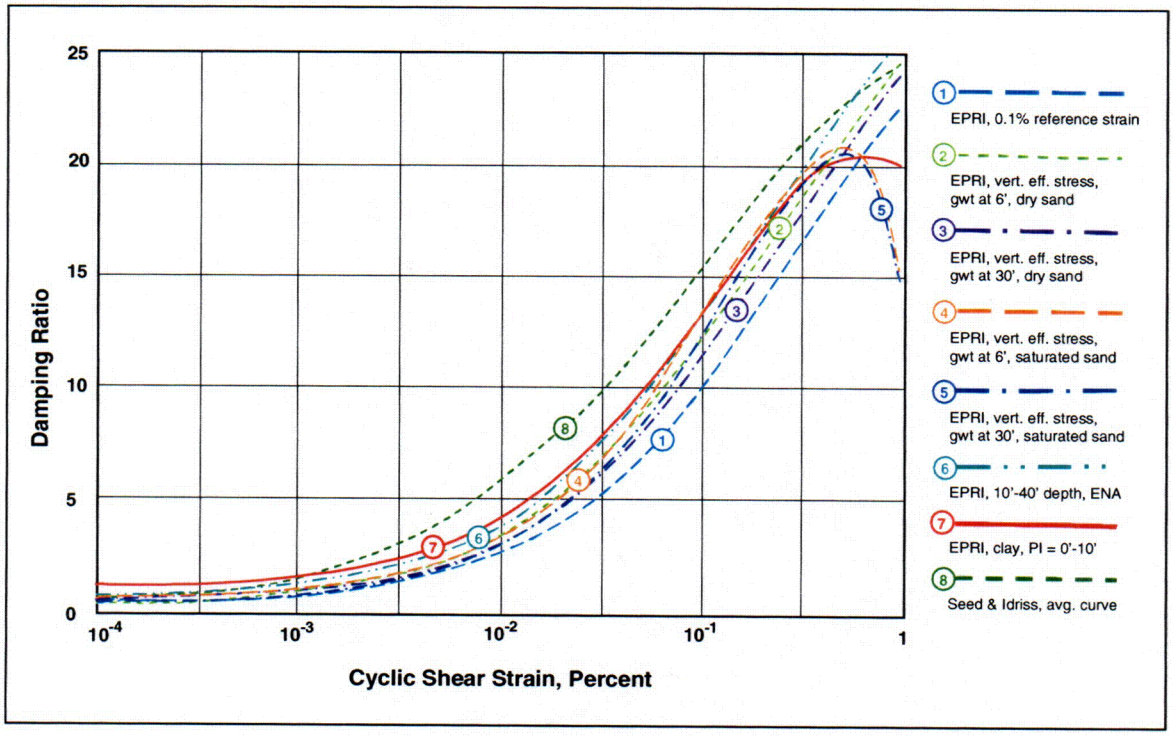

Figure 2. Damping Ratio versus Shear Strain Curves for Sands and Clay

C23

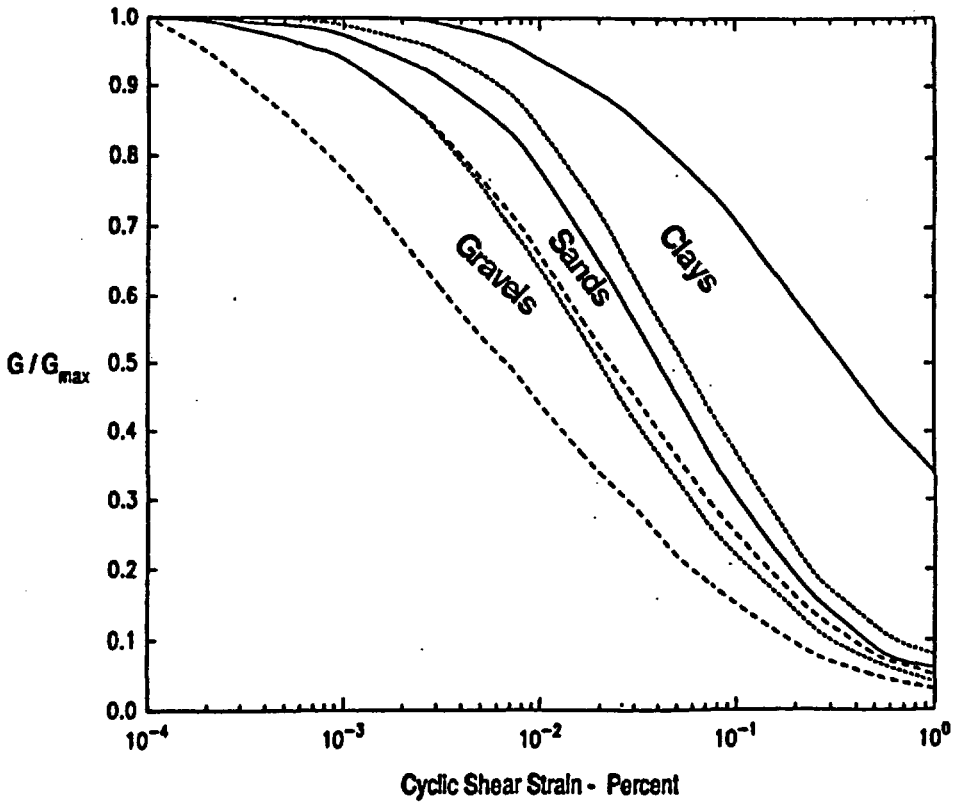

Exhibit 1. Typical Ranges for Modulus Reduction Curves

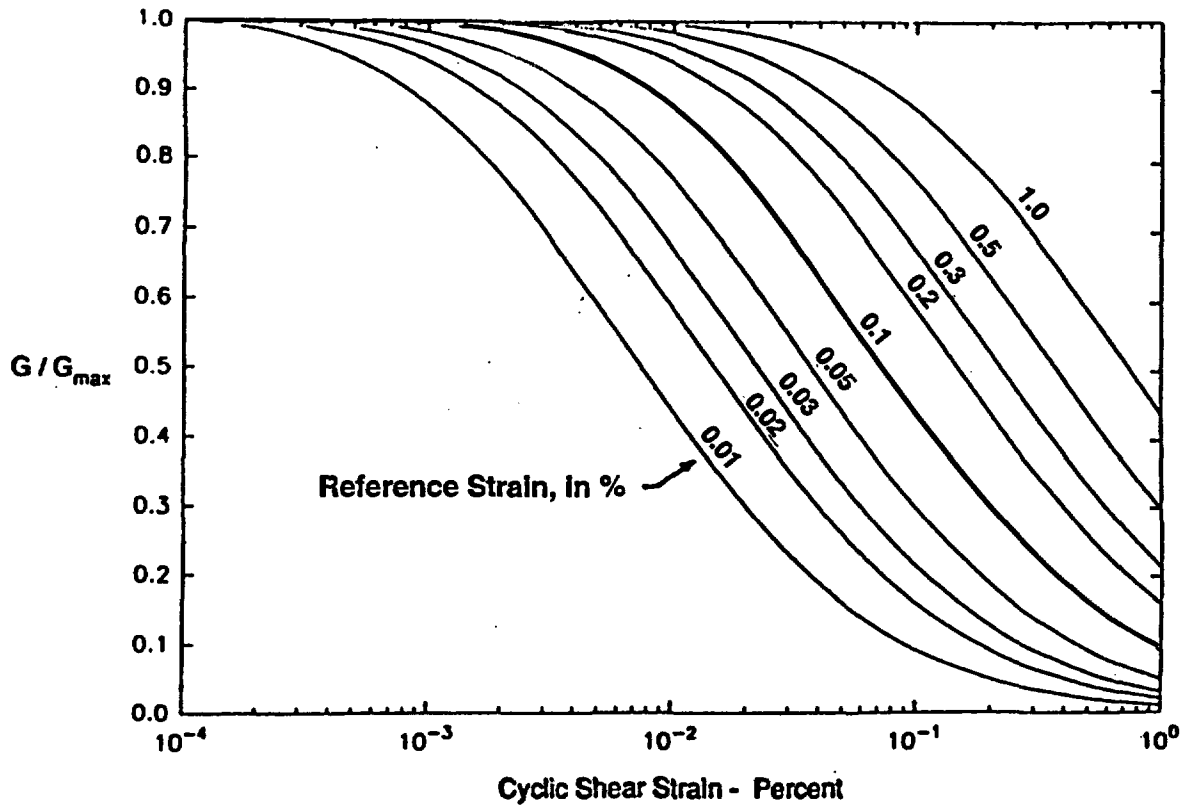

Exhibit 2: Recommended Modulus Reduction Curves
Page 1: Modulus Reduction as a Function of Reference Strain

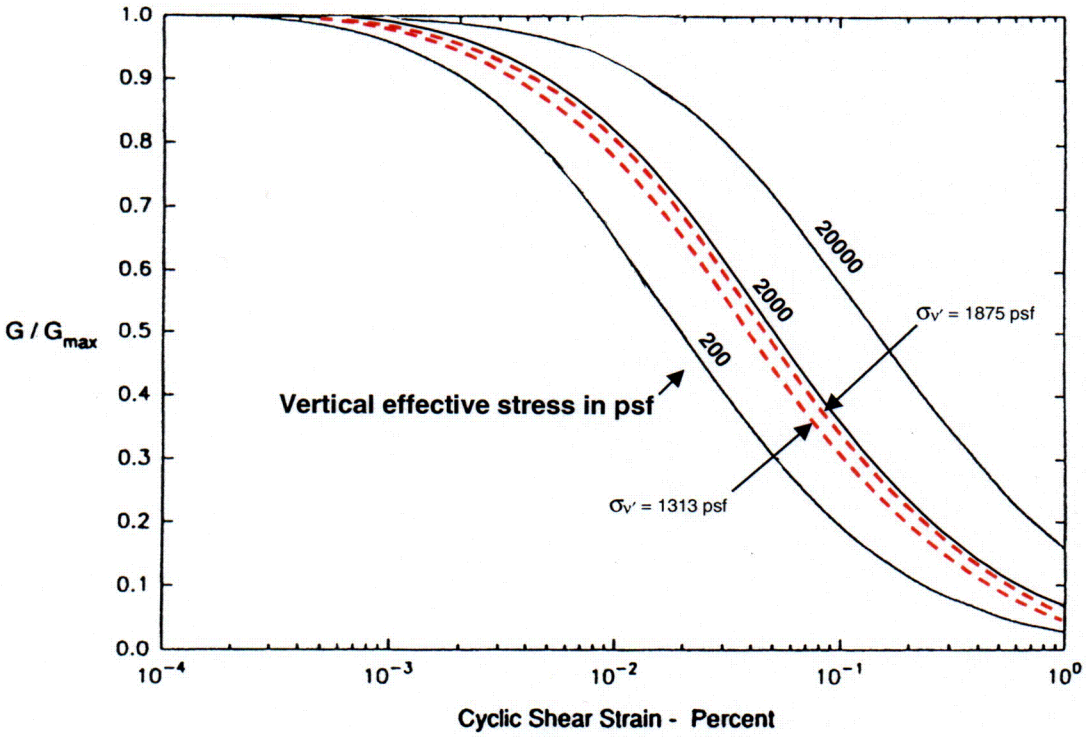

Exhibit 2: Recommended Modulus Reduction Curves
Page 2: Modulus Reduction Curves for Dry Sands

C24

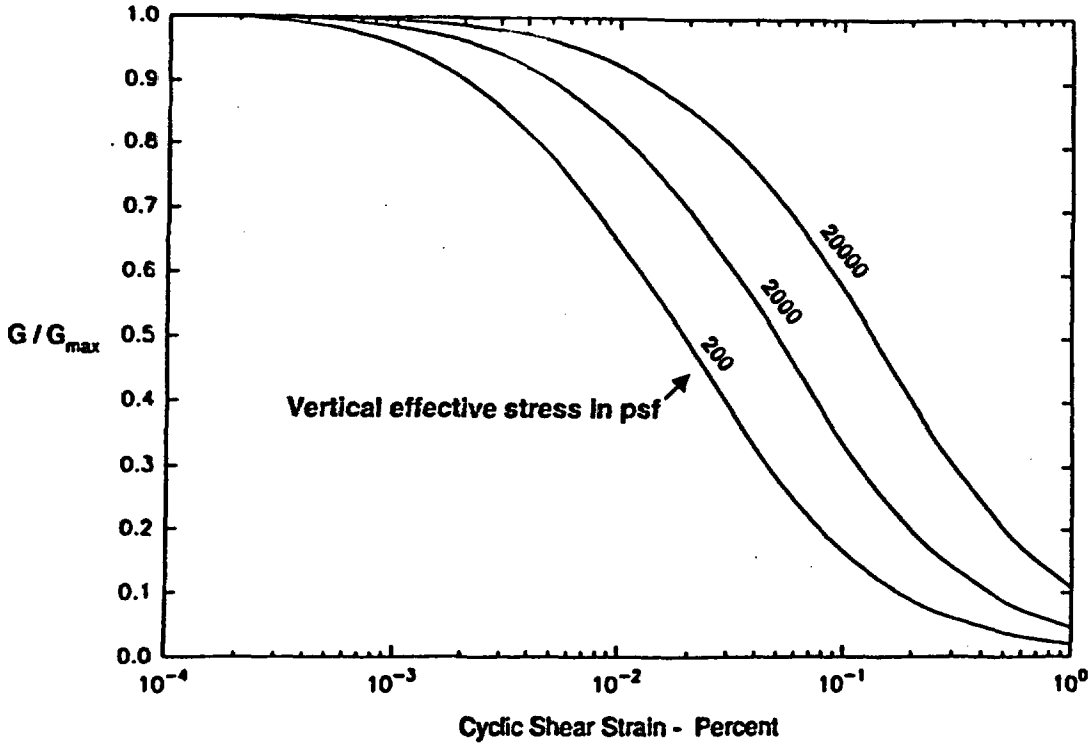

Exhibit 2: Recommended Modulus Reduction Curves
Page 3: Modulus Reduction Curves for Saturated Sands

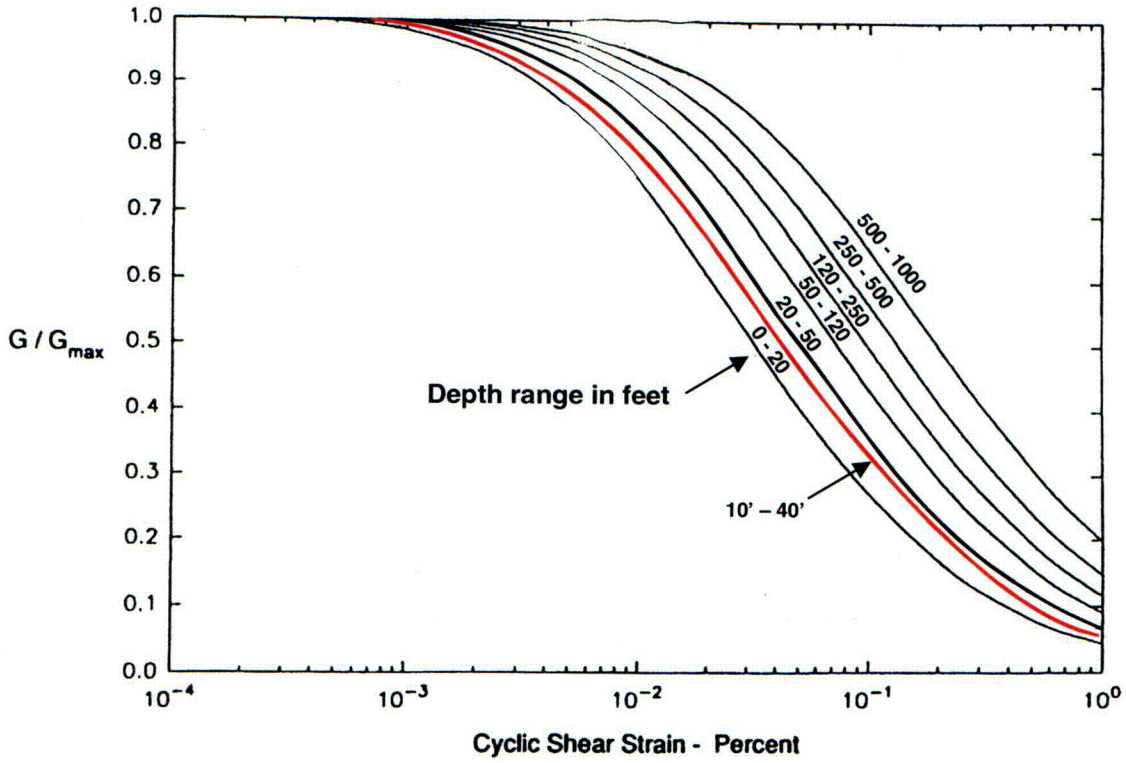

Exhibit 2: Recommended Modulus Reduction Curves
Page 4: Modulus Reduction Curves for Generic ENA Sites

C 25

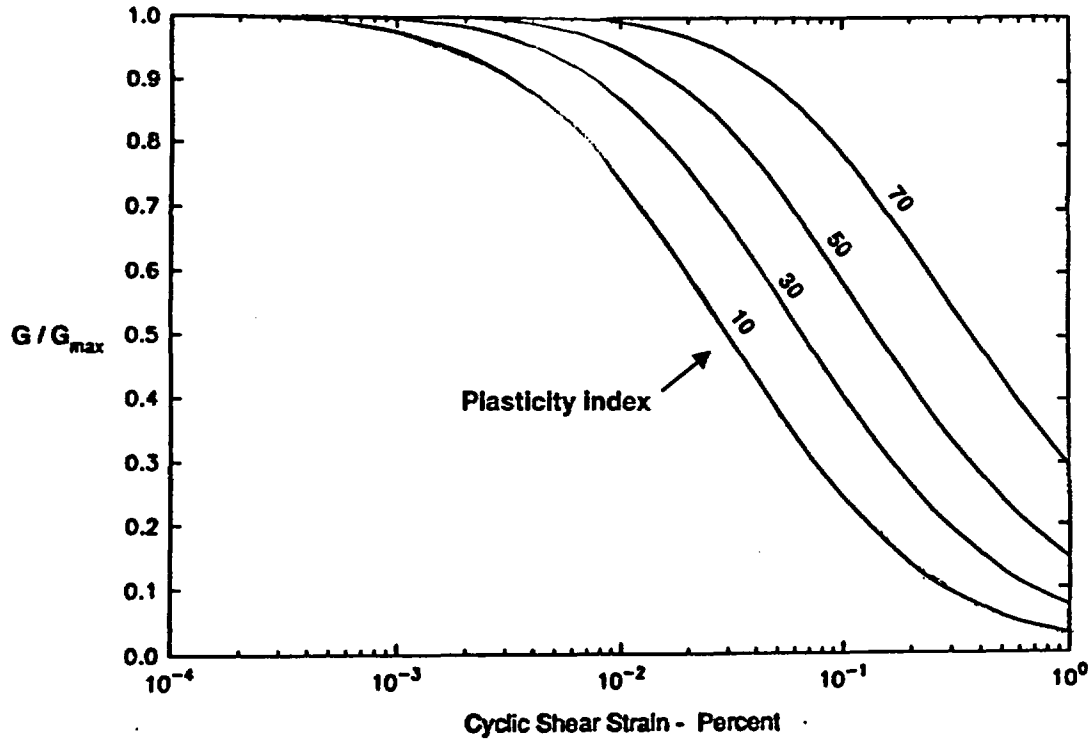

Exhibit 2: Recommended Modulus Reduction Curves
Page 5: Modulus Reduction Curves for Clays

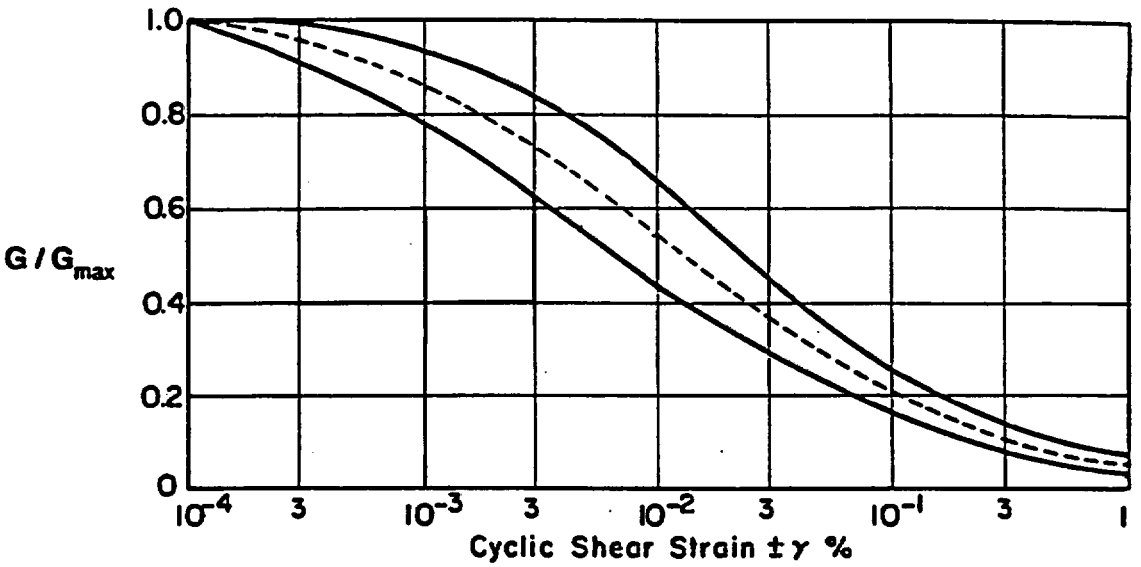

Exhibit 3: Modulus Reduction Curve for Gravel

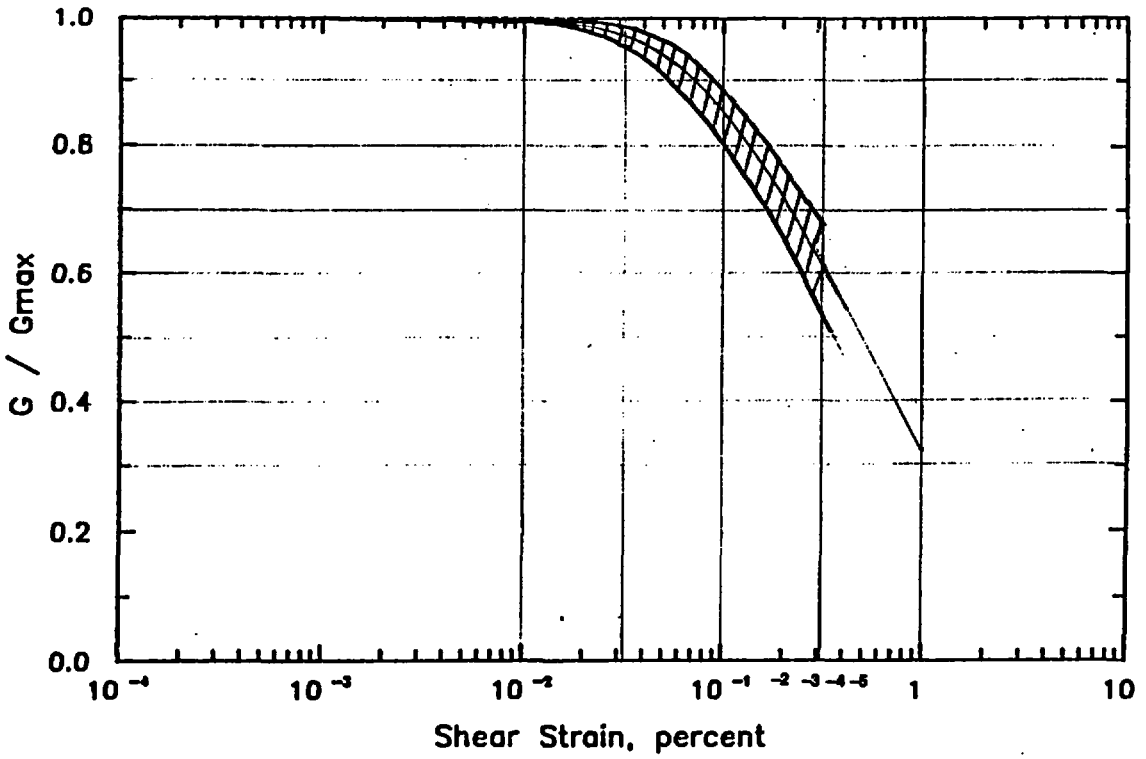

Exhibit 4: Modulus Reduction Curve for Mudstone

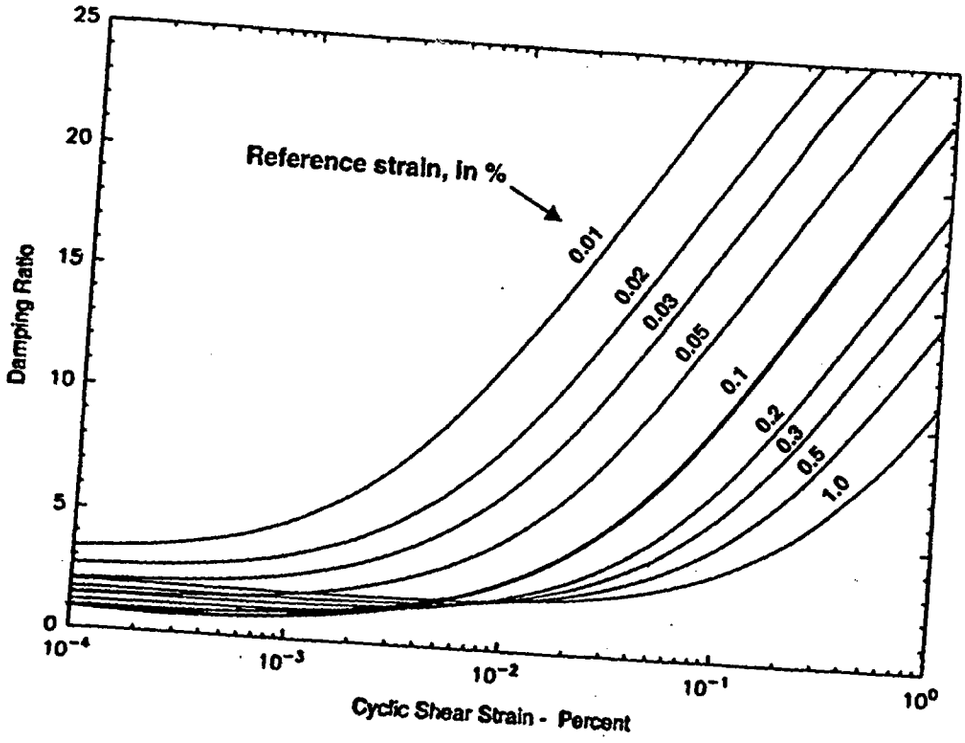

Exhibit 5: Recommended Damping Versus Strain Curves
Page 1: Damping Curves as a Function of Reference Strain

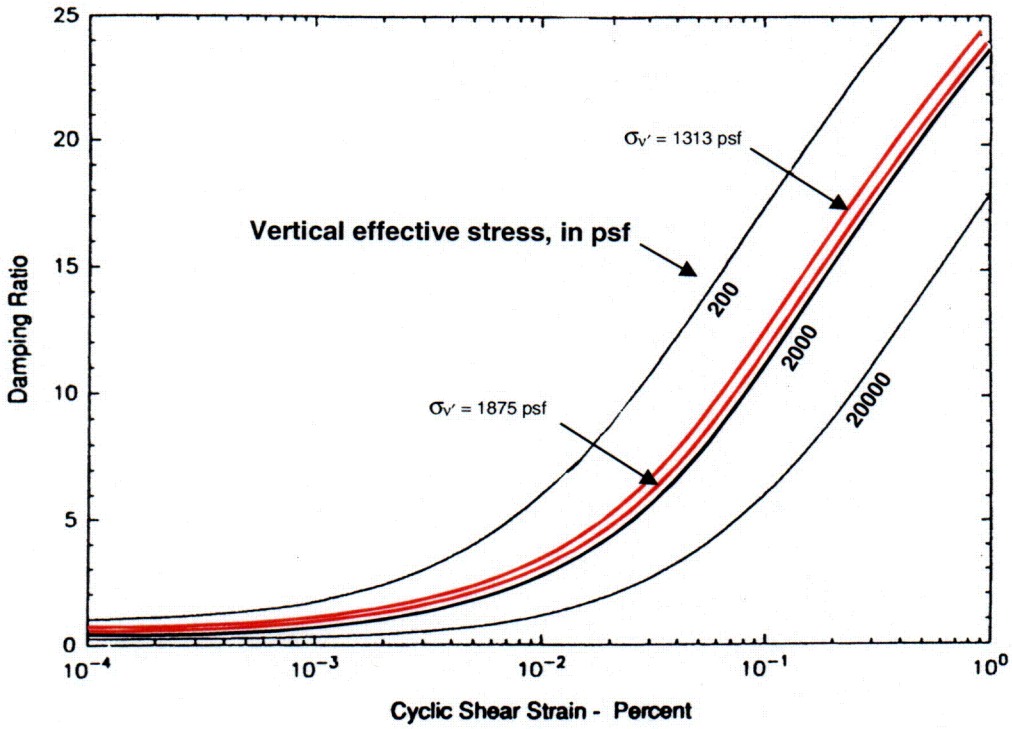

Exhibit 5: Recommended Damping Versus Strain Curves
Page 2: Damping Curves for Dry Sands

C26

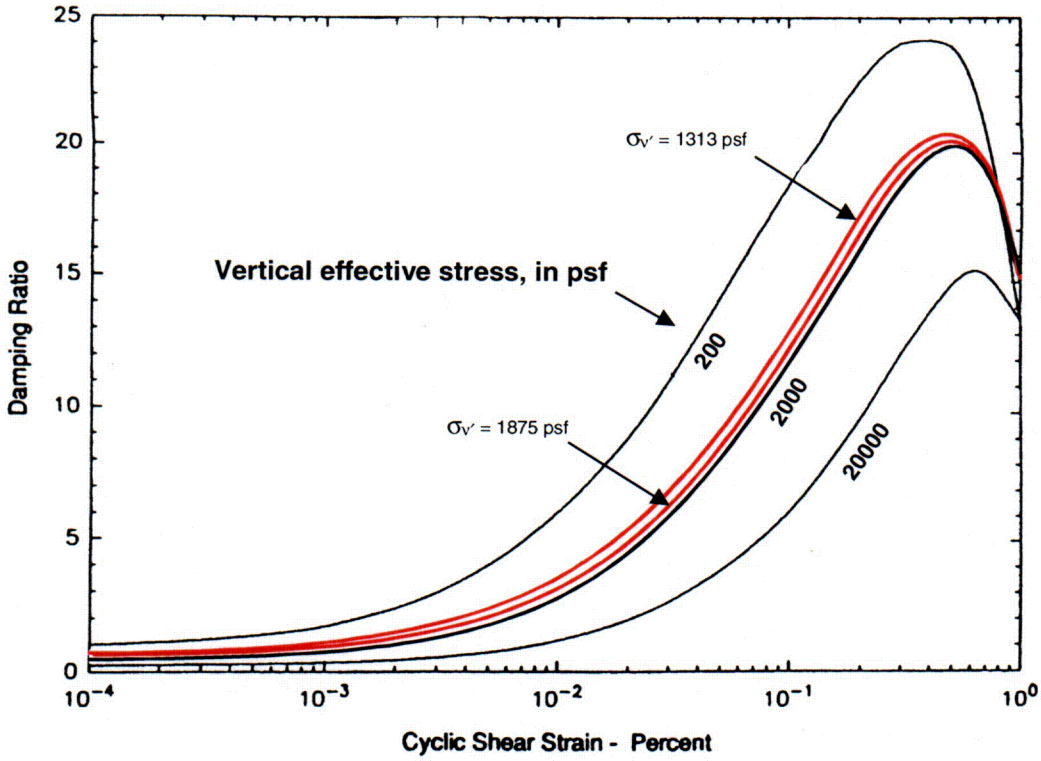

Exhibit 5: Recommended Damping Versus Strain Curves
Page 3: Damping Curves for Saturated Sands

C27

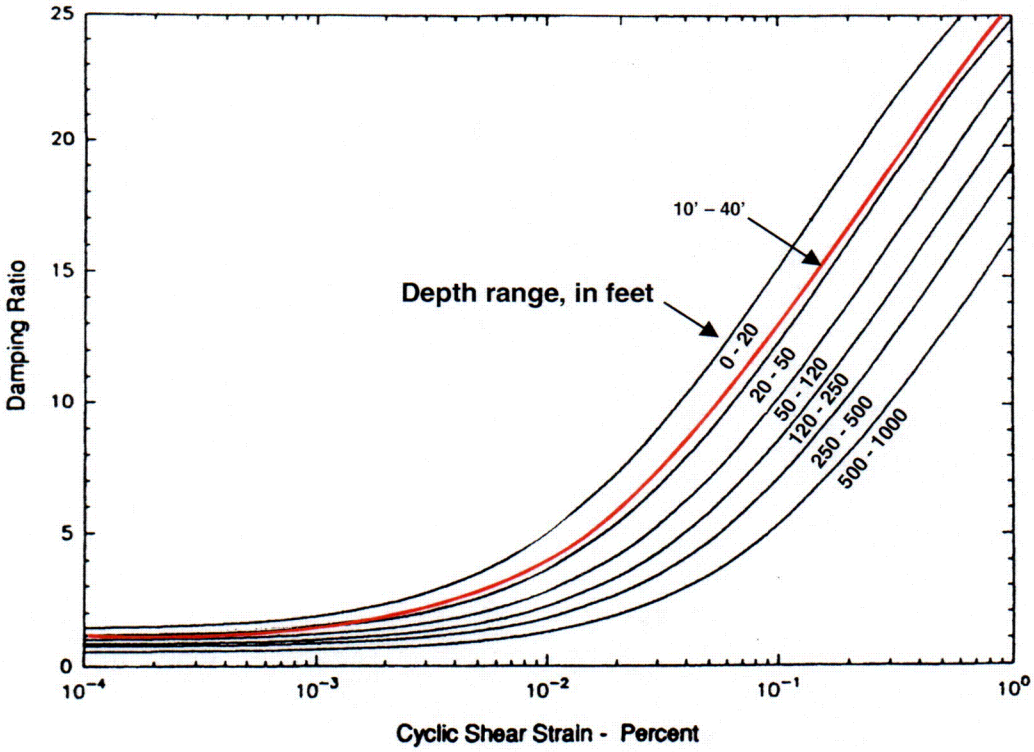

Exhibit 5: Recommended Damping Versus Strain Curves
Page 4: Damping Curves for Generic ENA Sites

C28

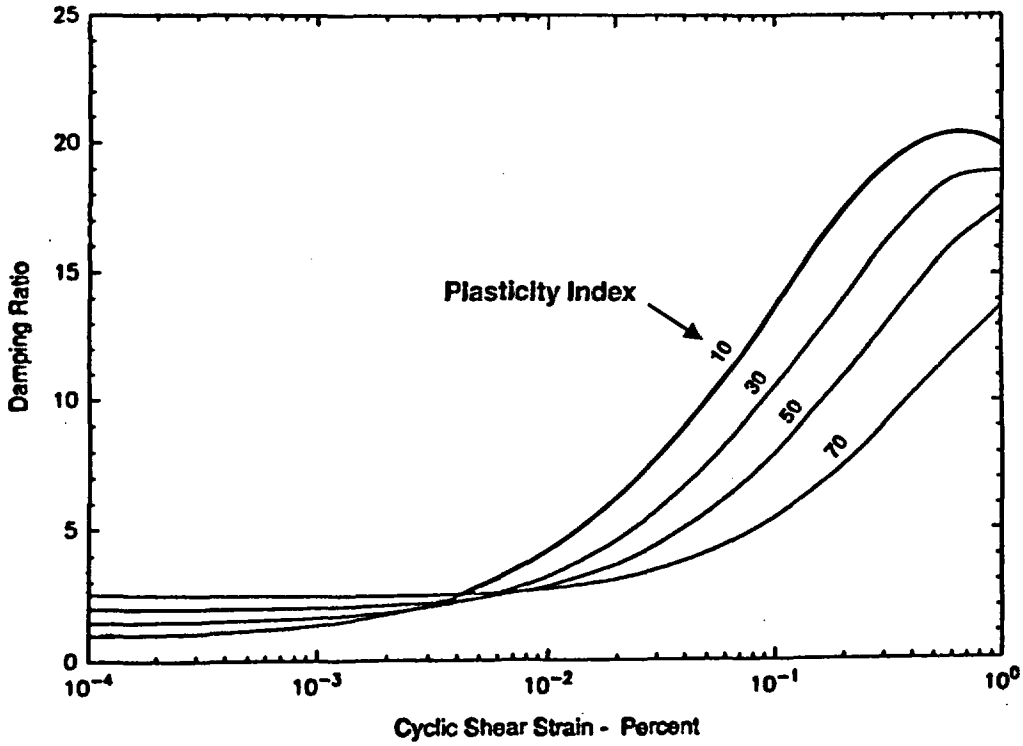

Exhibit 5: Recommended Damping Versus Strain Curves
Page 5: Damping Curves for Clays

RAI 2.5.4-11 (NRC 6/1/04 Letter)

Please provide a sample set of the calculations to substantiate the bearing capacities of soil and rock beneath major Category I structures, as shown in SSAR Table 2.5-47. Please indicate if and how the local site effects, such as the slope of the rock surface, fracture spacing, variability in properties, and evidence of shear zones, if any, were considered in determining the allowable bearing capacities of soil and rock for different structures.

Response

A copy of Bechtel Calculation 24830-G-004, "Bearing Capacity and Settlement Analysis," will be submitted by separate letter. The allowable bearing capacities given in SSAR Table 2.5-47 were derived in this calculation. These are reproduced below:

Table 1. Allowable Bearing Capacities	
Zone	**Allowable Bearing Capacity, q_a, ksf**
IIA	4
IIB	8
III	16
III-IV	80
IV	160

Table 2 below illustrates the structural foundations that would be placed on the various type materials.

Table 2: Structure Foundations by Zone		
Zone	**Used for Reactor Containment Structure Foundation?**	**Used for Other Category 1 Structure Foundations?**
IV	Yes	Yes
III-IV	Yes	Yes
III	No	Yes, as limited by bearing capacity. See Table 1.
II-B	No	Yes, as limited by bearing capacity. See Table 1.
Improved II-A(1)	No	Yes, as limited by bearing capacity. See Table 1.
II-A	No	No
I	No	No

(1) Improved Zone II-A saprolite is discussed in SSAR Section 2.5.4.12.

The maximum bearing pressure from the containment (reactor) building foundation is 15 ksf, which is only a fraction of the allowable bearing capacity of the bedrock. The allowable bedrock bearing capacity values given in the table are conservative presumptive values based mainly on building codes, and are themselves only a very small fraction of the theoretical ultimate bearing capacity of the rock. For example, the Zone III-IV rock has a design unconfined strength of 576 ksf, and the theoretical ultimate bearing capacity for mat foundations is several times the unconfined strength. The reason that the allowable bearing capacity is so much less than the theoretical ultimate capacity is because of the non-homogeneity of most rock masses, including variation in properties and the presence of fracture zones, referenced in the RAI. Thus the bearing capacity values for the Zone III-IV and Zone IV bedrock given in SSAR Table 2.5-47 take into account normal variations and fracturing in the rock. These bearing capacity values would only be affected if the bedrock were severely sloped, fractured, sheared, etc. This is discussed in the next paragraphs.

Sloped Rock Surface

As discussed in the response to RAI 2.5.4-1, bedrock level at the site is generally gently sloping, as shown on the two subsurface profiles in SSAR Figures 2.5-57 and 2.5-58, with steepest slopes in the 12 to 15% range. (Vertical exaggeration on these figures is approximately 5 and 2.5, respectively.) This is a normal rock surface slope.

Fracture Spacing

The recovery and rock quality designation (RQD) are typically good indicators of the degree of fracturing of cored rock. For the ESP borings, the recoveries for the Zone III-IV and Zone IV bedrock were around 90 and 100 percent, respectively, while the corresponding RQD values were around 50 and 95 percent. This puts the Zone III-IV rock into the "fair" category and the Zone IV rock into the "excellent" category according to Table 5.2 of Peck et al (1974). Some thin fracture zones found in the ESP borings are described in SSAR Section 2.5.1.2.3 and are discussed in the response to RAI 2.5.4-2. SSAR Section 2.5.1.2.6 concludes that, "The joints and fractures present in both zones (i.e., Zones III-IV and IV) are not considered to be of sufficient density or areal extent to affect the engineering behavior of the rock with respect to its foundation bearing capacity or integrity". Also, SSAR Section 2.5.4.10.1 states, "If excavation during construction reveals any weathered or fractured zones at foundation level, such zones would be overexcavated and replaced with lean concrete."

Variability of Properties

The variation in the strength of the bedrock was discussed in the response to RAI 2.5.4-6 Part c).

Shear Zones

As noted in SSAR Section 2.5.1.2.6 c:

> A shear zone was found in the Ta River Metamorphic Suite during the excavation for abandoned Units 3 and 4 at the North Anna Power Station. The shear zone was investigated by Dames and Moore (Reference 9) and the results presented to the U.S. Atomic Energy Commission. The results of the investigation concluded that movement occurred along the shear zone approximately 200 million years ago, and that movement has not occurred since, or at least not within the last one million years, given the relatively undisturbed thickness of residual soil that overlies the shear zone. The results of the investigation also concluded that the shear zone is of limited extent, and while it was traced through the Units 1 and 2 foundation area, no evidence of movement was observed along this section of the shear zone.
>
> The U.S. Atomic Energy Commission, following a review of the results of the above mentioned investigation, concluded that the shear zone at the site is not "capable", within the meaning of Section III (g) of 10 CFR 100, Appendix A (Reference 108).

No evidence of shear zones was found during the ESP subsurface investigation.

References

Peck, R. B., W. E. Hanson, and T. H. Thornburn. Foundation Engineering, Second Edition, John Wiley and Sons, Inc., New York, 1974 (Reference 182 of SSAR Section 2.5).

Application Revision

Table 2.5-47 will be revised as follows:

Table 2.5-47 Allowable Bearing Capacity Values

Zone	Allowable Bearing Capacity, ksf
IIB	8
III	16
III-IV	80(1)
IV	160(1)

(1) The new containment (reactor) buildings would be founded on Zone III-IV or Zone IV material.

Note: The above values include a factor of safety against bearing failure of at least 3. Minimum assumed foundation width is 5 feet. Minimum assumed foundation depth is 3 feet.

RAI 2.5.4-12 (NRC 6/1/04 Letter)

SSAR Section 2.5.4.11 (Design Criteria) states that geotechnical-related design criteria that pertain to structural design are not included in the application. Please provide the reasons for not providing the geotechnical-related design criteria that pertain to structural design (such as sliding, and overturning).

Response

SSAR Section 2.5 deals with site-related issues and not with specific structural design issues. The design criteria noted in SSAR Section 2.5.4.11 are either (a) not related to any specific structural design, e.g., factor of safety against liquefaction or slope stability failure, or (b) they are specific to the ESP site, e.g., allowable bearing capacity of the site soils and bedrock.

Structural criteria such as allowable wall rotation and factors of safety against structure sliding or overturning are not site specific and thus, for consistency, are not included in SSAR Section 2.5. These criteria would be established during detailed engineering and described in a design certification and/or COL application.

Application Revision

None.

RAI 17.1-2 (NRC 6/1/04 Letter)

Sections 8 and 9 of Dominion's Early Site Permit Application Development Quality Assurance Manual and Section 4 of Bechtel's Quality Assurance Program Plan state that the safety-related scope of the development of the ESP application would not involve the use of quality assurance measures for the identification and control of materials, parts, and components and for the control of special processes. Please describe why these quality assurance measures were not applicable to the development of the ESP application. Alternatively, if these quality assurance measures were applicable to the ESP application, please describe the quality assurance measures used by Dominion and the primary contractor (Bechtel) for these activities.

Response

1. Dominion ESP QA Manual

[Please note that Dominion's Early Site Permit Application Development Quality Assurance Manual addresses the quality requirements mentioned in the question in its Sections 9 and 10, not in Sections 8 and 9, as stated in the question.]

Under Dominion's overall direction, several companies were involved in the preparation of the North Anna ESP application. The quality requirements imposed on the various companies differed depending on their scope of work. For example, Section 9 of Dominion's own ESP QA Manual, "Identification and Control of Material, Parts and Components," was deemed not applicable to Dominion on the basis that no safety-related, materials, parts, or components were to be procured within Dominion's project scope. Section 10 of Dominion's ESP QA Manual, "Control of Special Processes," was also deemed not applicable to the ESP project because Dominion's project activities did not involve the use of special processes in the development of the ESP application.

More importantly, Section 5 of the Dominion ESP QA Manual, "Procurement Document Control," governs supporting company involvement to ensure that appropriate quality requirements are included in procurement documents defining the scope of the supporting companies' project involvement. In accordance with the Dominion QA Manual requirements, Dominion selected Bechtel as a primary contractor and awarded a contract for the development of the ESP application. The contract documents invoked 10 CFR 50 Appendix B and required that Bechtel prepare and submit a project-specific QA Program Plan for the project, meeting the Dominion ESP QA Manual requirements. Bechtel's Quality Assurance Program Plan (QAPP), which is based on the Bechtel Nuclear QA Manual (NQAM), was reviewed and approved by Dominion to verify that it met Dominion's ESP QA Manual requirements.

2. Bechtel Quality Assurance Program Plan

Bechtel's NQAM Policy Q-8.1, "Identification and Control of Materials, Parts, and Components," contains quality assurance measures for the identification and control of materials, parts, and components and Policy Q-9.1, "Control of Special Processes," contains requirements for the control of special processes. Both of these policies were not invoked in the ESP project-specific QAPP because the Bechtel scope of work for the ESP project does not include procurement and/or receipt of safety-related materials, parts, or components or other construction activities involving special processes. Dominion reviewed and approved the Bechtel QAPP.

However, to ensure that appropriate quality program requirements are specified in procurement documents for Bechtel suppliers/subcontractors, Bechtel NQAM Policy Q-4.1, "Preparation of Procurement Documents," governs. Policy Q-4.1 defines measures for determining and specifying appropriate quality program requirements for suppliers/subcontractors. Such quality program requirements receive a review and concurrence by Quality Assurance.

Bechtel used four subcontractors on the ESP project: MACTEC, Risk Engineering Incorporated (REI), Tetra-Tech NUS, Inc (TtNUS) and William Lettis & Associates (WLA). The activities of these subcontractors and the related quality program requirements are described below:

- MACTEC

  MACTEC provided surveying and sub-soil investigation services that included core drilling, sampling and laboratory testing of samples, etc. This included traceability of core samples. No special processes, such as, welding or non-destructive examination were included in MACTEC's scope of work.

  For the above services, Bechtel's specification defined the work scope and technical and quality requirements. The specification required that the subcontractor's QA program meet the requirements of 10 CFR 50 Appendix B. The specification also required labeling of core samples in accordance with the applicable ASTM D2113.

  MACTEC's QA program was satisfactorily audited by Bechtel to verify that appropriate program elements were covered and were being implemented. This included the 10 CFR 50 Appendix B, Criterion 8, "Identification and Control of Materials, Parts and Components."

- Risk Engineering

  REI provided computational and expert consulting services to prepare the SSAR Section 2.5 probabilistic seismic hazard sensitivity analyses. The work scope did not include any hardware requiring identification and control or special processes.

  Bechtel's service requisition defined the work scope and technical and quality program requirements. The service requisition required that the subcontractor's QA program meet the requirements of 10 CFR 50 Appendix B.

  REI's QA program was satisfactorily audited by Bechtel to verify that appropriate program elements were covered and were being implemented.

- Tetra-Tech NUS

  TtNUS provided services for preparing certain sections of the Environmental Report. These services included data collection, impact analysis, and document preparation. The work scope did not include any hardware requiring identification and control or special processes.

  The services of TtNUS are non-safety related. Bechtel's service requisition defined the work scope and technical and quality program requirements. The service requisition required that the subcontractor have a QA program that is compatible with the provisions and requirements of ISO 9000.

  TtNUS' QA program was satisfactorily audited by Bechtel to verify that appropriate program elements were covered and were being implemented.

- William Lettis & Associates

  WLA provided services related to geologic mapping and characterization of seismic sources for preparation of SSAR Section 2.5 and related ER sections. The work scope did not include any hardware requiring identification and control or special processes.

  Bechtel's service requisition defined the work scope and technical and quality program requirements. The service requisition required that the Subcontractor perform work in accordance with Bechtel's 10 CFR 50, Appendix B, QA program as described by the Bechtel QAPP and the implementing procedures contained in Bechtel's Project Engineering Procedures Manual.

Application Revision

None.